Title: Peripheral blood as a potential source for Alzheimer's disease biomarkers

Dissertation

zur Erlangung des akademischen Grades

Dr. rer. med

an der Medizinischen Fakultät der Universität Leipzig

eingereicht von:

David Larbi Simpong

geboren am 08.08.1984 in Aburi

angefertigt an der:

Universität Leipzig

Paul Flechsig Institute of Brain Research

Betreuer:

Prof. Dr. med. Thomas Arendt

Beschluss über die Verleihung des Doktorgrades vom: 25.02.2020

TABLE OF CONTENT

LIST OF ABBREVIATION

AD – Alzheimer's disease

APP – Amyloid precursor protein

AMPA – α-amino-3-hydroxy-5-methyl-4-isoxazolepropionic acid

Aβ – Amyloid beta

Aβ-PET – Amyloid beta positron emission tomography

BBB – Blood brain barrier

BSA – Bovine serum albumin also known as Albumin bovin Fraction V

B/S-N – Bjerrum Schafer- Nielsen

CERAD – Consortium to Establish Registry for Alzheimer's Disease

CNS – Central nervous system

CSF – Cerebrospinal fluid

CT – Computed tomography

DPBS – Dulbecco's Phosphate Buffered Saline

DMEM/HAM's F12 – Dulbecco's Modified Engle's Medium

DTI – Diffusion tensor imaging

ECL – Enhanced chemiluminescence

EDTA – Ethylenediaminetetraacetic acid

EGFP – Enhanced Green Fluorescent Protein

fPET – Fluorodeoxyglucose positron emission tomography

HAMAs – Human anti-mouse antibodies

HRP – Horseradish peroxidase

HUH.7 – Human hepatoma 7

HSP – Heat shock proteins

MMSE – Mini-Mental State Examination

MoCA – Montreal Cognitive Assessment

MRI – Magnetic resonance imaging

MTBR – Microtubule binding region

NFT – Neurofibrillary tangle

ndECVs – Neuron derived extracellular vesicles

N2A – Neuro2a

Opti-MEM – Improved Minimal Essential Medium

PE – Phycoerythrin (R- phycoerythrin)

PFI - Paul Flechsig institute of brain research

PNS – Peripheral nervous system

PVDF – Polyvinylidene difluoride

RNA – Ribonucleic acid

SDS – sodium dodecyl sulphate

SDS-PAGel – Sodium dodecyl sulphate-polyacrylamide gel

SDS-PAGE – Sodium dodecyl sulphate-polyacrylamide gel electrophoresis

SLUMS Saint Louis University Mental Status

SPECT – Single-photon emission computed tomography

Tau – Tubulin associated unit

TBS – Tris buffered saline

TEMED – Tetramethylethylenediamine

γ – Gamma

β – Beta

LIST OF FIGURES

1.   INTRODUCTION

1.1.   Alzheimer's disease

Alzheimer's disease (AD), first described in 1907 by Alois Alzheimer, is a neurodegenerative disorder [Alzheimer, 1907]. The term, AD was coined in 1910 by Kraepelin [Kraepelin, 1910], while the original research article was translated from German to English in 1995 by Stelzma and colleagues [Stelzma et al., 1995]. The disease is progressive and is characterized by cognitive defect [Glenner, 1982]. It begins at the hippocampus and progresses in a centrifugal manner, hierarchically from anterograde amnesia, speech impairment to loss of executive functions [Ray et al., 1998; Albert et al., 2011; Arendt et al., 2017]. Generally, AD is categorized into two forms; the sporadic and the familial [Lendon et al., 1997; Ray et al., 1998; Bekris et al., 2010]. The familial AD which constitute about 5% of the disease shows Mendelian inheritance [Lendon et al., 1997] while the sporadic AD which is influenced by environmental factors and/or genetic alteration account for about 95% of the disease [Bekris et al., 2010]. The disease can also be classified as early onset (30 – 60 years) or late onset (above 60 or 65), although old age is the major risk factor for the acquisition of AD [Bekris et al., 2010]. But, irrespective of which category or form (sporadic, familial, early onset or late onset) of the disease, AD is a dementing disorder and presents several symptoms [McKhann et al., 1984].

Clinical symptoms of AD include but not limited to memory decline [Markowitsch; Staniloiu, 2012], loss of executive function and judgement [Stokholm et al., 2006], Apraxia [Parakh et al., 2004], olfactory dysfunction [Rahayel et al., 2012], sleep disturbances [Ju et al., 2014], and seizures [Hauser et al., 1986]. Other symptoms include; motor signs defect [Portet et al., 2009], atypical presentation [Galton et al., 2000; Alladi et al., 2007] and mixed dementias [Galasko et al., 1994]. As disease advances, hypertonia, incontinence, mutism and myoclonus, pneumonia, malnutrition arises. And it is these complication (such as pneumonia, malnutrition, recurrent infection) that result in the death of an AD person and not the dementia which is the symptom of the disease [McKhann et al., 1984; Ray et al., 1998; Bekris et al., 2010]. Alzheimer's disease is characterised by two major histological hallmarks; neurofibrillary tangles (NFT) and neuritic plaques [KIDD, 1963; KIDD, 1964; Glenner; Wong, 1984; Glenner; Wong, 1986; Brion, 1998].

1.1.1. The neuritic plaque

The neuritic plaques are insoluble extracellularly deposits consisting of several proteins such as amyloid precursor protein (APP), apolipoprotein E, α_1- antichymotrypsin, IgG, several complements protein and glycosaminoglycans [Namba et al., 1991; Ghiso et al., 1993; Strittmatter; Roses, 1996]. However, of all the protein constituents, amyloid beta (Aβ), a proteolytic cleavage (39 - 43 amino acid long) derived from amyloid precursor protein is the major component of neuritic plaque [Ghiso et al., 1993; Ray et al., 1998]. The APP belongs to the type I membrane protein family and is found in a variety cells but particularly in brain cells [Zheng; Koo, 2011; Coronel et al., 2018]. The actual biological function of this protein is unclear, but it has been suggested to function in neural growth, maturation, synaptogenesis and axonal outgrowth after injury [Wang et al., 2014; Coronel et al., 2018]. In the brain, APP is produced in the astrocytes and neurons [Puig; Combs, 2013; Brothers et al., 2018]. Typically, APP is constitutively cleaved by alpha (α), beta (β) and gamma (γ) secretases to produce soluble fragments such as secreted APPα (sAPPα or sAPPβ), Aβ peptides (including Aβ_{1-40}, A$\beta_{1-42,}$ or Aβ_{1-43}), and 3-kDa peptide (P^3) respectively [Chow et al., 2010; Nhan et al., 2015]. However, due an unclear mechanism in the brain, Aβ monomers self-assemble [Tycko, 2016] to aggregate and form oligomers [Brothers et al., 2018]. Further aggregation of the peptides progresses to oligomers, protofibrils and finally fibrils. Other cellular components subsequently combine with the aggregated fibril and then form insoluble deposit called Aβ plaque (amyloid plaque). Since APP is a membrane protein, the generated insoluble Aβ fragments becomes extracellular deposits. The commonly produced monomeric peptides of amyloid protein in this pathology are the Aβ_{40} and Aβ_{42} [Thinakaran; Koo, 2008; Grimm et al., 2013; Dawkins; Small, 2014; Coronel et al., 2018]

1.1.2. The neurofibrillary tangles

Neurofibrillary tangles on the other hand are intracellular deposits consisting mainly of a microtubule associated protein, tubulin the associated unit (tau) within dystrophic neurons [Strittmatter; Roses, 1996; Ray et al., 1998]. The tau protein belongs to the family, microtubule associated proteins (MAPs) and it was discovered in the year 1975 [Weingarten et al., 1975; BERKELEY, 2009]. In human central nervous system (CNS), tau

gene is located on the long arm of chromosome 17q21 [Neve et al., 1986] and alternative splicing of the tau transcript gives rise to six (6) isoforms in the CNS [Goedert et al., 1989]. Natively, the protein is unfolded, flexible, mobile [Guo; Lee, 2011] and consists of four (4) regions; N terminal (1 to 150 amino acid), proline rich (151 to 243 amino acid region), the microtubule binding region (MTBR) and the C-terminal (370 to 441 amino acid region)[Guo et al., 2017]. In adult human brain, the MTBR on a single isoform of tau exist in either 3 or 4 repeats (3R or 4R) with a 50:50 ratio.

Tau protein uses its MTBR region to bind microtubules and stabilize them [Spires-Jones et al., 2009]. The binding affinity between the MTBR of the tau and the microtubules is regulated by several post-translational modifications (such as nitration, phosphorylation, glycosylation, proteolysis and glycation), however, phosphorylation is the primary mechanism controlling this binding process [Morris et al., 2015]. The tau protein has about 85 potential phosphorylation sites [Buerger et al., 2002; Hansson et al., 2006; Goossens et al., 2017] and the ability for the protein to become phosphorylated is tightly regulated by the balance between kinases (such as glycogen synthase kinase 3β and cyclin dependent kinase 5) and phosphatases (such as protein phosphatase 2A) activities [Mazanetz; Fischer, 2007].

1.1.3. Pathophysiology of NFT

Due to an unclear mechanism in pathological state, kinases activity becomes upregulated while phosphatases become downregulated leading to abnormal phosphorylation (hyperphosphorylation) of the tau protein [Kolarova et al., 2012]. And as tau protein becomes hyperphosphorylated its binding affinity for microtubules becomes very weak and it therefore detaches [Lindwall; Cole, 1984; Bramblett et al., 1993]. Once tau protein dissociates from the microtubules it relocates into the somatodendritic region of the cell. At the somatodendritic compartment, tau protein undergoes further modification such as phosphorylation which subsequently aggregate to form tau filaments [Spires-Jones et al., 2009] or sequester other neuronal microtubules associated proteins, MAP1 and MAP2 [Alonso et al., 1997]. Further aggregation of the fibril develops into tangles (neurofibrillary tangles) which become toxic species to the cell leading to its death and

loses, a phenomenon that characterised AD. And as the tau protein is intracellularly located, the tangle that form is also intracellularly deposited [Spires-Jones et al., 2009]

Again, tau protein, which is primarily found in the axons of neurons, functions as a glue to hold and stabilize the microtubules thereby bridging the cytoskeletal connection [Goedert et al., 1989; Gu et al., 1996; Brion, 1998; Guzmán-Martinez et al., 2013]. This key function of tau protein is necessary to maintain the normal morphology (such as growth) and the biological role (such as intracellular transport) of neuronal cell [Weingarten et al., 1975; Grundke-Iqbal et al., 1986; Mandelkow; Mandelkow, 2012]. But, when the tau protein dissociates from the microtubules, it destabilizes bridging connectivity within the cytoskeleton and potentially collapse the axonal region leading to obstruction of information flow within the neuron [Masliah; Terry, 1993]. Following this obstruction of communication dynamics and axonal transport within the cell, neuronal cell death and loses which is generally term, neurodegeneration arise [Terry et al., 1981; Kolarova et al., 2012]

Neuronal death has a rippling effect on the neighbouring cells because the aggregated deposit from the dead cells obstruct synaptic transmission to healthy neurons and subsequently lead to synaptic loses [Hof et al., 1990; Masliah; Terry, 1993]. And as intact synapses are a fundamental requirement for the physiological functioning of the neurons, a quantitative decrease in these structures (synapses) affect the neurons and result in massive pathological changes in the brain [Hof et al., 1990; Masliah et al., 1991]. An extensive review of tau protein in neurodegeneration is provided elsewhere [Buée et al., 2000; Avila et al., 2004; Spires-Jones et al., 2009; Kolarova et al., 2012; Arendt et al., 2016; Pîrşcoveanu et al., 2017].

1.2.   Epidemiology and socio-economic burden of Alzheimer's disease
In 1990, about 20.2 million people had dementia, however, this number increased to 43.3 million in 2015 with women recording the highest number [Nichols et al., 2019]. In 2016, 27.0 million women and 16.8 million men had dementia and currently dementia linked associated complication is the fifth leading cause of death, accounting 2.4 million death [Nichols et al., 2019]. And of these numbers, AD constitutes between 60% - 80% of all the

cases [Alzheimer's Association, 2019]. More so, a projection of approximately 131 million people are likely to suffer from the disease by 2050 worldwide [Homolak et al., 2018], a figure that is alarming.

The prognostic outcome after administering AD drugs (such as donepezil, galantamine, rivastigmine, memantine, neuronal IGF-1 or Docosahexaenoic acid) to individuals diagnosed of AD has resulted in unsatisfactory outcome [Tariot et al., 2009; Homolak et al., 2018], possibly because the disease is diagnosed at its advanced stage [Hogervorst et al., 2003]. Each year over 5 million cases of AD are reported globally [Bekris et al., 2010]. And until pragmatic efforts are made towards prevention, early diagnosis or treatment of the disease, AD will constitute an increasing heath care challenge globally. As of 2015 the care of about 35 million persons living with AD and other dementia was estimated to be around $600 billion [Marešová et al., 2015]. Besides, AD patients stay in hospital beds twice longer in a year than older person, and this affect other emergency service [Hurd et al., 2013].

Alzheimer's disease faces two major challenges; definite factors that trigger the disease which is unknown, and a lack of affordable diagnostic platform for early detection of the disease. This is particularly important because molecular and cellular aberrations occur long (almost 20 years) before the onset of detectable clinical symptoms [Lendon et al., 1997].

1.3.   Clinical diagnosis of Alzheimer's disease

The guideline for the diagnosis of AD was established 35 years ago [McKhann et al., 1984] however, this criterion has gone through series of revisions over the past years. Currently, the predictive diagnostic criteria for AD is based on neuropsychological evaluation test, neuroimaging and biochemical measures of cerebrospinal fluid (CSF) protein markers [McKhann et al., 2011; Arevalo-Rodriguez et al., 2015].

The neuropsychological test commonly employed include the Mini-Mental State Examination (MMSE) [Folstein et al., 1975] Montreal Cognitive Assessment (MoCA) [Nasreddine et al., 2005], Saint Louis University Mental Status (SLUMS) [Tariq et al., 2006] and Consortium to Establish Registry for Alzheimer's disease (CERAD) [Morris et al., 1989].

Magnetic resonance imaging (MRI), computed tomography (CT), [18]fluorodeoxyglucose

positron emission tomography (^{18}fPET), single-photon emission computed tomography (SPECT), Aβ positron emission tomography (Aβ-PET) and diffusion tensor imaging (DTI) are among the commonly used neuroimaging technique for the diagnosis of AD [Ferreira; Busatto, 2011]. The MRI visualizes general brain atrophy in the medial temporal lobe and white matter lesions [Whitwell et al., 2012], the CT identifies gross abnormality of the brain, and the DTI demonstrate loss of white matter integrity in the limbic and cortico-cortical tracts [Ferreira; Busatto, 2011]. Amyloid beta deposition in the brain can be identified by Aβ-PET [Rabinovici; Jagust, 2009], while possible regional brain hypoperfusion and hypometabolism can be demonstrated by SPECT and ^{18}fPET respectively [Cummings, 2012]. In recent times, the advent of tau-specific tracers for use with PET has enabled in vivo quantification of NFT, particularly tau deposition in the brain, and this diagnostic pathway is currently under clinical validation [Saint-Aubert et al., 2017; Okamura et al., 2018; Leuzy et al., 2019]. However, of all the neuroimaging techniques, Aβ-PET is the gold standard method for diagnosing AD [Morris et al., 2016].

The biochemical measurement of β-amyloid, total tau and phosphorylated tau proteins in the CSF are the current fluid-based diagnostic method for AD in clinical use [McKhann et al., 2011]. The rationale behind the measurement of CSF β-amyloid (either Aβ$_{40}$ or Aβ$_{42}$) stems from the fact that, in AD there is an aggregation and sequestration of amyloid protein to forming cerebral plaque. And because of this aggregation and accumulation of the amyloid in the brain, the CSF becomes deficient of the protein and hence less accessible for measurement [Pawlowski et al., 2017]. On the contrary, an increase in CSF tau protein concentration is an indication for positive predictive diagnosis for AD. This follows the assumption that, in AD, neurons rapidly expel the intracellularly accumulated toxic tau protein into CSF to relief the cell of stress and neuronal death. And this increases the tau protein content in the fluid. Hence, the CSF tau protein levels are directly proportional to the intensity of neuronal damage in the brain [Blennow et al., 2012; Pawlowski et al., 2017]. Altogether, an increase in CSF tau and decrease in β-amyloid protein level is considered as one of the useful indications for predicting probable AD.

1.4.   Challenges associated with the current diagnosis of AD

Despite the diagnostic value of the neuropsychological testing, neuroimaging or CSF biomarkers, definite diagnosis of AD requires histopathologic examination which can be performed at post-mortem and this does not benefit the patient. In addition to the fact that the available antemortem diagnostic methods only identify the disease in its advanced stage, the methods are challenged by several factors [Hogervorst et al., 2003; Nagasaka et al., 2005; Khan; Alkon, 2015]. For instance, the neuropsychological test which can be performed without sophisticated equipment is influenced by a person's education and race [Crum et al., 1993]. The neuroimaging techniques which can provide both qualitative (standardized) and quantitative evaluation of AD diagnostic markers is not only expensive but there are issues regarding what constitutes a positive test and the interpretation of positive result [Yang et al., 2012].

Again, the biochemical assay of CSF biomarkers which provide quantitative information on possible AD patients is characterised by some drawback. For instance, circadian rhythm as well as old age phenomenon (or old age-associated diseases) are potential factors that can influence the levels of CSF markers [Kang et al., 2009; Homolak et al., 2018]. Also, the predictive value of increased CSF tau level and deceased $A\beta_{1-42}$ for AD diagnosis is insufficient. This is because a decreased CSF tau and increased $A\beta_{1-42}$ has also been observed in control subjects [Motter et al., 1995; Gasparini et al., 1998] and raises further concern about the sensitivity and specificity of this diagnostic tools. Besides, the CSF markers are also involved in secondary inflammation [Akingbade et al., 2018], sampling for CSF involves lumber puncture, an invasive and uncomfortable technique.

To overcome these challenges associated with AD diagnosis, there is the need to explore other potential sources for AD biomarkers that can unambiguously predict the disease antemortem. Characteristically, such an ideal clinical biomarker should be indicative of damage, detect the disease before the onset of histopathological alteration and must be sensitive. Besides, such a marker should correlate significantly with the severity of damage, be analytically stable and measurable in the peripheral tissue such as blood and produce same result irrespective of the species. Fundamentally, such a possible diagnostic marker should have a known mechanism and able to localize damage [Robinson et al., 2008]. Several AD-linked biomarkers have been evaluated in peripheral tissue. These includes: the Aβ peptides (Aβ1–40, Aβ1–42), Tau proteins (total tau, p-tau-

181), Inflammatory proteins (C-reactive protein, antichymotrypsin, macroglobulin, interleukins, tumour necrosis factor, complement factors, homocysteine), metabolism (lipidomics & proteomics) and other (Clusterin, APOE) [Khan; Alkon, 2015]. The outcome has been interesting; for instance, although a decrease in β-amyloid has been observed in the blood of AD patients, subsequent studies were inconsistent [Irizarry, 2004; Khan; Alkon, 2015]. Similarly, a dysregulation in the signaling pathways as well as differences in the distribution of leucocytes has been observed in the blood of AD and mild cognitive impaired patients [Wyss-Coray, 2006; Ray et al., 2007; Khan; Alkon, 2015].

Recently, extracellular vesicles (ECVs) have come in focus in the field of biomarker research. Thus, ECVs have been found to be an important source of diagnostic biomarkers for cancers [Tai et al., 2018], human immunodeficiency virus disease [Patters; Kumar, 2018]. Similarly, there are growing concerns about the potential role of these ECVs in the diagnosis of AD.

1.5.   Extracellular vesicles

Extracellular vesicles (ECVs) are heterogeneous, lipid bilayer membrane-bound carriers [Maas et al., 2017]. Although these vesicles are referred to by several names such as exosomes, microvesicles (ectosomes), microparticles and oncosomes [Maas et al., 2017], they are broadly categorized as exosomes and microvesicles [van Niel et al., 2018]. The exosomes which are the smallest in terms of diameter, were discovered in 1983 by Pan and Johnstone in one research group [Pan; Johnstone, 1983], and Harding and Stahl in another research group [Harding; Stahl, 1983]. Microvesicles were also described by Tram and colleagues somewhere in the 20th century [Trams et al., 1981]. However, until now a major controversy exists regarding the definite distinction between exosomes and microvesicles [Słomka et al., 2018]. An extensive review of extracellular vesicles is available elsewhere [van Niel et al., 2018; Słomka et al., 2018]. Mindful of the considerable overlap between exosomes and microvesicles [Lai; Breakefield, 2012; Raposo; Stoorvogel, 2013], the term ECVs is adopted in this current research for clarity.

1.5.1. Formation of ECVs (ectosomes and exosomes)

Microvesicles (ectosomes) are formed by the outward budding of the plasma membrane into extracellular milieu [Lai; Breakefield, 2012]. On the contrary, the formation the smallest ECVs (the exosomes) are via a more complex pathway. The formation of exosomes starts when a receptor on the plasma membrane is internalized (invaginated) to form early endosome containing ubiquitinated cargo. In the cell, endosomal sorting complex required for transport (ESCRT) facilitate the maturation of the early endosome into late endosomes [Lai; Breakefield, 2012; Colombo et al., 2014]. Further inward budding of the late endosome results in a progressive accumulation of intraluminal vesicles to form a multivesicular body.

Following a regulation mechanism control by ESCRT, a multivesicular body has two fates; either it gets phagocytosed by lysosomes or exits the cell via the exocytic pathway [Colombo et al., 2014]. Possibly due to the composition of the intraluminal vesicles, a multivesicular body destiny for exocytic pathways is further regulated by both dependent and the independent (involving tetraspanins) activities of ESCRT [; Kanninen et al., 2016; Vogel et al., 2018]. But whichever pathway (dependent or independent of ESCRT) a multivesicular body adopts, it ultimately fuses with the plasma membrane (exocytic multivesicular body) and release its contents (intraluminal vesicles containing cargos) into the extracellular space as ECVs. And, since different pathways of ESCRT (such as the dependent and independent) are involved in the biogenesis of multivesicular bodies, a given cell may release several subpopulations of ECVs having varied composition [Bebelman et al., 2018]. The ECVs are found in several biological fluids such as blood, semen, urine, breast milk, ascites, cerebrospinal fluid, malignant pleural effusions, amniotic fluid, tears, saliva, mucus, lymph, and bronchial lavage [Simpson et al., 2008; Lakhal; Wood, 2011; Ibrahim; Marbán, 2016].

1.5.2. Size, density and composition of ECVs

Extracellular vesicles are characterized based on their size (diameter), density and composition [Kanninen et al., 2016]. The smallest category of ECVs is known to have a size range 30nm to 150nm [Théry et al., 2002; Muller et al., 2014; Zeringer et al., 2015;

Matsumoto et al., 2017], while the larger ones are between 100nm to 1000nm [Raposo; Stoorvogel, 2013; Słomka et al., 2018]. Typically, ECVs float at a buoyant density ranging from 1.08 to 1.22g/ml [Tauro et al., 2012; Muller et al., 2014; Colombo et al., 2014; Kalani et al., 2014; Pérez-González et al., 2017]. Based on their composition, ECVs contain several marker proteins which are either located on the surface or lumen of the vesicles. These markers include; tetraspanin proteins (CD9, CD63, CD81 and CD82), the heat shock protein (HSP70 and HSP90), the membrane trafficking protein (Rabs and Annexins). Others are; the proteins involve in multivesicular bodies biogenesis, the immune regulator molecules, the cytoskeletal, signal transduction proteins and metabolic enzymes [Frühbeis et al., 2012; Colombo et al., 2014; Jakobsen et al., 2015; Sastre et al., 2017; Li et al., 2017]. Most cells can release ECVs which contain repertoire of signatories from the parental cells [Kanninen et al., 2016]

Although several cells such as neural stem cell, neurons, oligodendrocytes, astrocytes and microglia cells can release ECVs, these cell-specific vesicles are distinguishable [Ghidoni et al., 2011; Lachenal et al., 2011; Vogel et al., 2018]. This is possible because cell specific ECVs contain unique marker proteins in addition to the general marker proteins that characterised the vesicles [Simons; Raposo, 2009]. For instance, ECVs release by neurons are uniquely characterized glycosylphosphotidylinositol anchored prion protein, GluR2/3 subunit of the AMPA receptor and Cell adhesion molecules L1/ CD171 [Fauré et al., 2006; Maness; Schachner, 2007; Chivet et al., 2012; Mustapic et al., 2017; Yoo et al., 2018]. Microglial cells' ECVs contain CD13 and monocarboxylate transporter, while, oligodendrocytes ECVs contain myelin proteins and associated lipids [Kanninen et al., 2016]. Therefore, the presence of these cell-specific markers has been helpful for the identification ECVs subpopulations.

1.5.3. Functions of central nervous system ECVs

Functionally, ECVs released from the CNS may dispose unwanted cellular materials or provide signalling information to other cells. The signalling information carried by ECVs may include proteins, RNA and lipids which can modulate the state of the recipient cell [Frühbeis et al., 2012]. Although ECV has emerged as a third (beside direct cell-cell

contact and transfer of secretory molecules) way for intercellular communication [Simons; Raposo, 2009], the role of these vesicles in the CNS is attracting major attention. For instance, astrocyte derived ECVs carries synapsin1, a protein capable of facilitating the survival of neurons during oxidative stress [Frühbeis et al., 2012]. Similarly, the cargo (miRNA) of neuronal derived ECVs can also activate the functions of glial cells which subsequently contribute to the clearing of Aβ deposition in the brain [Soria et al., 2017]. And, both neurons and microglia can take-up oligodendrocytes derived ECVs to mediate neuroprotection [Kanninen et al., 2016]. Neurons can internalize glia ECVs, utilize its content and subsequently releases more neuron ECVs [Frühbeis et al., 2012]. Therefore, Glia and neuron ECVs have been suggested to be responsible for inter-neuronal transfer of physiological information within the brain circuit [Chivet et al., 2012]. Non-coding RNAs, miRNAs, RNAs, lipids and proteins are among the major constituent molecules of ECVs [Lai; Breakefield, 2012; Kalani et al., 2014]. Therefore, the phenotypic state of these cargo molecules may mirror the nature of their originating cell [Kalluri, 2016]. ECVs have been proposed to represent a novel mode of intracellular communication which could lead to immunological responses and other cellular processes [Zhang et al., 2017]. For instance, ECVs secreted by B lymphocytes have the capacity to act as a vehicle to shuttle 'major histocompatibility complex' class II peptide between cells [Colombo et al., 2014].

Although ECVs have been suggested to participate in functional cellular processes, they have also been implicated in several pathological states including trans-synaptic transmission of pathogenic proteins [Lachenal et al., 2011]. The possible role of ECVs in pathological conditions is gaining concerns. Thus, it is emerging that ECVs can parade as vectors and facilitates the exchange of pathological proteins [Fauré et al., 2006]. The presence of tau protein inside ECVs [Polanco et al., 2016] and the ability of this vesicle to cross the blood brain barrier [Süssmuth et al., 2001; Lakhal; Wood, 2011] raises further suspicion about the potential role of ECVs in the propagation of PHF in AD.

1.6.   Tau protein, ECVs and peripheral blood
As the protein loses it functional properties and detaches from the microtubules in the axons it relocates into the neuronal cytoplasm. But because this abnormally modified tau

is toxic to the neurons [Alonso et al., 1997], the cell may expel this lethal protein in an enclose structure such as ECVs. This is possible because, the mechanism by which ECVs transfer functional proteins among neurons is suggested for how pathologic tau protein are also shuttled [Bartheld; Altick, 2011]. Thus, neurons release pathologic tau proteins into the extracellular space by activity dependent fashion to be taken up by other neuron [Bodea et al., 2016], a mechanism that can equally be employed by ECVs. Since ECVs and tau protein enter recipient neurons by endocytosis [Lu et al., 2007; Frühbeis et al., 2012; Michel et al., 2014] via ECVs mediated mechanism [Saman et al., 2012], the two (ECV and tau) may be closely linked. Hence, ECVs may provide as a vehicle that transport tau protein [Saman et al., 2012].

Previous studies have demonstrated that AD-like tau proteins are present in peripheral blood [Fiandaca et al., 2015; Abner et al., 2016; Winston et al., 2016; Guix et al., 2018]. But, since free floating tau proteins are susceptible to proteolytic degradation by thrombin [Arai et al., 2005], it is practical to suggest that, the protein is transported in an enwrapped medium. Enwrapping of tau protein may be an important process to shield it from truncation or degradation by thrombin. This is particularly important as tau can cross the blood brain barrier (BBB) [Lakhal; Wood, 2011], transverse cerebrospinal fluid into peripheral circulation [Weinstein; Seshadri, 2014], or shuttle among neuron, a process that an unwrapped protein may not survive it.

And as the formation and release of ECVs are ubiquitous and cell type-specific, neuron derived extracellular vesicles (ndECVs) may be the specific vesicles that transport this abnormal tau protein. Particularly, as it is known that ndECVs can cross the BBB into CSF [Süssmuth et al., 2001; Lakhal; Wood, 2011; Kanninen et al., 2016] and subsequently into the peripheral blood circulation [Weinstein; Seshadri, 2014].

Beside the fact that ndECVs contain signatories of their parental cell, such vesicles may also harbour useful information that reflects the state of the originating cells. Therefore, this study hypothesized that blood-based ndECVs could represent a reliable source for AD diagnostic marker, tau protein and further provide as a surrogative source for quantifying AD-linked tau protein using flow cytometry technique.

1.7. Aim of the study

The detection and quantification of tau protein in blood-based ndECVs has been reported [Guix et al., 2018], however, the significance of this proteins in the ECVs for diagnosis of AD remain largely unclear. Hence, this study aimed to quantify tau protein in blood-based ndECVs using flow cytometry technique and evaluate the significance of the measured proteins in the diagnosis of AD.

Flow cytometry is a reliable, simple and a sensitive analytical technique that uses light to either qualitatively or quantitatively profile biological particles such as cells or vesicles in suspension. Flow cytometry technique has been employed in several studies that were aimed to quantify biological molecules such as DNA [Hedley et al., 1983], apoptosis [Riccardi; Nicoletti, 2006], cell cycle [Pozarowski; Darzynkiewicz, 2004], haematopoietic cells [Lanier; Warner, 1981], and therefore it is appropriate to adopt the technique in this current study.

1.8. Objectives

As blood contains a mixture of ECVs from several cells, a research aimed at a cell type-specific vesicle should first concentrate, isolate, purify, characterize and verify the vesicles before quantifying the cargo proteins content in the vesicles. Therefore, this study set the following objectives:

(i)   Establish a protocol for the isolation and characterization of ECVs and ndECVs using western blot and flow cytometry technique

(ii)   Use the flow cytometry platform to quantify tau protein in the blood-based ndECVs of clinical patients who had already undergone the routine clinical diagnostic procedures (such as CSF tau, CSF p-tau, CSF β-amyloid or MMSE evaluation),

(iii)   Evaluate the significance of tau protein in the ndECVs as a potential biomarker for AD.

2.   METHODOLOGY

2.1.   Study design

This study employed both retrospective and prospective cross-sectional design and was performed from 2016 to 2019 at Paul Flechsig institute of brain research (PFI), Universität Leipzig, Leipzig, Germany. Blood samples from humans as well as *Mesocricetus auratus,* and cell cultured supernatant from human neuroblastoma cell line SH-SY5Y that has been transfected with cDNA for human tau protein were used.

2.2.   Ethical issues

This study was approved by Leipzig research ethical committee and had a reference number, 329/16-ek. Participants' identity remained anonymous to this study and only arbitrary numbers were assigned to the samples. Blood samples from *Mesocricetus auratus* (TVV 17/13) were provided by PD Dr.rer.nat. Max Holzer of Paul Flechsig Institute of Brain Research (PFI), Universität Leipzig, Leipzig, Germany. Human blood samples were obtained from colleagues at Paul Flechsig Institute of Brain Research and patients from Klinik für Psychiatrie der Universität Leipzig.

2.3.   Materials

Table 1: List of biological samples used

Samples type	Total number	source	purpose
Human (healthy young adult)	9	PFI	protocol establishment
Human (patient samples)	28	clinic	quantification of tau protein
Mesocricetus auratus	20	PFI	Positive control
SH-SY5Y cell	N/A	PFI	Positive control
Neuro-2A cells	N/A	PFI	Negative control (WB)

PFI - Paul Flechsig institute of brain research, WB - western blot, N/A – not applicable

Table 2: List of antibodies used for western blot analysis

Antibody (primary)	CatLog number	company	Dilution	country
Monoclonal mouse HSP70	L1813	Santa Cruz Biotechnology	1:2000	Germany
Polyclonal goat anti CD63	AB0047-200	SICGEN	1:3000	Germany
Polyclonal rabbit anti-CD9	L1214	Santa Cruz Biotechnology	1:3000	Germany
Polyclonal rabbit anti-human tau	A0024	Dako	1:4000	Germany
Antibody (secondary)				
Polyclonal rabbit anti-Mouse immunoglobulins HRP	P0260	Dako	1:10,000	Germany
Polyclonal rabbit anti-goat immunoglobulin HRP	P0449	Dako	1:10,000	Germany
Polyclonal goat anti-rabbit immunoglobins HRP	P0448	Dako	1:10,000	Germany

Table 3: List of antibodies used for flow cytometry

Antibody (primary)	CatLog number	company	Dilution with bead	ECVs volume
Mouse monoclonal anti-human CD171Biotin	Clone 5G3	eBiosciences	1:5	50µl
Mouse monoclonal anti-human CD9 (HBM-CD9-20)	140815	HansaBioMed Life sciences	1:200	100µl
Mouse monoclonal anti-CD63Biotin clone H5C6	B191782	BioLegend	1:5	5µl
ALEXA Fluor 488 (HBM-A488)	070915	HansaBioMed Life sciences	1:1000	N/A
Mouse monoclonal PE anti CD9 (clone HI9a)	312105	BioLegend	1:10	N/A

N/A – not applicable

Table 4: List of equipment including consumables

Equipment	CatLog number/ID	company	country
Abbe-refractometer	Modell G	Jena	Germany
Amersham™ Hydond™ PO.45 (PVDF)	10600023	GE Health Life Sciences	Germany
Blood test tube (S-monovette® 7.5ml)	7030411	SARSTEDT	Germany
Dnr Bio-Imaging System	MF-chemiBis 1.6	Biostep® GmbH	Germany
Eppendorf tube		Eppendorf	Germany
ELISA plate washer	hydrospeed	Tecan	Germany
Greiner bio-one	650180	CELLSTAR	Germany

Table 4 (continuation): List of equipment including consumables

Equipment	CatLog number/ID	company	country
Guava easyCyte^{TM}		M Millipore	USA
Heraeus multifuge X1R	rotor 75003658	Thermo Fisher Scientific	Germany
Electro-blotter 20 X 20cm (TV 400-EBK)	300017547	Biostep GmbH	Germany
Master cycler gradient		Eppendorf	Germany
Micro-ultracentrifuge (SORVALL MTX 150)	Rotor S52-ST, 2045	Thermo Fisher Scientific	Germany
Multichannel Finnpipette	C93910	Labsystems	Germany
PCR tubes (0.2ml)	G006-TUCA	Kisker Biotech	Germany
SIGMA laboratory centrifuge (3K30)	rotor 12154-H	Thermo Fisher Scientific	Germany
Rotating roller (RM5.40)	705977	Assistant	Germany
SETON open-top centrifuge tube (13 x 51mm)	32516	polyclear^{TM}	USA
SORVALL® COMBI PLUS	AH 629	Thermo Fisher Scientific	Germany
96 well Greiner plate	E14011AY (655061)	Greiner	Germany

Table 5: List of reagents

Reagent	CatLog number	company	Country
Acrylamide/Bis 37:7:1	10688.01	SERVA	Germany
Aldehyde/Sulfate Latex bead (4% w/v, 4μm) – 1.5μl	A37304	Thermo Fisher Scientific	Germany
Ammonium persulfate	9592.2	ROTH	Germany
Cyto-last™ buffer	B181625	Miltenyi Biotec	Germany
Dulbecco's Modified Eagles Medium	0685G,FG4815	Dulbecco	Germany
EXO-Prep	HBM-EXP-B5	Hansa BioMed Life Sciences	Estonia
exosome standard	06032	Hansa BioMed Life Sciences	Estonia
Fetal calf serum	BS255756	BIO & SELL	Germany
Glycine	3908.3	ROTH	Germany
Greiner bio-one (10cm dish)	E130702L	CellStar®	Germany
Gentamycin 50mg/ml (1000x)	BS. AB17.03.03100	BIO & SELL	Germany
HBM-SB sample buffer	091015	HansaBioMed Life Sciences	Estonia
Inside Fix	5140807265	Miltenyi Biotec	Germany
Inside Perm	5140807265	Miltenyi Biotec	Germany
JetPEI (polyethylenimine)	614201	Polysciences	Germany
Lumigen ECL utra solution A and B	TMA-100	Lumigen	USA
non-essential amino acid	K0293	M Biochrome GmbH,	Germany
Opti-MEM®	11058-021	gibco	UK
Protease inhibitor (2% cOmplete™ EDTA free)	4693132001	Roche	Germany
Sodium hydroxide (NaOH)	502790987	Praha Chemapol	Czechoslovakia
Streptavidin MagneSphere^R (1μm) – 5μl	Z5481	Promega	Germany
Tetramethylethylenediamine	2367.1	ROTH	Germany
Tris	4855.5	ROTH	Germany
Tween® 20	327259797	ROTH	Germany
BSA/ Albumin bovin Fraction V	170146	SERVA	Germany
VISIPAQUE™ 320	10328257	Amersham	Germany
triton x-100	37240	SERVA	Germany

Table 6: List of prepared consumables

10% SDS-PAG	SDS running buffer	10ml 4X SDS sample loading buffer
Separating gel	Tris base – 30.3g	2ml 1M TRIS HCl PH 6.8
Distilled water – 4.88ml	Glycine – 144.4g	0.8g SDS
1.5M tris-HCL, pH 8.8 – 3.0ml	SDS – 10g	4ml Glycerol
Acrylamide/Bis solution –4ml	1L of ddH$_2$O	400µl of 14.7M β-mercaptoethanol
10% SDS – 120µl		8mg bromophenol blue
10%APS – 100µl	**TBS**	
TEMED – 10µl	50mM Tris	
	150mM NaCl	**1% BSA sample buffer**
Stacking gel	DdH$_2$0	BSA – 1g
Distilled water – 4.41ml		PBS – 100ml
1.0M tris-HCL, pH 6.8 – 0.75ml		
Acrylamid SL – 0.78ml	**B/S-N blot buffer (10x, 1litre)**	
10% SDS – 60µl	48mM Tris	
10%APS – 60µl	38mM glycin	
TEMED – 6µl	distilled water	

Table 7: List of antibodies used for enzyme linked immunosorbent assay (ELISA)

Antibody	CatLog number	company	Final concentration	ECVs volume
Anti tau antibody clone 1G2 (non-phospho-epitope)	0714-02	AJ Roboscreen	4µg/ul	25µl
Anti-human tau antibody clone 7E5	07/17-02	AJ Roboscreen	0.16µl/ml	N/A
HAMAs blocking reagent (Mouse IgG)	57224	Jackson immune Research	1µg/ul	N/A
Tau lyophilized standard (10µl)	0118-01	AJ Roboscreen	N/A	N/A

N/A – not application

2.4. Methods

2.4.1. Blood sampling

Blood samples (from human and *Mesocricetus auratus*) was collected into heparin (for plasma) or heparin free (for serum) test tube (table 4) and centrifuge using Heraeus multifuge X1R (table 4) at 2500xg for 10minutes at 20°C to obtain plasma or serum respectively. The obtained plasma or serum was stored at -80°C until needed.

2.4.2. SH-SY5Y Cell culture processing

As a positive control, SH-SY5Y cells were obtained from the cell line bank of PFI and processed as described elsewhere [Park et al., 2015] but with major modification. Briefly, SH-SY5Y cells were cultured in Dulbecco's Modified Eagles Medium (DMEM) Ham´s F-12, 1:1 (table 5) which has been supplemented to 10% fetal calf serum (FCS), 1x non-essential amino acid and 1x Gentamycin (table 5). Subsequently, SH-SY5Y cells (4.9 x 10^{6}) were seeded in a Greiner bio-one 10cm dish (table 4) containing DMEM until a confluence of at least 80% was observed.

To avoid the potential contaminates from exogenous ECVs in DMEM containing FCS, the medium to be used to grow the transfected cells was ultracentrifuge at 100,000 x g for 18 hours using SORVALL® COMBI PLUS (table 4) with the aim of pelleting any vesicle that may be present. The supernatant collected was considered as ECV-free medium. Seeded SH-SY5Y cells in ECV-free medium were transfected with cDNA (1µg/µl, self-prepared) for human tau protein. Prior to the transfection, the cDNA was re-suspended in a mixture of JetPEI and Opti-MEM® (table 5). The transfected cells were incubated at 37°C with CO_2 for 48hours. The cell supernatant (40ml) containing the released ECVs was harvested and pre-cleaned. Cell lysate from the SH-SY5Y cell as well as a 48-hour seeded neuro-2A cells lysate were included as positive and negative controls respectively where necessary.

2.4.3. Isolation of ECVs

2.4.3.1.   Pre-cleaning of serum, plasma and cultured supernatant

To get rid of dead cells, cells and other contaminants samples were subjected to increasing sequential centrifugation, starting with 300xg for 10 minutes, followed by 3000xg for 10 minutes and then finally 10,000xg for 30 minutes. All the centrifugations were performed using SIGMA laboratory centrifuge (table 4) at a temperature of 4°C.

2.4.3.2.   Precipitation of ECVs

The procedure for exosome isolation from serum or plasma outlined in the HansaBioMed, EXO-Prep (One step Exosome isolation Reagent) datasheet was followed. Regarding the suggested volumes, 100µl of plasma and 250µl of serum were used. All reagents used for this experiment were all enclosed in the obtained HansaBioMed EXO-Prep kit.

2.4.3.3.   Pelleting of ECVs

To pellet ECVs, serum or plasma was aliquoted into a 13 x 51mm SETON open-top centrifuge tube (table 4) and the tube was filled to ¾ with 10% Dulbecco's phosphate buffered saline (PBS). The PBS was added to the serum to reduce viscosity and to prevent possible collapse of the tube during ultracentrifugation. The ECVs were pelleted and washed at 100,000xg for 2 hours at a temperature of 4°C using micro-ultracentrifuge (table 4). The pelleted ECVs were resuspended in 1/10th the starting material of PBS.

2.4.3.4.   Density gradient ultracentrifugation and fractionation

To prepare density gradient, the method described by Lane and colleagues [Lane et al., 2017] was modified and adopted. Here, iodixanol (VISIPAQUE^{TM} 320) or sucrose density gradient was prepared. A discontinuous iodixanol (VISIPAQUE^{TM} 320) gradient with concentrations 40% (w/v), 30% (w/v), 20% (w/v), 10% (w/v) and 5% (w/v) was self-prepared from a stock solution (62.5% w/v) of VISIPAQUE^{TM} 320 (table 5) and PBS. Similarly, a discontinuous sucrose gradient with 5 different concentrations; 2.4M, 2.0M, 1.5M, 1.0M and 0.5M was also self-prepared from a sucrose stock solution (2.5M) and

PBS. The gradients were formed by overlaying 920µl of each of the iodixanol or sucrose concentrations in 13 x 51mm SETON open-top centrifuge tube polyclear^{TM} (table 4) starting with the highest concentration at the bottom and sequentially to the lowest at the top. Pelleted ECVs were carefully overlaid on top of the lowest concentration and allow to sediment into the iodixanol or sucrose by ultracentrifugation at a speed of 100,000xg for 18 hours at 4°C using micro-ultracentrifuge (table 4). Twenty-four (24) fractions each approximately 195µl were collected in decreasing order of concentration with a self-assembled fractionator (Figure 2-1) into a sterile round bottom 96-well Greiner bio-one plate (table 4). The procedure is summarised in the flow chart of figure 2-1.
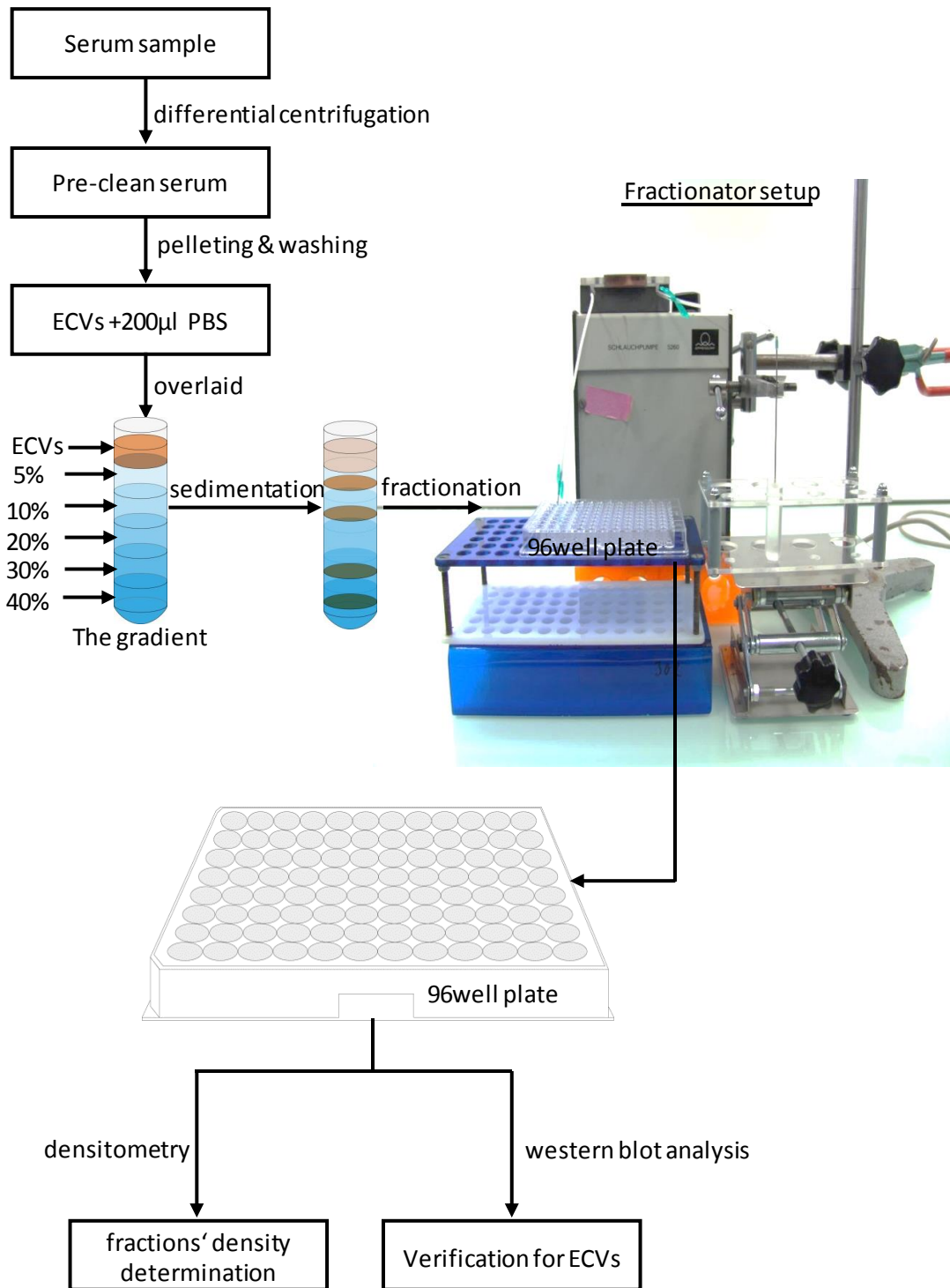
Figure 2-1: A flow chart showing the sequential process as well the fractionator setup for the purification of ECVs.

2.4.3.5. Bead-assisted technique

Flow cytometric analysis can be the simplest and most sensitive technique for detecting ECVs [Zhu et al., 2014]. But, as the modern flow cytometers were designed to study cells, particles with size less than that of cells are difficult to be a resolved by the scattering light using the conventional flow cytometers [Steen, 2004; van der Pol et al., 2012; Morales-Kastresana; Jones, 2017]. The basic principle in flow cytometer is its ability to measure scattered light in either forward or sideward direction at an angle following a passage of a cell or particle through a laser beam. Typically, the limit of ungated scattering light in the commercial flow cytometers is around 300nm – 500nm [Steen, 2004]. And as ECVs have varied sizes, vesicles less than 300nm has the tendency of not scattering forward light and this may affect the acquisition of forward scattering light and lead to interpretation issues. To overcome this challenge, a suitable bead can be coated with the ECVs. Coupling of ECVs onto beads increases their size and makes them discernible enough to be reliably resolved in the flow cytometer [Morales-Kastresana; Jones, 2017]. In addition to the fact that the beads increase the size of the ECVs, it also concentrates these vesicles and improves the outcome of the forward scattering light. Based on this background information, the bead-assisted (specific) technique for the isolation of ECVs was exploited. In this technique, beads interact with specific antibodies to generate high affinity binding, bead-antibody complex. The complex is then used to capture the ECVs via specific antigens on the vesicles.

The bead-assisted techniques for isolating ECVs or ndECVs as described [Oksvold et al., 2015; Park et al., 2015; Pedersen et al., 2017] was modified for this study. Briefly, Streptavidin MagneSphere[R] beads (table 5) were washed and resuspended in 0.1% BSA sample buffer in an Eppendorf tube. Into the washed magnetic beads, the primary antibody, CD63Biotin or CD171Biotin (table 3) was added and incubated for 30 minutes at room temperature on a rotating roller (table 4). Unbound antibodies were washed off by placing the tube on a magnetic stand and pipetting off the clear supernatant. The remaining magnetic bead-antibody complex was resuspended in 0.1% BSA sample buffer and pelleted ECVs added. The entire mixture was incubated overnight (18hours) at $4^{o}C$ with gentle agitation. Either the captured ECVs on the bead or the uncaptured ECVs in the suspension were collected separately and named as ECVs or non-ndECVs respectively; or

ndECVs (CD171$^+$) or non-ndECVs (CD171$^-$) respectively. To prevent potential degradation of proteins by proteases, protease inhibitor cocktail (table 5) was added to each sample that was to undergo further downstream analysis.

An ideal volume of beads for a given test was determined to be 5µl (2.36x10^{5}particles/µl). This suitable volume was obtained after several test-trials (not shown here) and it was also found to be suitable for measuring by flow cytometer.

2.4.4. Detection, characterization and quantification of ECVs and the cargo tau protein

2.4.4.1. Western blot analysis

The Laemmli's principle [Laemmli, 1970] of using sodium dodecyl sulphate (SDS) as detergent for electrophoretic separation of small proteins in polyacrylamide gel (PAG) was adopted in this study as well as the procedure for performing western blot outlined earlier [Mahmood; Yang, 2012] was modified and adopted. Here, into PCR tubes (table 4), 3 parts of the isolated ECVs was added to 1 part of 4X SDS sample buffer (table 6). The mixture was heated at 95°C for 5 minutes using master cycler gradient (table 4) to heat denatures the ECVs. Equal volumes (20µl) of the ECVs lysate were loaded into each lane of a self-prepared 10% SDS-PAG (table 6) and electrophoresed at a constant 170V for about an hour in SDS running buffer (table 6). The separated proteins were subsequently electro-transferred at 26V onto polyvinylidene difluoride (PVDF) membrane (Table 4) in Bjerrum Schafer- Nielsen (B/S-N) transfer buffer (table 6) overnight at 4°C using electro-blotter tank device (table 4). The membrane was washed in Tris-buffered saline (TBS) and blocked in 1% bovine serum albumin (BSA) fraction V (table 5) in TBS containing 0.01% Tween$^®$ 20 (table 5) for 1 hour at room temperature. The PVDF membrane was stained with primary antibody (table 2) and incubated overnight at 4°C with gentle shaking. The PVDF membrane was washed in TBS containing 0.01% Tween$^®$ 20 to remove any unbound primary antibody and was subsequently stained with the detection (secondary) antibody (table 2) for 2 hours at room temperature. The membrane was developed with enhanced chemiluminescent (ECL) reagents, Lumigen ECL utra solution A and B (table 5) and visualized using "Dnr Bio-Imaging System" (table 4).

2.4.4.2.   Determination of the density of the isolated ECVs

To determine the buoyant density of the isolated ECVs, the densitometry technique described by Théry and colleagues [Théry et al., 2006] was modified and adopted. Here, the refractive indices of the entire fractionated fractions (1- 24) obtained earlier (2.4.2.4) were measured using Abbe-refractometer (Modell G, Jena, Germany). Fractions that show positive reaction for the ECVs markers proteins were noted and their respective densities determined.

2.4.4.3.   Detection of ECVs using flow cytometry technique

The ECVs were pelleted by ultracentrifugation as described earlier (2.4.3.3). Beads were coated with antibodies (table3) directed against ECVs' generic marker protein CD63 or cell type-specific marker protein CD171 as described (2.4.3.5). Coupled beads-antibody complex were used to capture and concentrate the pelleted ECVs. The captured ECVs on the beads were subsequently detected by a second antibody that has been conjugated with the fluorophore, phycoerythrin (PE, table 3). As negative control, 1% BSA in PBS was added to immunomagnetic bead instead of isolated ECVs. All dilutions and resuspension were made in 1% BSA sample buffer (table 6)

Data on the detected ECVs was acquired in the flow cytometer, guava easyCyte^{TM} (table 4) and analyzed using the Flowjo version 10. The qualitative mean intensity of the detection antibody is shown by both histogram and bar chart. The entire procedure is summarized in figure 2-2.
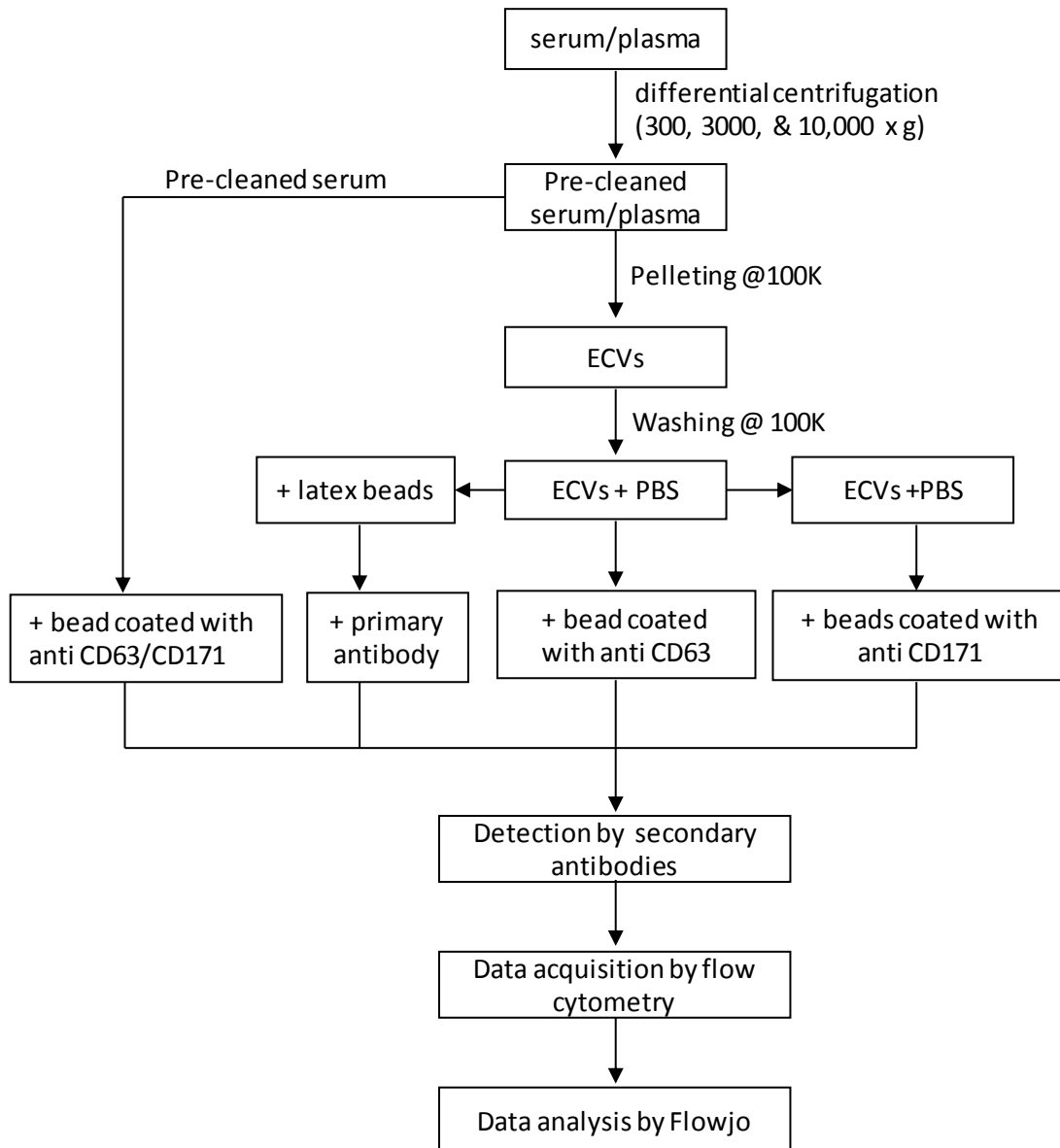
Figure 2-2: A flow chart showing the sequential approach used in the isolation, detection and verification of ECVs from serum or plasma using bead-assisted technique. **PBS** represent phosphate buffered saline, 100k represent the 100,000xg, the speed at which ultracentrifugation was performed.

2.4.4.4.   ECVs' cargo protein detection using flow cytometry

The procedure outline in Miltenyi Biotec datasheet (Inside Stain Kit) for "Intracellular staining of eukaryotic cells", specifically, the protocol for solid phase intracellular staining for flow cytometric analysis was followed but with slight modification. Briefly, serum sample was obtained (2.4.1) from young healthy donor, pre-cleaned (2.4.3.1) and ECVs pelleted by ultracentrifugation as described earlier (2.4.3.3). Beads were coupled with

antibody directed against ECV generic marker protein CD63 or cell type specific marker protein CD171 as described by the bead assisted technique (2.4.3.5). The beads that have been coupled to the antibodies were used to capture the pelleted ECVs as described earlier (2.4.3.5). Captured ECVs on the beads were resuspended in 50µl of cyto-last buffer (table 5). Subsequently, 50µl of Inside Fix (table 5) was added, mixed well and incubated at room temperature for 20 minutes. The fixed ECVs on the beads were permeabilised and stained with a cocktail containing 4µl of anti HSP70-PE diluted in 36µl (such as 1:9) of Inside perm (table 5). Following incubation (10 minutes), the stained cargo in the pellet was resuspended in Inside perm (100µl). As a negative control, an irrelevant coupled antibody (isotype control) that has been conjugated to the fluorophore, PE was diluted in the Inside perm and incubated along with the experiment. Two positive controls were included, pelleted ECVs from SH-SY5Y cells suspension and SH-SY5Y cells. Data was acquired by the flow cytometer (2.4.4.3).

2.4.4.5. Enzyme linked immunosorbent assay (ELISA) analysis technique

To make tau protein in the vesicles accessible for ELISA quantification analysis, the pelleted ndECVs (CD171$^+$) and non-ndECVs (CD171$^-$) were lysed with 1% Triton-100 (table 5) as described [Osteikoetxea et al., 2015] was modified and adopted. Briefly, into 1ml Eppendorf tube, 45µl of CD171$^+$ or CD171$^-$ ECVs were aliquoted into with 5ul of Triton-100 added and incubated on ice for at least 5 minutes. Subsequently, 450µl of PBS was added to reduce the concentration of the Triton solution in the sample. Also, the dilution of the lysis buffer was necessary to avoid possible interference with the subsequent ELISA analysis. Potential cross reactivity and nonspecific binding sites in the samples were blocked with 1µg/µl anti human anti-mouse antibodies (anti-HAMAs) (table 3). Of the processed sample, 25µl was aliquoted for the subsequent downstream enzyme linked immunosorbent assay (ELISA) analysis.

A 96 well mircoplate (table 4) was coated with 50µl each of 0.1M carbonate buffer (PH 9.7) containing 4µg/ul antibody 1G2 (table 3) and incubated overnight (16 hours) on gentle a shaker at 4°C. The incubated plate was washed 6 times with 10mM TBS containing 0.05% tween 20 (TBS-T20) using ELISA plate washer (table 4). Nonspecific

binding sites on the coated antibodies were blocked with 150µl of 1% BSA sample buffer (table 6) in TBS-T20 containing 1µg/µl HAMAs for at least 1 hour. The detection antibody-mix was prepared by diluting one part of antibody 7E5-HRP (3µg/µl, table 3) in 6000 part of 0.1M carbonate of P^H 9.7 containing 3% BSA and 0.05% Tween 20. Twelve (12) multichannel Finnpipette (table 4) was used to aliquot 25ul of the detection antibody mix into the 96 well, and 25ul of the prepared human samples (serum, supernatant, $CD171^+$ ECVs or $CD171^-$ ECVs) were added. Tau lyophilized standard (table 3) was used to prepare different concentrations in 1% TBS-T20 containing 0.01µg/µl HAMAs and was used to draw the standard curve. A summary of the entire process is presented in figure 2-3.
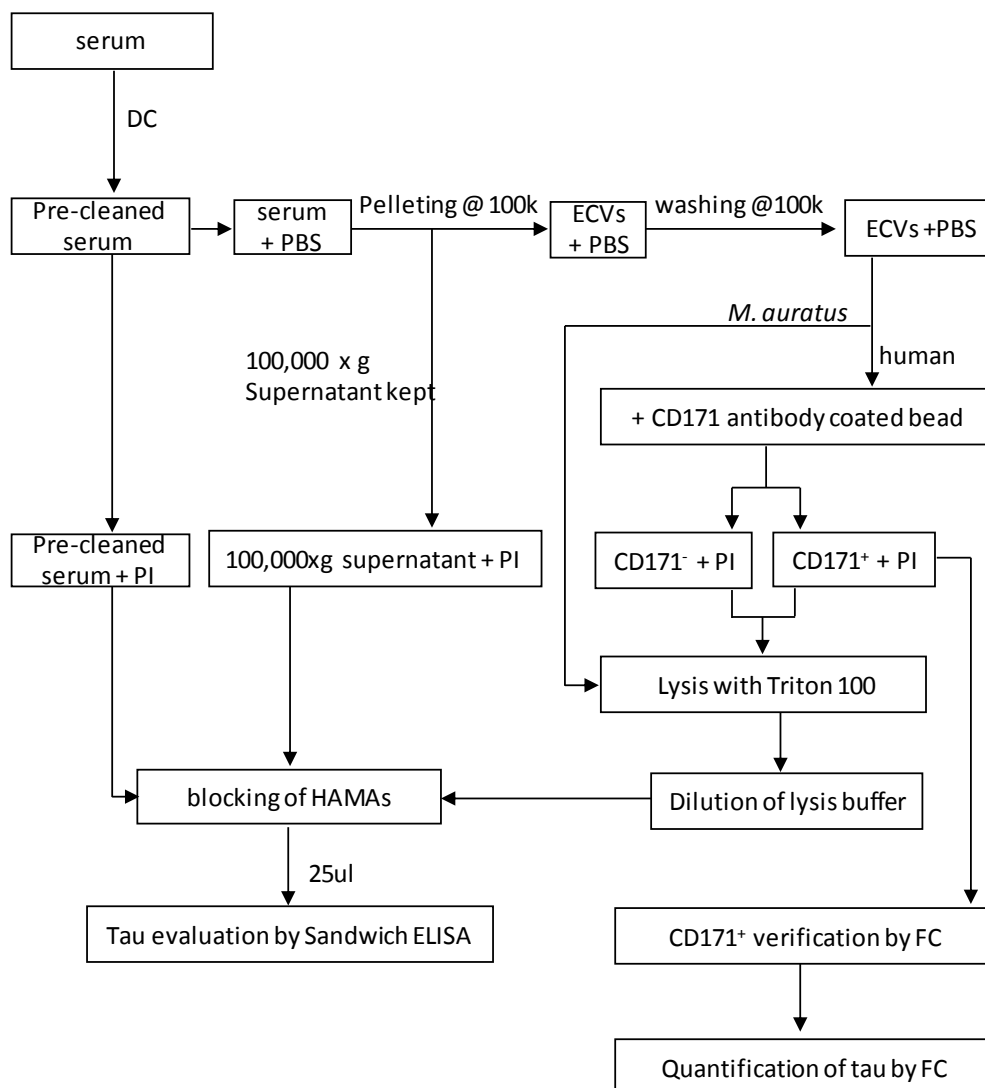
Figure 2-3: A flow chart summarizing the procedure prior to ELISA and flow cytometry (**FC**) analysis. The **PI** represent protease inhibitor while the **HAMAs** represent a blocker of human anti-mouse antibodies, **DC** represent differential centrifugation.

Two positive controls were included in this experiment to provide as a proof that tau protein was measurable in the vesicles. The first being SH-SY5Y cells that have been transfected with cDNA for human tau protein (2.4.2). While the second was blood samples from *Mesocricetus auratus* hibernators that were in the torpid state (5 - 10°C). For negative control, 1% BSA sample buffer containing 2% protease inhibitor and 1µg/ml mouse IgG was included.

2.5.   Statistical analysis

To show whether tau protein was measurable in serum, ndECVs (CD171$^+$) or non-ndECVs (CD171$^-$), scatter plot (GraphPad prism 8.1.0) was used to demonstrate the frequency of the measured concentration. To compare the means of tau protein concentration serum to that of CSF, unpaired student t-test (GraphPad prism 8.1.0) was performed to determine the significant difference between them. Subsequently, Pearson correlation coefficient (GraphPad prism 8.1.0) was used to determine possible relationship between tau protein in the ndECVs or serum and four validated markers of AD (CSF-tau, CSF-ptau, CSF-Aß and MMSE). Finally, unpaired t-test was used to evaluate tau protein from the serum of hamsters (positive control).

3.   RESULTS

3.1.   Establishment of protocol for the isolation and characterisation of ECVs

The result is broadly presented into two (2) parts. The first part (3.1) presents series of analysis performed with the aim to establish a valid protocol for the isolation and characterisation of ECVs. Having established a reproducible protocol for the isolation and characterisation of the vesicle, the next part (3.2) is focused on detection and quantification of cargo proteins in the isolated ECVs.

3.1.1.   Precipitation versus ultracentrifugation techniques of isolating ECVs

The use of precipitation technique for the isolation of ECVs is common however, majority of studies using this technique are often interested in the evaluation of the RNAs content of the ECVs [Li et al., 2014; Prendergast et al., 2018; Patel et al., 2019]. Hence possible contaminant from protein aggregate was not considered an issue. Since this study was focused towards quantification of tau proteins in the ECVs there was the need to identify a suitable technique that will not introduce protein contaminates. Therefore, the precipitation technique of isolating ECVs was compared to the ultracentrifugation technique.

Here, ECVs that have been isolated by either precipitation (2.4.3.2) or ultracentrifugation techniques (2.4.3.3) were verified using western blot analysis (2.4.4.1). Precipitated ECVs' proteins were electro-transferred onto membrane A (Figure 3-1A) while ultracentrifuge pelleted ECVs' proteins onto membrane B (Figure 3-1B), and both membranes stained with ECVs' marker protein HSP70 and detected by anti-mouse immunoglobulins HRP. As HSP70 is one of the cytosolic protein markers for ECVs, a positive reaction in any of the preparation (precipitation or ultracentrifugation) suggests that the ECVs are present. Also, the HSP70 protein has a molecular weight of 70kDa, and therefore a migration to this region is suggestive of a positive reaction. From the results shown (Figure 3-1A & 3-1B), no obvious positive reaction for HSP70 was detected in the precipitated sample (either serum or plasma). On the contrary, an obvious positive reaction for HSP70 was detected in the ultracentrifuge sample (plasma and serum). Also, included on the membrane B

(Figure 3-1B right) is a serum sample that underwent only pre-cleaned (Pc) process (2.4.3.1), and like the precipitation method, ECVs' marker protein HSP70 was not detected. SH-SY5Y cells lysate was included to provide a positive control.
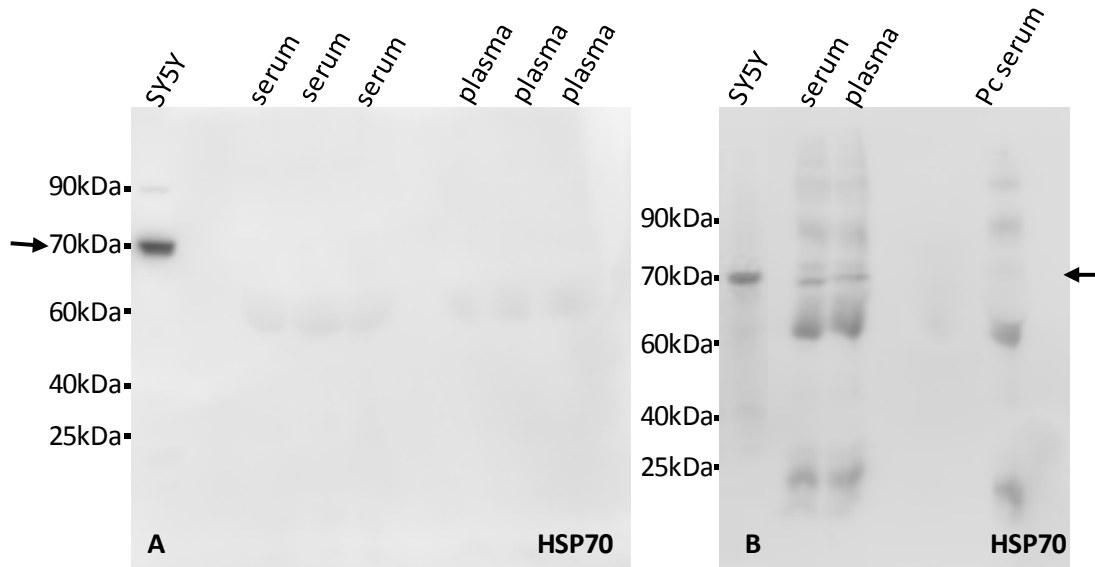
Figure 3-1: Western blot analysis result of HSP70 ECVs. Precipitated ECVs (membrane **A**) shows no detectable reactivity for HSP70 (70kDa). Membrane **B (left,** plasma & serum) ultracentrifuge ECVs shows detectable reactivity for HSP70 (70kDa). Membrane **B (right**), pre-cleaned ECVs shows no detectable reactivity for HSP70 (70kDa). "**Pc**" represents pre-cleaned. The arrows point to the region where the ECVs' marker protein, HSP70 reactivity is expected.

3.1.2. Purification of ECVs using iodixanol or sucrose density gradient

Generally, either iodixanol or sucrose density gradient is used to purify ECVs; however, this study wanted to identify which of these two is ideal. To achieve this, a serum sample that has been pre-cleaned (2.4.3.1) and ECVs pelleted by ultracentrifugation (2.4.3.3). Pelleted ECVs were sedimented through either iodixanol or sucrose gradient (2.4.3.4) was compared. Sedimented ECVs were subjected to western blot analysis (2.4.4.1). The ECVs' proteins on the membrane were stained with the primary antibody directed against the protein HSP70 and detected by a second antibody, anti-mouse immunoglobulins that have been conjugated to horseradish peroxidase (HRP). As shown in the result (Figure 3-2), a positive reactivity at 70kDa as well as sharp bands (fraction 5 – 9) are observed in the iodixanol gradient prepared samples compared to that of sucrose gradient preparation. Since HSP70 has molecular weight of 70kDa, the observed reactivity at 70kDa region of

iodixanol gradient is considered HSP70 containing ECVs. From the result, it is observed that purification of ECVs by iodixanol density gradient produce appropriate outcome compared to sucrose gradient. Therefore, the iodixanol gradient was used in subsequent analysis where purification of ECVs was needed.
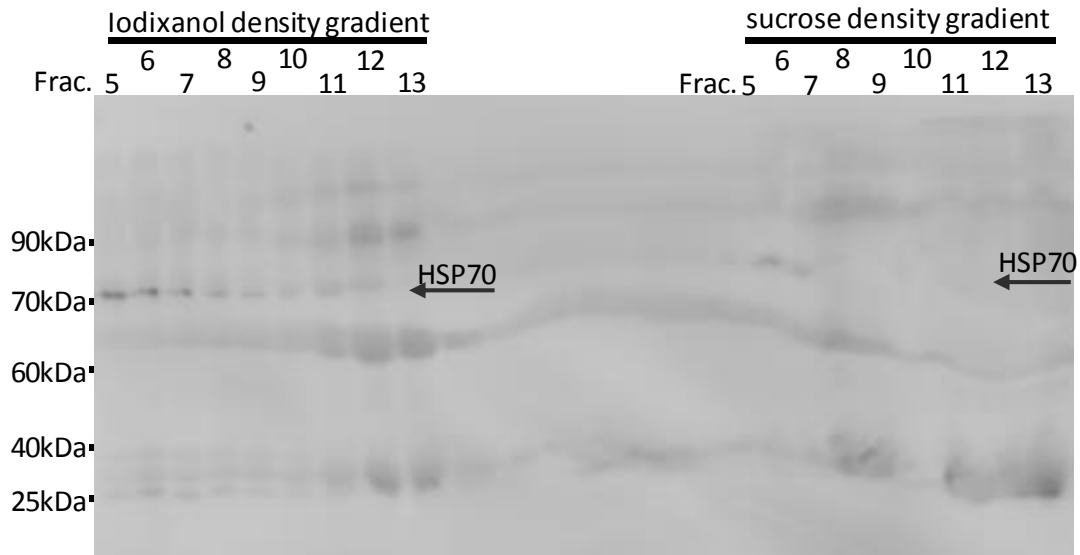
Figure 3-2: Western blot analysis of purification of ECVs by iodixanol (left) and sucrose (right) density gradient. An obvious positive reactivity for HSP70 (70kDa) is seen in the iodixanol purified ECVs (**left**). The ECVs purified by sucrose gradient (right) could not demonstrate sharp or positive reactivity for HSP70 (70kDa). The arrows point to the region where the ECVs' marker protein HSP70 reactivity is expected. "**Frac**." represent fractions.

3.1.3. Demonstration of other marker proteins of ECVs

Since at least one cytosolic and one transmembrane protein are required to be demonstrated in a vesicular structure to be considered as ECVs, this study simultaneously verified for the presence HSP70, CD9 and CD63 proteins in the same processed serum. These marker proteins were considered because they the abundant tetraspanin (CD9 and CD63) or cargo (HSP70) protein of ECVs. Here, serum was obtained from a single donor, pre-cleaned (2.4.3.1), pelleted by ultracentrifugation (2.4.3.3), and purified by iodixanol gradient (2.4.3.4). The obtained vesicles were subsequently processed by western blot technique (2.4.4.1). Electro-transferred ECVs protein on the PVDF membrane were stained with primary antibody directed against the tetraspanin protein CD9 (Figure 3-3A), CD63 (Figure 3-3B) or the cargo protein HSP70 (Figure 3-3C). For detection, anti CD9, anti CD63 and anti HSP70 stained membrane were respectively stained with second antibodies, anti-rabbit immunoglobins HRP, anti-goat immunoglobulin HRP and anti-

mouse immunoglobulins HRP were used to stain the CD9. The molecular weight of the protein CD9 is about 25kDa, CD63 is between 35 – 65kDa, and HSP70 is 70kDa. As shown in figure 3-3 the isolates showed positive reaction at 25kDa (A), 35 – 65kDa (B), and 70kDa (C) for ECVs' protein CD9, CD63, and HSP70 respectively. This suggests that, the pelleted and purified vesicles contained ECVs which settle within iodixanol fractions numbered 5 – 10. Included in this experiment are SH-SY5Ycell lysate (positive control) and neuro-2A cell lysate (negative control) stained with anti-CD63 (D). The smear appearance shown in the membrane stained with CD63 is due to glycosylation.
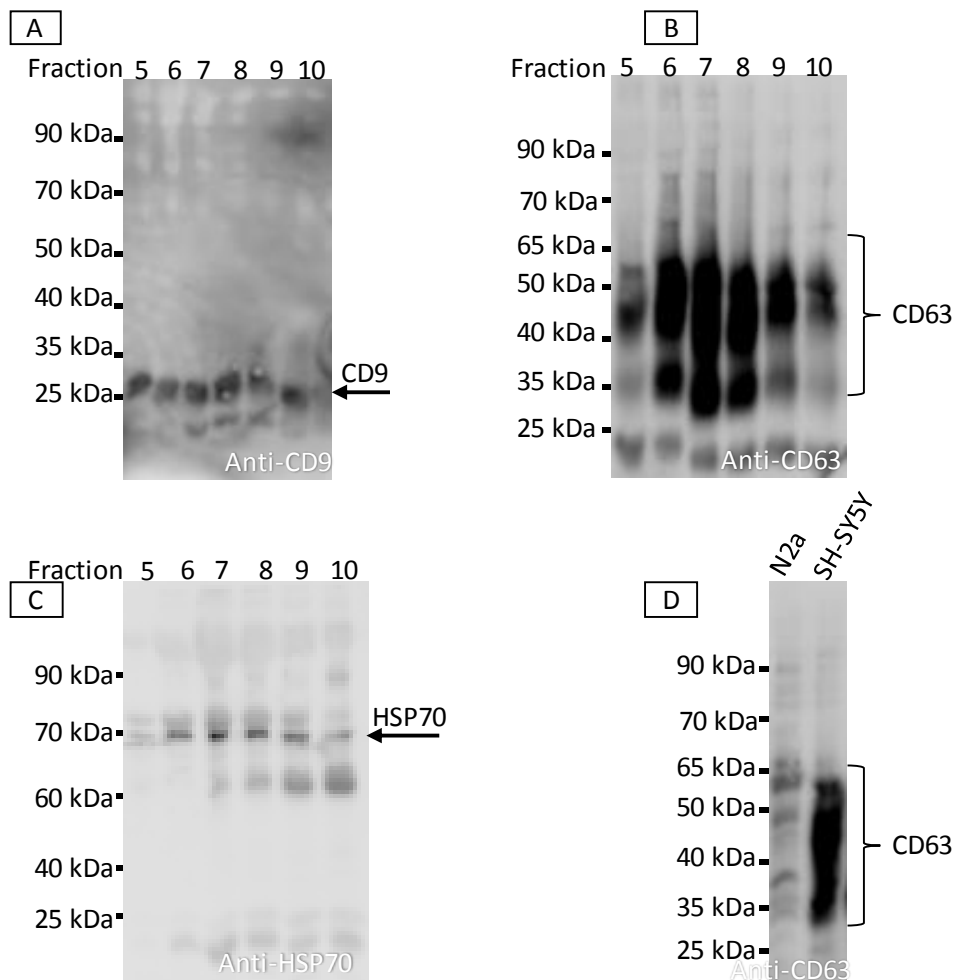
Figure 3-3: Western blot analysis showing 3 marker proteins of ECVs. Membrane **A** was stained with anti-CD9, **B** anti-CD63, and **C** HSP70. Obvious positive reactivity is seen at 25kDa (CD9) region (**A**), 65 – 35kDa (CD63) region (**B**) and 70kDa CD63 region (**C**), The control (**D**) was stained with anti-CD63. The arrows point to the region where the ECVs' marker protein reactivity is expected. The smear seen in the CD63 stained membrane is due to glycosylation.

3.1.4. Analysis of reproducibility

Having isolated and purified ECVs from a single donor, the study proceeds to find out if the procedure could be reproduced. To achieved this, serum samples were obtained from 3 healthy young donors and process as described earlier (2.4.3.1, 2.4.3.3, & 2.4.3.4). Following the fractionation of the iodixanol gradient containing the ECVs, fractions numbered 4 to 10 were selected for each donor and subjected to western blot analysis. Membrane containing ECVs' proteins were stained with a primary antibody directed against the protein HSP70 and detected by a second antibody, anti-mouse immunoglobulins HRP. An obvious positive reactivity was observed consistently in the iodixanol fractions 4 to 10 for all the 3 donors (Figure 3-4). While the obtained result demonstrates that the samples contained ECVs, it also shows that the procedure used was reproducible. Also shown on the membrane (Figure 3-4) an SH-SY5Y cell lysate served as positive control.
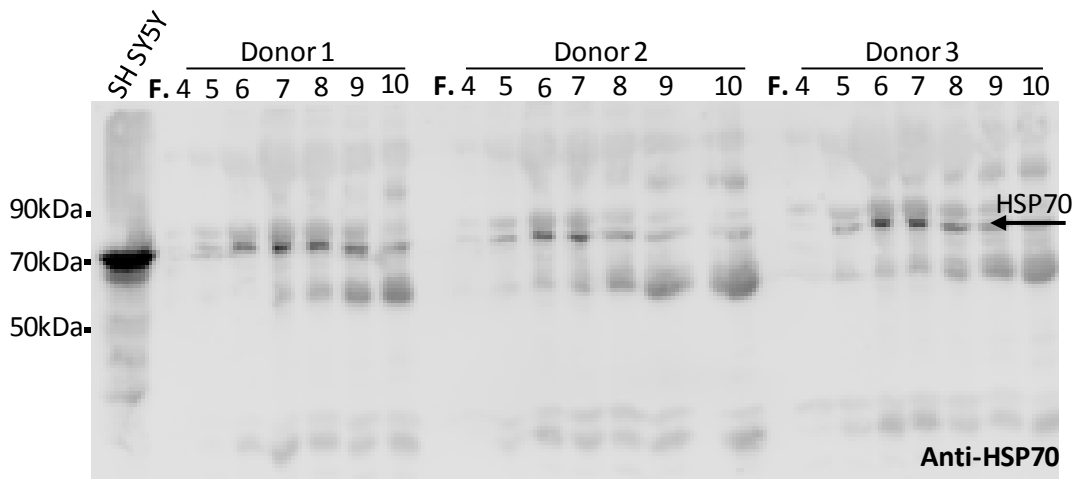
Figure 3-4: Western blot analysis of ECVs' marker protein HSP70 in the serum of 3 young healthy donors. The ECVs were purified by iodixanol density gradient. An obvious positive reactivity is shown in fraction 4 to 10 for all donors. The arrow points to the region where ECVs' marker protein HSP70 reactivity is expected. The '**F**' represents Fractions.

3.1.5. ECVs' density determination

Having observed that the procedure for the isolation and verification of ECVs was reproduceable, and that, the ECVs constantly settled in the same fractions, the study proceeds to determine the densities of these iodixanol fractions. Here, all the refractive indices of the 24 fractions (2.4.3.4) were measured and their respective densities plotted (Figure 3-5). Since the verified vesicles settled within fraction 4 and 13 which have densities 1.196g/ml and 1.079g/ml respectively, the isolated ECVs were assumed to have same buoyant density. The recorded density range for the isolated ECVs in this current study falls within the previously reported density range of 1.22 g/ml to 1.08 g/ml [Théry et al., 2006; Tauro et al., 2012; Muller et al., 2014; Pérez-González et al., 2017]
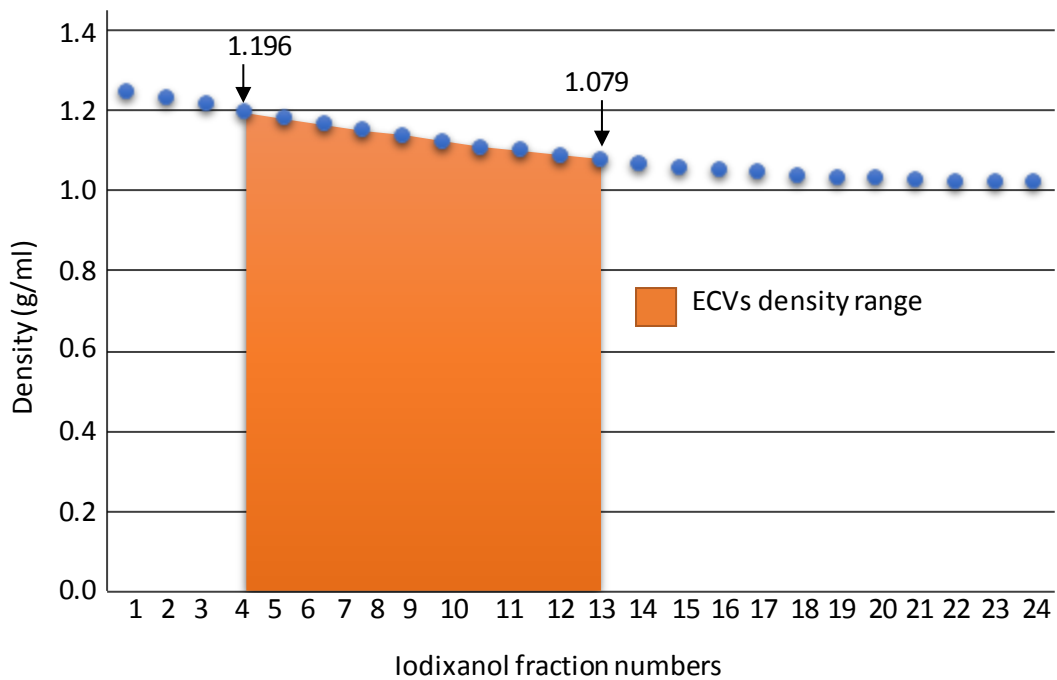
Figure 3-5: A graph showing the density range where ECVs settle in iodixanol gradient.

3.1.5.1.   Immunomagnetic isolation of ECVs

To be able to address isolated vesicles to their parental cells, there is the need to adopt a strategy that can define a subpopulation of the ECVs. The bead-assisted technique can be used to isolate and concentrate ECVs in general or cell type specific ECVs. Before attempting to isolate cell type specific ECVs using this strategy, it is important to first use the technique to isolate ECVs in general. Therefore, beads were coated with antibodies directed against ECVs' generic marker protein CD63 using the bead-assisted technique (2.4.3.5). The CD63-antibody coupled beads were used to capture the pelleted ECVs (from 2ml serum). The serum was obtained from a young healthy donor (donor 1) and pre-cleaned (2.4.3.1) before pelleting by ultracentrifugation.

The captured ECVs on the beads were detected by a second independent antibody directed against the tetraspanin CD9. This second antibody (CD9) has been conjugated with the fluorophore, phycoerythrin (PE). The tetraspanin proteins, CD9 and CD63 are both generic marker proteins of ECVs. Therefore, a positive signal for CD9 suggests a successful isolation of ECVs, and as CD63 was used to capture the vesicles, further confirms the sensitivity of the isolation process. Data on the detected ECVs was acquired by flow cytometry (2.4.4.3). As a negative control, 0.1% BSA in PBS was substituted for the ECVs. The flow cytometry verification result for the detected ECVs is shown in figure 3-6. An increased CD9 reactivity (positive signal) is observed for the pelleted ECV (Figure 3-6A). The quantitative mean intensity of the measured CD9-PE in the pelleted ECVs is higher than that of negative control (Figure 3-6B). As a positive signal is observed for the ECVs' marker protein CD9, further confirms that the isolate also contain CD63 marker protein, hence the protocol was considered appropriate for ECVs isolation.
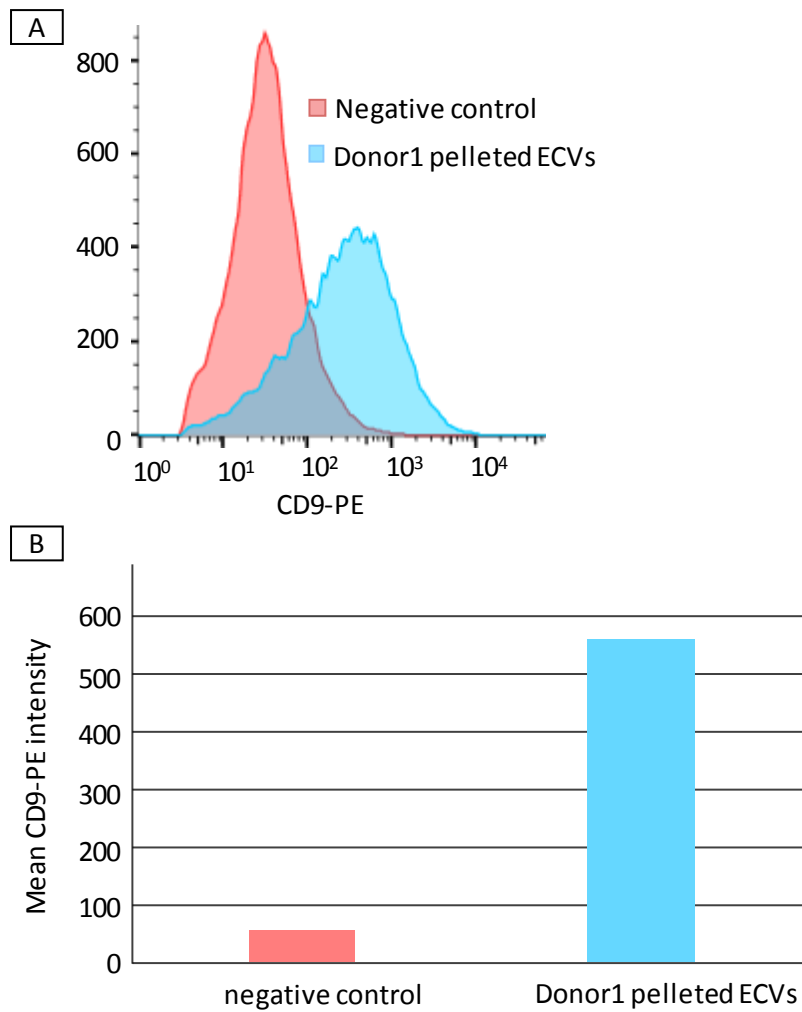
Figure 3-6: ECVs verification result. A histogram (**A**) that shows the marker protein CD9 in pelleted serum. The quantitative mean intensity of the detected CD9-PE is shown on the bar chart (**B).**

3.1.5.2. Cell type-specific ECVs (ndECVs) using bead-assisted technique

Having established a valid protocol for the isolation and detection of ECVs in general (3.1.5.1), this study subsequently narrowed to isolating cell type-specific vesicle, the ndECVs. Here, beads were coated with antibodies directed against the cell type specific ECVs' marker protein CD171 using the bead-assisted technique (2.4.3.5). The CD171 coupled beads were used to capture ECVs from ultracentrifuge pelleted serum (2ml) obtained from young healthy donors (donor 1 & 2) and has been pre-cleaned (2.4.3.1).

For detection and analysis of the captured vesicles, a CD9-specific antibody that has coupled to a fluorophore, PE was applied. As CD9 is a generic ECV marker protein, a positive signal would confirm a successful isolation of ECVs. Whiles the use of a CD171 specific antibody for capturing, on the other hand, guarantees the specificity of ndECVs. Also, since it is known that SH-SY5Y cells release vesicles which are positive for the protein marker CD171, ECVs pelleted from the supernatant of these cells were included to provide as positive control. As a negative control, 0.1% BSA in PBS was substituted for the ECVs. Data on the detected ndECVs was acquired by flow cytometry (2.4.4.3).

As shown in the result (Figure 3-7), an increased CD9 reactivity (positive signal) is observed for donor 1 and 2 compared to the negative control (Figure 3-7B). Since CD9 is a generic marker protein for ECVs, the observation confirms that the isolation process for the ECVs was successful. And, as the ECVs were captured by CD171-specific antibodies, the result further provides assurances that the isolates were indeed ndECVs. Besides, the SH-SY5Y cells (positive control) also demonstrated positive signal (right shift) for marker protein CD9 (Figure 3-7A). The quantitative mean CD9-PE intensity of donor 1 and 2 as well as the positive control (SH-SY5Y) are observed to be higher than that of negative control sample as shown in the bar chart (Figure 3-7C).
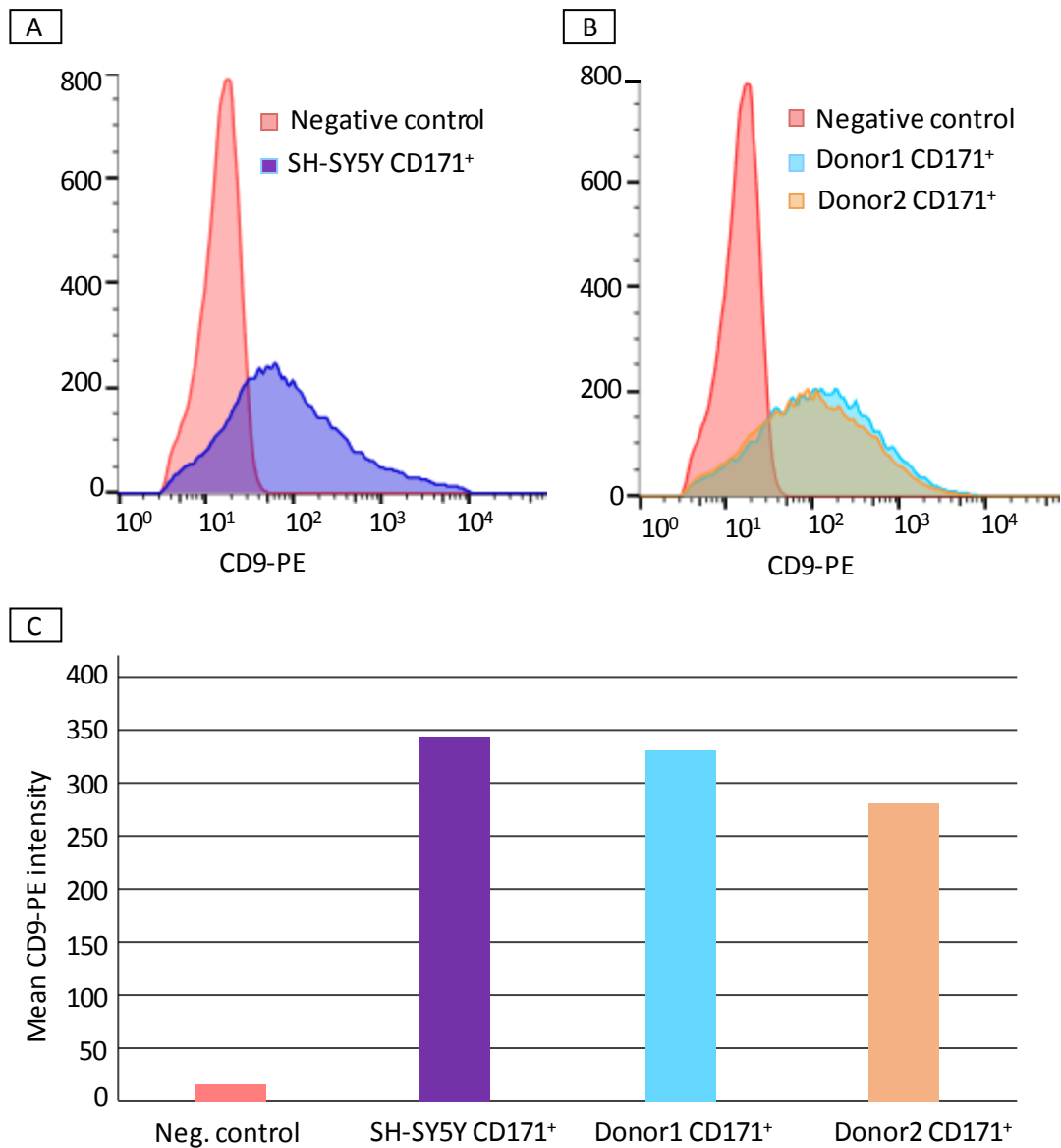
Figure 3-7: Verification result for immunomagnetically captured CD171^{+} that were analysed by flow cytometry. 'A' and 'B' are histogram that showing CD171^{+} in the pelleted SH-SY5Y supernatant (positive control) in donors' serum (B) respetively. 'C' is a bar chart showing the quantitative mean intensity of the CD9-PE (**C**). ''Neg.'' represents negative.

3.1.6. Comparing serum and plasma as ideal starting material

Next, the study compared serum and plasma to identify which was the ideal starting material for the isolation of ndECVs. The basis for this comparison was to find out if one has advantage over the other regarding ndECVs isolation. Here, serum (1ml) and plasma (1ml) were obtained from a single donor, pre-cleaned (2.4.3.1) and ECVs pelleted by ultracentrifugation (2.4.3.3). The ndECVs from both materials (plasma and serum) were

immunomagnetically captured with biotinylated CD171 antibody coupled beads as described earlier (2.4.3.5). The captured ndECVs were detected by a second antibody CD9. Data on the detected ndECVs was acquired by flow cytometry (2.4.4.3). The flow cytometry verification result for the captured ndECVs from both serum and plasma is shown in figure 3-8. An approximately equal increased CD9 reactivity (positive signal) is observed for the ECVs pelleted from either serum or plasma compared to the negative control (Figure 3-8A). Similarly, both plasma and serum showed approximately equal quantitative mean intensity of CD9-PE compared to the negative control (Figure 3-8B). Based on this finding, either plasma or serum is suitable for the isolation of ECVs.
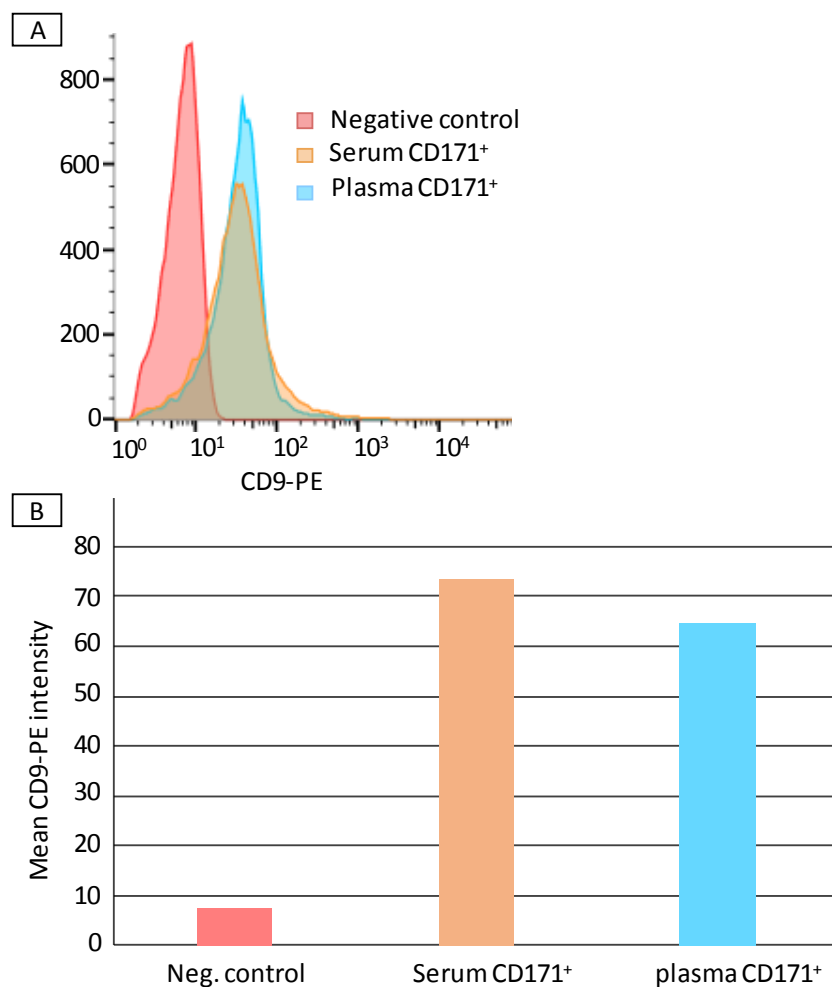
Figure 3-8: Verification result for the immunomagnetically captured ndECVs from plasma and serum of the same donor. 'A' is a Histogram showing the positive signal (right shift), and a bar chart (**B**) showing the quantitative mean intensity of the detected CD9-PE from both samples.

3.1.7. Optimal minimum starting volume of serum

Having identified serum as equally suitable material for isolation of ndECVs, the study next identified the optimal minimum volume of the serum needed to fully saturate the applied beads for capturing the vesicles. Here, ndECVs were isolated from 4 different volumes (150µl, 250µl, 500µl and 750µl) of serum from a single donor using the ultracentrifuge pelleted technique and the beads assisted technique
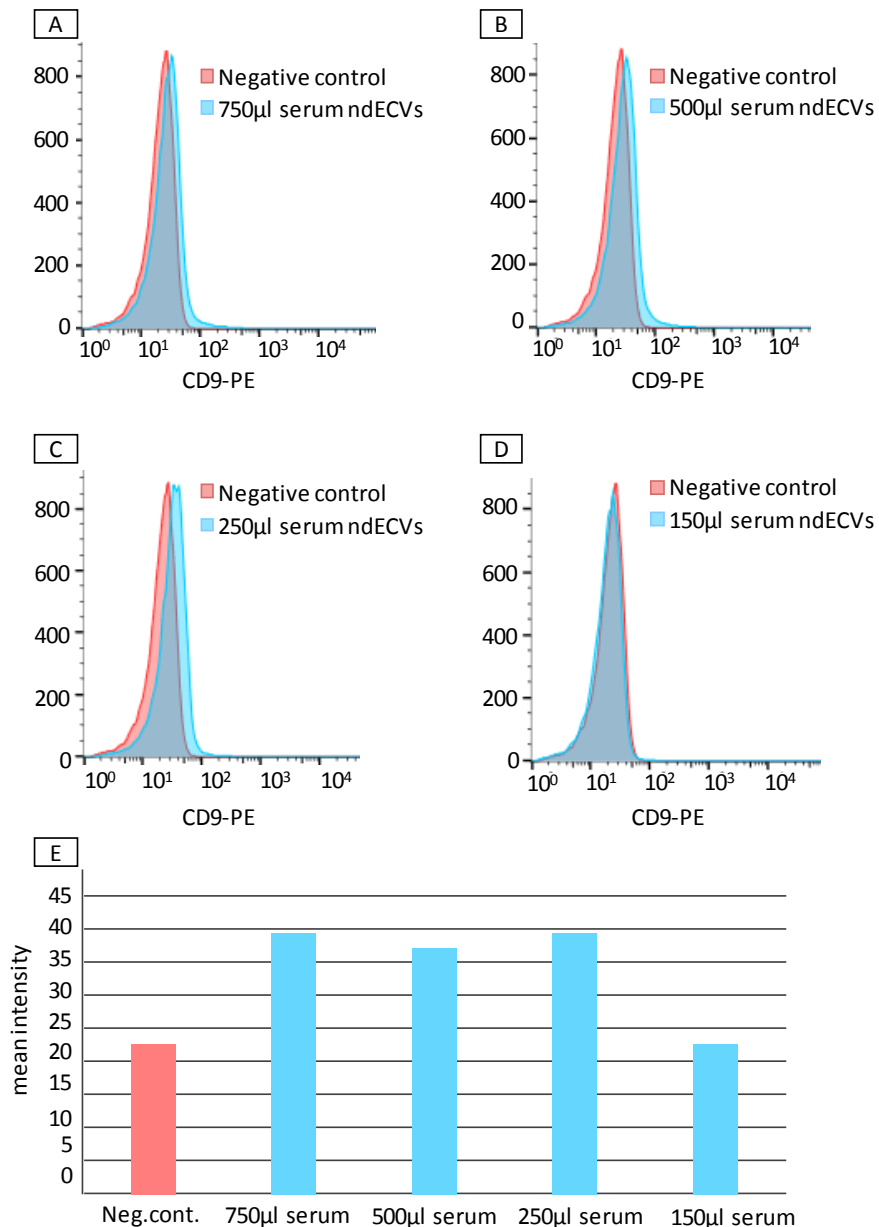
Figure 3-9: Flow cytometry verification result of ndECVs from four different volumes of serum. The CD9-PE intensity of the captured ndECVs is shown by histogram (**A**) and bar chart (**B**).

Beads coated with CD171 antibodies were used to capture the ndECVs. Captured ECVs on the beads were detected by a second independent antibody directed against the tetraspanin CD9. Data on the detected ndECVs was acquired by flow cytometry (2.4.4.3). From the result above (Figure 3-9), ndECVs could be isolated from 250µl of serum sample. In this experiment, the volume (5µl) of the bead used was always kept constant. As a negative control, 0.1% BSA in PBS was substituted for the ECVs.

3.1.8. Isolation of ndECVs from ultracentrifuge or pre-cleaned serum

It is generally recommended that, the capturing of ECVs should be performing in small volumes. Therefore, this study tested whether this was necessary as ultracentrifugation process consumes time, material and may not be beneficial to the sample. Here, beads that have been coupled with CD171 biotinylated antibody were used to capture ndECVs from either 0.5ml pre-cleaned (2.4.3.1) or pelleted 50µl ECVs in PBS (original/starting serum 0.5ml). For detection and analysis, a second antibody directed against the tetraspanin protein CD9 was used. As a negative control, 0.1% BSA in PBS was substituted for the ECVs. Data on the detected ndECVs was acquired by flow cytometry (2.4.4.3).

From the verification result (Figure 3-10), an increased CD9 reactivity (positive signal) is observed for the ndECVs marker protein in both the pre-cleaned and pelleted serum compare to the negative control (Figure 3-10A). However, the CD9 signal (reactivity) for pelleted ECVs was more pronounced than that of the pre-cleaned serum. Quantitatively, a higher CD9-PE mean intensity was observed in the pelleted serum compared to the pre-cleaned serum (Figure 3-10B).
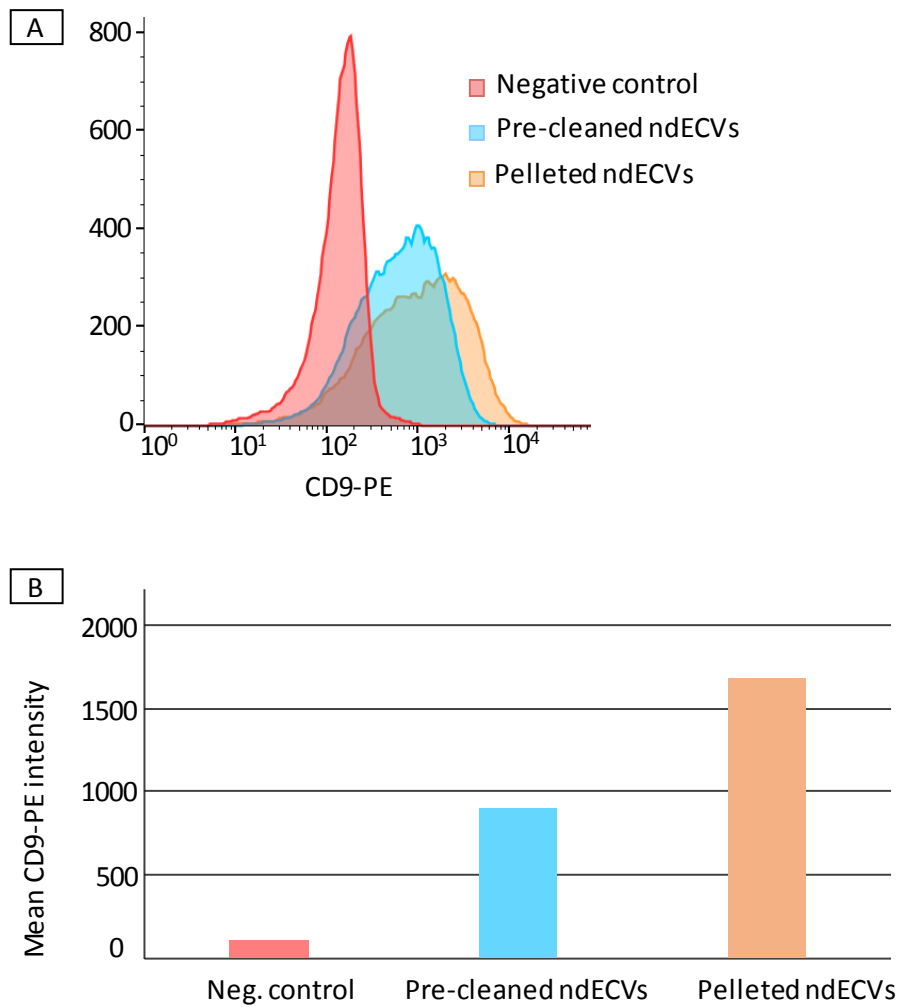
Figure 3-10: Isolation of ndECVs from either pre-cleaned serum or ultracentrifuge pelleted serum using bead-based technique. A Histogram (**A**) showing the ndECVs that were detected in the pre-cleaned as well as in the pelleted serum. A bar chart (**B**) showing the quantitative mean CD9-PE intensity. Based on the result, ndECVs were detected in both samples but pronounced in the pelleted serum

3.2. Detection and quantification of ECVs' cargo proteins, HSP70 and tau

Having established a reliable and validated platform for isolation and characterization ECVs and ndECVs (3.1.1 – 3.1.8), the study next focused on the quantification of tau protein in the ECVs.

3.2.1. Western blot technique

This current study was aimed to quantify tau proteins in the ECVs, however, the cargo HSP70 was included to provide a guarantee of procedure. The HSP70 is known to be abundant in ECVs and has been demonstrated extensively in this study (Figure 4B, Figure 5, Figure 6C and Figure 7). Therefore, tau protein and HSP70 were evaluated from different volumes of serum. Here, two 11ml each and one 80ml serum were obtained from a young healthy donor. The sample was pre-cleaned (2.4.3.1), pelleted by ultracentrifugation (2.4.3.3) and purified by iodixanol density gradient (2.4.3.4). The 11ml and 80ml serum volumes were arbitrary selected. The purified ECVs were subjected to western blot analysis. ECVs obtained from one of the 11ml was stained with antibody directed against the protein HSP70, while the ECVs obtained from the other 11ml as well as the 80ml serum were stained with polyclonal anti-human tau. For detection, a second antibody anti-mouse immunoglobins HRP was used for the membrane that was stained previously by HSP70 antibody, while antibody anti-rabbit immunoglobins HRP was used for the membrane stained with anti-human tau.

The tau proteins have molecular weight ranging from 65kDa to 35kDa because of their different isoform and proteolytical processing, while HSP70 has a molecular weight of 70kDa. From the result (Figure 3-11), there is no obvious tau protein reactivity in fraction 5 – 10 of the 11ml serum (Figure 3-11A), however, there is a weak positive reactivity for tau protein in fraction 5 – 10 of the 80ml serum (Figure 3-11B). On the other hand, the cargo protein HSP70 showed obvious positive reactivity in fraction 5 – 10 (Figure 3-11C). Since HSP70 was clearly shown in 11ml serum, the western blot procedure adopted was successful; however, due to low levels of tau protein in ECVs, one may require at least 80ml of serum to demonstrate tau protein using this analysis platform.
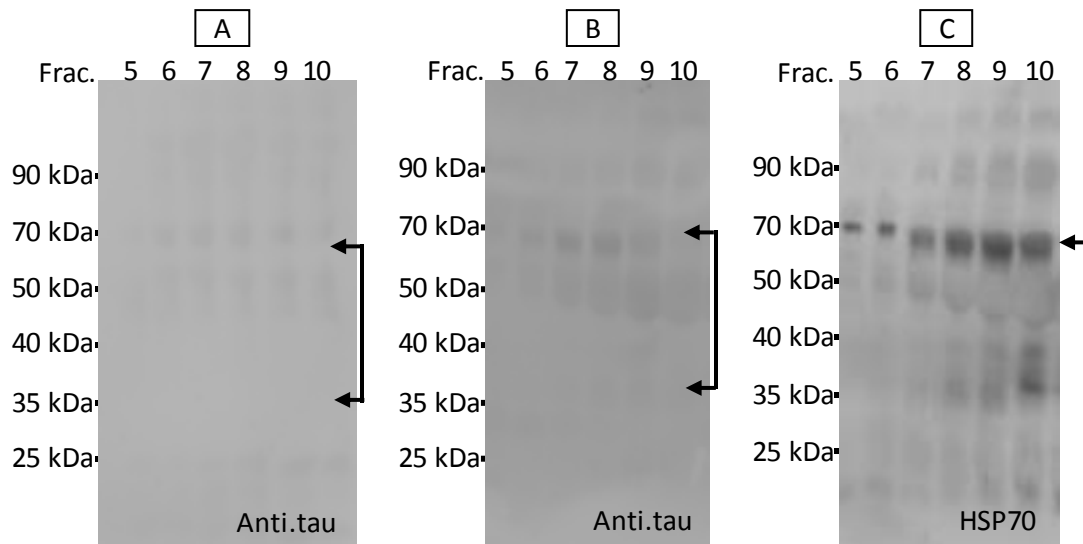
Figure 3-11: Demonstration of ECVs' cargo proteins, HSP70 and tau in different volumes of serum. Membrane **A,** 11ml serum stained with anti-tau but shows no obvious positive reactivity below 70kDa. Membrane **B,** 80ml stained with anti-tau and showed weak positive reactivity below 70kDa. Membrane **C**, 11ml stained with anti-HSP70 and showed obvious positive reactivity at 70kDa. The arrows point to the region where the ECVs' cargo protein tau or HSP70 reactivity is expected. The '**Frac.'** represents fraction.

3.2.2. Flow cytometry

Although tau proteins in ECVs were demonstrated by western blot analysis, at the least a serum volume of 80ml was required and this may pose a challenge. Hence, the flow cytometry, a well-established fast and a sensitive technique for quantitative and multiparametric analysis of particles was exploited to quantify the tau protein in the ECVs. Prior to using the flow cytometry analysis platform to quantify tau protein in the ECVs, the technique was first employed to measure HSP70 in the vesicle to provide a proof of principle for the procedure. Here, serum (10ml) was obtained from a young healthy donor pre-cleaned (2.4.3.1) and ECVs pelleted by ultracentrifugation (2.4.3.3). The pelleted ECVs were captured by beads (2.4.3.5) that has been coupled with an antibody directed against the tetraspanin protein CD63.

The captured ECVs on the beads were fixed and permeabilized as described earlier (2.4.4.4). For detection, the permeabilized ECVs were stained with second antibody directed against the ECVs' cargo protein HSP70. The anti HSP70 was couple to a fluorophore, PE. Data on the detected ndECVs was acquired by flow cytometry (2.4.4.3).

Cultured SH-SY5Y Cells in suspension were used as positive control. As a second positive control was ECVs pelleted from the supernatant SH-SY5Y cultured cells was included. For negative control, permeabilized ECVs were stained with irrelevant PE coupled antibody (isotype control), and the result shown in figure 3-12.
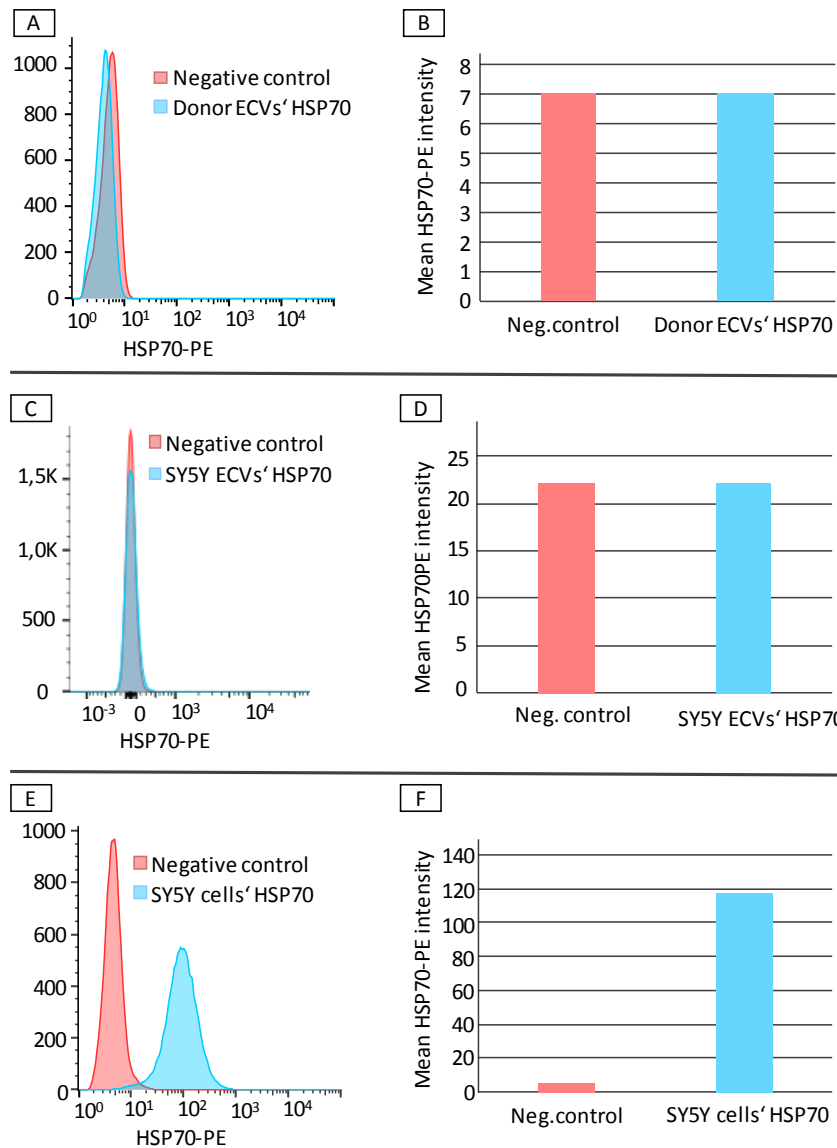
Figure 3-12: Flow cytometry result showing ECVs' cargo protein, HSP70 analysis. No obvious positive signal is seen for HSP70 in the ECVs from the donor serum (**A & B**) as well as ECVs from the SY5Y cells (positive control, **C & D**). An obvious positive signal is observed HSP70 from SH-SY5Y cells (also positive control, **E & F**).

From the result above (Figure 3-12) no obvious reactivity (positive signal) for HSP70 was observed in the ECVs obtained from the donor (Figure 3.12A and 3-12B). Also, the ECVs pelleted from the supernatant of the SH-SY5Y cultured cells (positive control) did not

show any obvious reactivity (Figure 3-12C and 3-12D) for HSP70. On the contrary procedure was able to stain intracellular HSP70 in the SH-SY5Y cells (Figure 3-12E and 3-12F). Indeed, as HSP70 was detectable in the SH-SY5Y cells, the established platform was considered feasible except that at present it could not demonstrate the cargo protein in the ECVs.

3.2.3. ELISA as an alternative approach to quantify of tau protein in ndECVs

As the detection of cargo proteins in the ECVs using the flow cytometry technique and western blot analysis did not show obvious positive reactivity, this study switched to using ELISA as an alternative approach to quantify the tau protein in these vesicles. Here, serum (1ml) was obtained from 28 clinical participants who have already undergone the routine clinical diagnosis for AD. The serum was pre-cleaned (2.4.3.1) and ECVs pelleted by ultracentrifugation (2.4.3.3). A volume 50µl each of the pre-cleaned serum was kept as pure serum (serum without ultracentrifugation). Pelleted ECVs were resuspended in 100µl of sample buffer (table 6). Beads that have been coated with CD171 were used to capture the ndECVs as described by the bead-assisted technique (2.4.3.5).

Captured ndECVs were resuspend in 50µl of sample buffer. From the 50µl of the resuspended captured ndECVs 5µl was aliquoted to verify for the presence of CD171$^+$ vesicles using flow cytometry (2.4.4.3). The remaining 45µl was lysed with Triton 100 to expose the tau protein. Protease inhibitor and anti-HAMAs were added to all samples. The ELISA technique (2.4.4.5) was used to detect and measure tau protein in ndECVs and non-ndECVs as well as free (soluble) floating tau in serum (pre-cleaned serum). As a positive control, ndECVs obtained from SH-SY5Y cells that was transfected with cDNA (2.4.2) for human tau protein was included. As a negative control sample buffer 1% BSA in PBS was included.

The result for the measurement of the tau protein is shown in figure 3-13. Based on the shown result, the ELISA technique could detect and measure tau protein in human serum, ndECVs and non-ndECVs. Also, from the result (Figure 3-13) a higher tau protein concentration was measured in the pure serum compared to that of the ECVs.
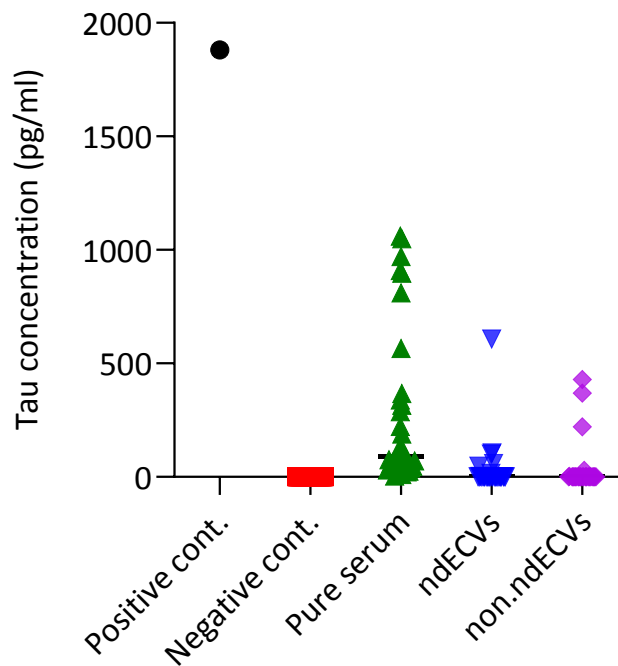
Figure 3-13: A scatter plot showing the measured tau protein concentration in serum, ndECVs and non-ndECVs. Also shown is the positive and the negative control results. From the graph higher tau protein concentration was measured in the pure serum (serum that underwent only pre-cleaning). As a positive control, SH-SY5Y cells that has been transfected with cDNA for human tau protein was used.

3.2.3.1.   Comparing the mean tau protein measured in serum and in CSF.

Since tau protein was measured in the serum and the clinically validated CSF tau protein measurement for the same participants were available, this study compared the two results. To determine the mean difference between the two measurement of tau protein (from serum or CSF), unpaired student t-test was performed. A p-value of 0.05 or less will imply that there is a significant difference between the two means. However, the study observed that, there was no significant difference (p=0.2708) between the means (Figure 3-14). As the p-value is greater than 0.05, it suggests that there is no significant difference between the mean tau protein measured in the serum and that of CSF.

Figure 3-14: A graph comparing mean tau protein concentration in serum and CSF. The '**ns**' represent no significance. There is no significant difference between the mean serum tau protein concentration and the mean CSF tau protein concentration.

3.2.3.2.   Correlation between serum tau protein and four AD predictive markers

Since the clinically validated results (CSF tau, CSF p-tau, β-amyloid and MMSE) of seventeen (17) participants were available, this study went further to determine a possible correlation between any of this clinically validated AD markers and the measured serum tau protein. This was necessary because where strong correlation would be observed could serve as basis for further evaluation or monitoring. For instance, if serum tau protein correlated strongly with CSF tau protein or β-amyloid, then serum tau measurement could be evaluated further and if possible, substitute for these validated makers.

Therefore, Pearson correlation analysis was performed and the correlation coefficient (r) of serum tau concentration and the AD predictive markers was determined. Generally, r value of +1 is considered as strong positive correlation and r value of -1 is a strong negative correlation. An r value of zero (0) is considered no correlation. Therefore, in an experiment where correlation coefficient is determined, the obtained r value is compared to these values (+1 to -1). In this current study, the r for serum tau protein and CSF tau protein was 0.146 (Figure 3-15A), and that of serum tau protein and CSF p-tau was 0.249

(Figure 3-15B). Also, the r for serum tau protein and CSF β-amyloid was -0.467 (Figure 3-15C), while that of serum tau protein and MMSE was -0.187 (Figure 3-15D).

As none of the correlation coefficient was zero (Figure 3-15), but close to zero there is no strong correlation between the serum tau protein concentration and CSF tau, CSF p-tau or MMSE. However, of major interest is the trend for a correlation between serum tau protein and CSF β-amyloid (Figure 3-15C). The r value between these markers is − 0.467 (p=0.059). This trend for a negative correlation (r = -0.467, p=0.059) observed demonstrates a pattern that may suggest that AD related reduction of Aβ is accompanied by a serum tau increase. But since the p-value was higher than 0.05, the correlation between the two markers are not significant. The statistical analysis showing the correlation coefficient (r) and the p-value are shown in figure 3-15.

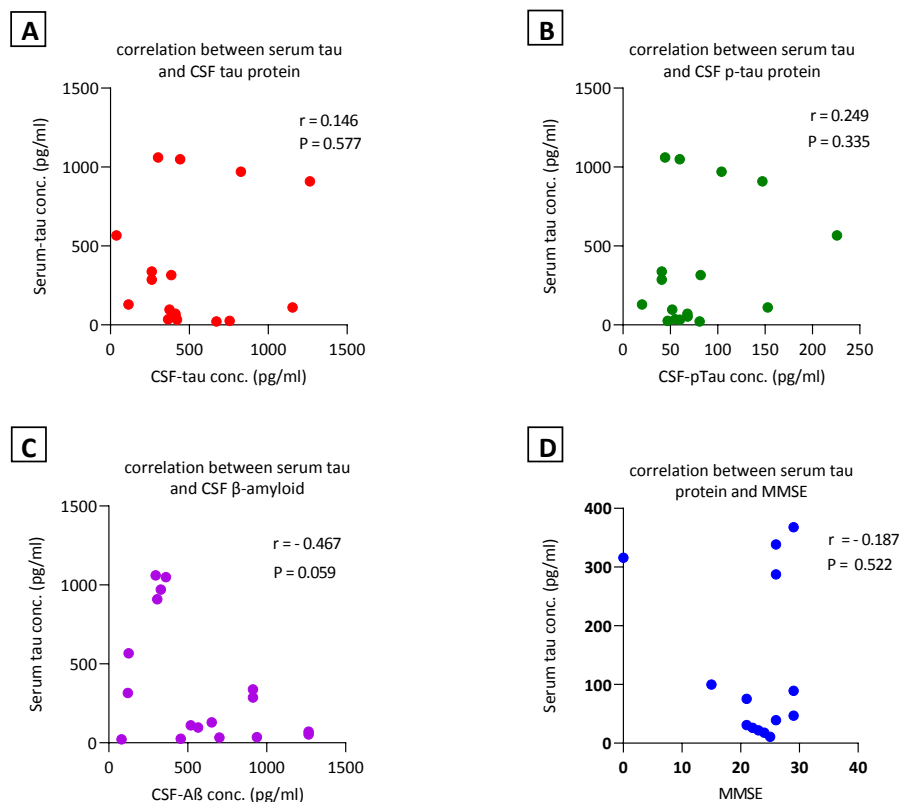

Figure 3-15: Correlation of serum tau protein concentration and four predictive markers of AD. Serum tau protein concentration is plotted against; CSF tau (**A**), CSF p-tau (**B**), CSF β-amyloid (**C**) and MMSE (**D**).

3.2.3.3. Correlation between ndECVs' tau protein and four AD predictive markers

Again, as tau protein was measured in serum-based ndECVs, this study next, correlated the tau protein in these vesicles to the four (4) clinically validated AD predictive markers (CSF tau, CSF p-tau, β-amyloid and MMSE). With the aim of identifying which of these validated makers correlate with ndECVs' tau protein. Therefore, the Pearson correlation coefficient (r) between ndECVs' tau protein and CSF tau, CSF p-tau, Aβ-amyloid or MMSE were performed. From the result (Figure 3-16), the r values of ndECVs' tau protein concentration and CSF tau (Figure 3-16A), CSF p-tau (Figure 3-16B), CSF β amyloid (Figure 3-16C) or MMSE (Figure 3-16D) are -0.259, -0.200, 0.024 or -0.185 respectively. Like the explanation for r given earlier (3.2.3.2) here also, none of the r values was zero but considering the closeness to zero there was no strong correlation.
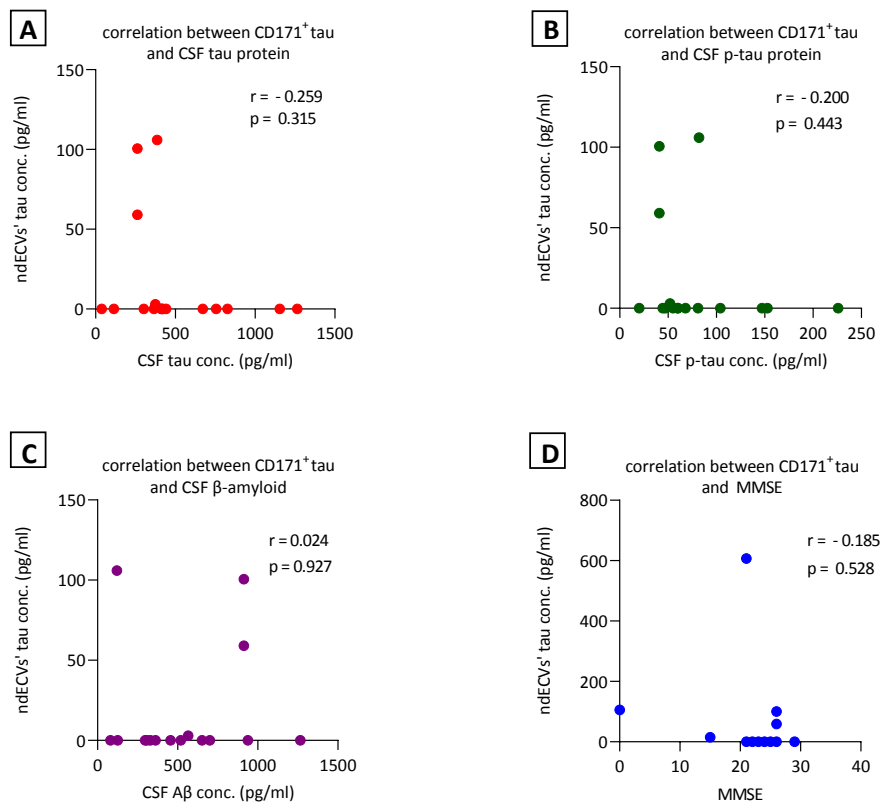
Figure 3-16: Correlation between tau protein in ndECVs against CSF tau (**A**), CSF p-tau (**B**), CSF Aβ amyloid (**C**) or MMSE (**D**). Also shown on the graphs are the correlation coefficient (r) as well as the p values. As none of the r values is zero but close to zero, it appears there was no strong correlation between ndECVs' tau and the AD predictive markers.

Finally, as the established ELISA technique (3.2.3) could quantify tau protein in serum and in ECVs of human, the study further attempted quantifying tau protein in hibernating

animals that are in the torpid state. The inclusion of these animals was necessary to serve as an additional (beside the SH-SY5Y cells) positive control for ECVs' tau protein measurement using the ELISA technique. It is known that torpid state hibernators show AD-like tau protein in their brain [Arendt et al., 2003; Härtig et al., 2007], and therefore is possible to detect and measure the protein in their blood. A successful measurement of tau protein in the ECVs of these animals would further strengthen the claim that the protein was measured in the human samples.

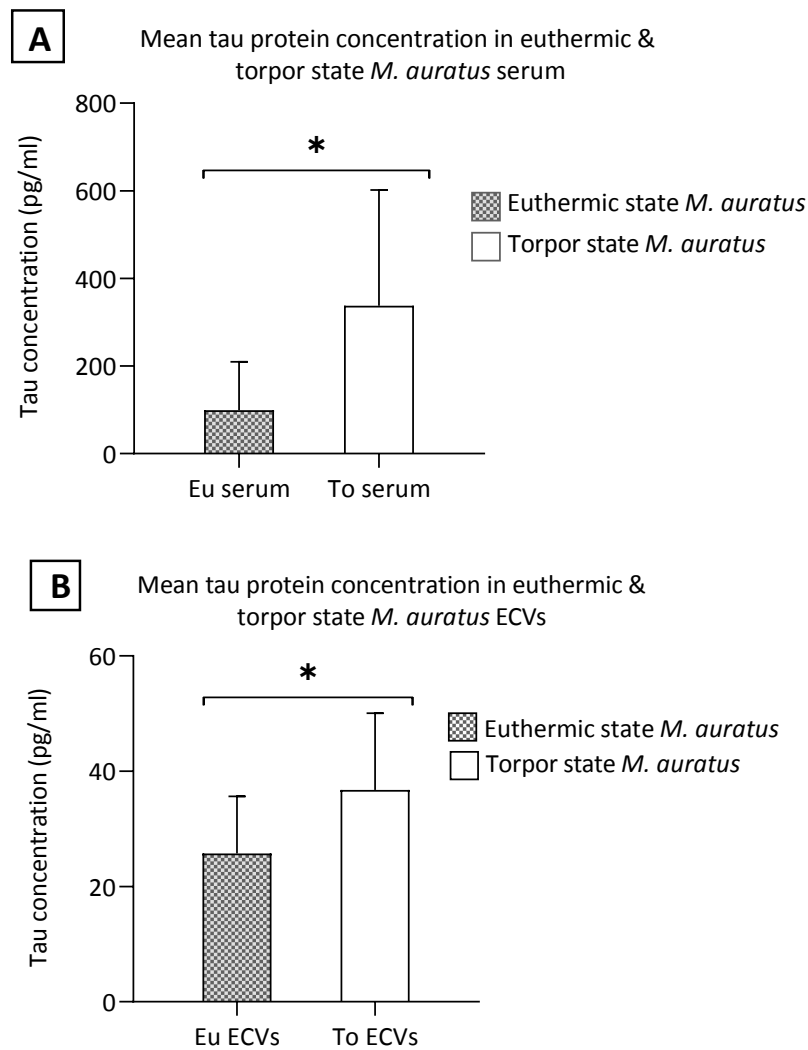**Figure 3-17:** A bar graph showing mean tau protein concentration in serum (**A**) and CD171^{+}ECVs (**B**) of *M. auratus* (either in torpor or euthermic state). Also shown is the significant difference (*) between the means.

Here, ten (10) torpid state *M. auratus* and ten (10) euthermic state *M. auratus* were used. Serum was obtained from each set of the animal and pre-cleaned as described (2.4.3.1).

Each pre-cleaned serum was divided into two parts; one part was subjected to ultracentrifugation (2.4.3.3) to pellet the ECVs and the other part kept plain as "serum". Tau protein concentration was measured in both the serum and ECVs for each animal.

Unpaired t-test was used to compare the mean tau protein concentration between the torpid state and the euthermic states animals. Regarding tau protein concentration in the serum (Figure 3-17A), a mean value of 99.23pg/ml was recorded for the euthermic state *M. auratus* is while the torpor state *M. auratus* had a mean value of 337.5pg/ml. Also, there was a significant difference in the means of these two measurements which is shown by an asterisk on the bar (Figure 3-17A).

Similarly, the mean tau protein concentration in the ECVs of the euthermic state *M. auratus* was 25.74pg/ml while that of the torpid state *M. auratus* was 36.76pg/ml (Figure 3-17B). Like the serum, here also there was a significant difference between the two means and is shown by an asterisk in figure 3-17B.

4.   DISCUSSION

4.1.   Basis for considering blood-based markers for the diagnosis of AD

In AD, altered metabolic pathways and signalling cascades are not localised to the CNS alone but include also peripheral tissue [Gasparini et al., 1998; Stieler et al., 2001; Khan; Alkon, 2015]. This postulation is supported by several studies [Ray et al., 2007; Rezai-Zadeh et al., 2009]. An alteration in the signalling transduction processes involving protein kinase C, cyclic AMP, calcium homeostasis, phosphoinositide metabolites and ion channel permeability has been observed in both the brain and fibroblast of AD patients [Favit et al., 1998; Alkon et al., 2007]. Also, an altered glucose consumption, reduced a-ketoglutarate dehydrogenase, increased lactate production, decreased glutamine oxidation and declined cytochrome c oxidase are significant in both fibroblast and the platelets of AD patient [Peterson; Goldman, 1986; Sims et al., 1987; Parker; Parks, 1995; BLASS et al., 1997]. Moreover, three important enzymes; Erk1, Erk2 and glycogen synthase kinase 3β which are involved in tau phosphorylation are all regulated by protein kinase C, an enzyme which is not restricted to the CNS alone [Alkon et al., 2007]. Hence, the concomitant dysregulation in the signalling transduction machinery of these enzymes in both the brain and the peripheral tissue of AD patient suggests that the disease is ubiquitous in nature [Khan; Alkon, 2010; Khan; Alkon, 2015].

In addition to the altered signalling transduction pathways in peripheral tissue, the simultaneous impairment of immune function in the CNS as well as peripheral tissue of AD patients further suggest that the disease is not limited to the brain alone. In AD, the formation of plaques and tangles activate microglia, astrocytes, and induce other immune response such as cytokines, complement proteins, proteinase, chemokines and cell surface immune molecules in the brain [Bonotis et al., 2008; Rezai-Zadeh et al., 2009; Morris et al., 2014b]. The activation of these neuroinflammatory response in the brain of AD, and the fact that, T-lymphocytes can cross the BBB [Wekerle et al., 2000], is reflective of the observed dysregulation in the peripheral immune cells [Stieler et al., 2001; Morris et al., 2014b]. An extensive illustration of CNS and peripheral tissue immune response in AD is available elsewhere [Tollefson et al., 1989; Ikeda et al., 1991; Tan et al., 2002; Chen et al., 2006; Richartz-Salzburger et al., 2007].

In the peripheral blood, a significant decrease in tumour necrotic factor (TNF) and lymphocyte in person with severe cognitive impairment compared to heathy cognitive control has been observed [Bonotis et al., 2008]. A positive correlation of peripheral blood CD4 subpopulation as well as a negative correlation of interleukin-2 with MMSE was observed in severe cognitive impaired individuals [Bonotis et al., 2008]. Further, peripheral lymphocytes of AD patients showed decreased proliferative markers after mitogenic stimulation compared to cognitive normal control [Stieler et al., 2001; Rezai-Zadeh et al., 2009; Yoon et al., 2010]

From the above discussion (inflammatory responses and signalling mechanism), it stands to reason that AD is likely more systemic, and that peripheral tissue such as blood may provide as important source for early diagnostic markers for the disease. Currently, CSF tau, CSF p-tau and β amyloid are among the biomarkers used to diagnose AD. Although these biochemical measurements are the gold standard in clinical use, it can also be influenced by circadian rhythm [Kang et al., 2009]. Besides, the lumbar puncture sampling technique for CSF is invasive and not useful for marker screening, and only detects AD in its advance stage [Nagasaka et al., 2005; Khan; Alkon, 2015].

4.2. Basis for targeting tau protein in peripheral blood

Although neuritic plaques and NFT are the typical features of AD, abnormal deposition of plaque (β-amyloid) have been observed in cognitive healthy individuals [Davis et al., 1999; Price et al., 2009; Kang et al., 2009; Morris et al., 2014a]. This raises further question about the specificity and the sensitivity of the diagnostic value of β-amyloid.

Again, unlike plaques, the degree of NFT deposition in the brain correlates positively to the severity of clinical symptoms of neuronal dysfunction [Holzer et al., 1994; Brion, 1998; Hampel et al., 2010]. It has been demonstrated extensively that, the accumulation of NFT in the brain follows a hierarchical pattern beginning from the neurons in the trans-entorhinal region [Hyman et al., 1987; Braak; Braak, 1991; Gómez-Isla et al., 1996], then, over years spread across the limbic, and then finally to the isocortical associated areas [Braak; Braak, 1991]. This centrifugal spreading pattern of NFT in the brain is consistent with the progressive nature of AD symptoms which also begin with anterograde amnesia,

speech impairment, mood imbalance and finally lost of executive function [Hyman et al., 1987; Hyman; Trojanowski, 1997; Calignon et al., 2012]. And since abnormal hyperphosphorylated tau protein is the major component of NFT, evaluation of the protein in peripheral blood could yield more reliable marker for monitoring AD progression [Hampel et al., 2010; Wren et al., 2018].

4.3. Potential role of ndECVs in the transportation of tau protein

In recent times, the evaluation of blood-based tau protein as reliable marker for predicting AD is on the rise [Fiandaca et al., 2015; Abner et al., 2016; Winston et al., 2016; Guix et al., 2018]. The rationale for considering a possible diagnostic role of blood-based tau protein is rooted on several logical assumptions. Beginning from the fact that, as tau protein becomes hyperphosphorylated, it detaches from the microtubules and relocates into the somatodendritic compartment, further phosphorylation and aggregation makes it more rigid, insoluble and neurotoxic. The insulted neuron, to overcome the stress from this intracellularly accumulated tau deposit, will attempt to expel deposition in a secluded manner. And ndECVs has been suggested as the potential culprit that provides a medium for the transportation of this abnormal folded tau protein [Kanninen et al., 2016].

Again, the ability for both ndECVs and tau protein to enter recipient cell via a similar mechanistic pathway (endocytosis) further suggest that, ndECVs and tau protein are closely linked [Frühbeis et al., 2012]. Also, the sequential spreading pattern (trans-entorhinal, limbic and to the cortices) of NFT in the brain can be executed by a well-structured and unrestricted medium such as ndECVs. The ndECVs and its contents, tau protein can cross the blood brain barrier into CSF [Süssmuth et al., 2001; Lakhal; Wood, 2011; Kanninen et al., 2016]. And, on daily basis, about 500µl of CSF is absorbed into peripheral blood stream, so ndECVs containing tau protein may use this intermediary (CSF) to transverse into peripheral blood [Weinstein; Seshadri, 2014]. In healthy state, approximately 2000 trillion ECVs are available [Kalluri, 2016], however, in pathological state such as cancers and neurodegenerative conditions, this number is actually change [Melo et al., 2015; Kalluri, 2016; Soria et al., 2017]. The quantities of ECVs increase proportionally in neurodegeneration [Soria et al., 2017]; hence, the same can be true for

ndECVs and its cargo, tau protein in same pathology. Since, ECVs possess signatures of their parenting cells, and tau protein is primarily found in the neuron, blood-based ndECVs and its cargo, tau may provide useful information that reflects the state of brain neuron.

Based on this background information, this study first aimed at establishing a valid protocol to isolate ndECVs and then evaluate the tau protein content within these vesicles.

4.4.   Establishment of protocol for isolation and characterisation of ECVs

Since AD is not localised and the disease occurs several years before the onset of clinical symptoms, quantification of tau protein in peripheral blood can be used to monitor at-high-risk individuals. And as mounting evidence suggests that ECVs may be involve in the transmission of AD-like tau proteins from the CNS to peripheral blood, further makes the evaluation of the protein in the peripheral blood attractive. Blood sampling technique is less invasive, does not require sophisticated tools and it involves less time.

To accept blood based ECVs in clinical settings as a potential source of AD diagnostic markers (such as tau protein), the isolation strategy of the vesicle should be efficient and reliable. This is because several cells release ECVs into blood, and therefore a method that can distinctively define a specific population would be helpful for downstream analysis. A plethora of studies have reported on several protocols for isolating ECVs, however there are some experimental concerns or issues that still needs to be clarified. For instance, whether a protocol designed for cell cultured suspension may be applicable for human serum, plasma or urine. It is always important to first define the study goal clearly. As this current study was aimed at detecting and quantifying tau protein in ndECVs, it first modified and compared several existing ECVs isolation methods and established the most suitable one.   Discussed below are the various modifications, comparison and the established valid protocol for isolating ECVs and specifically ndECVs.

As baseline knowledge, ECVs are extracellularly located in body fluids. Hence, to avoid the possibility of introducing intracellular structures from disrupted cells and tissues, the body fluid (plasma or serum) ought to be sampled and processed gently. This is one of the

reasons why plasma or serum is progressively centrifuged (pre-cleaned) prior to isolation of ECVs. Also, pre-cleaning is performed before isolation of ECVs is to remove dead cells, protein aggregates and debris which can potentially trap or contaminate the vesicles. Therefore, all samples obtained were first pre-cleaned before using.

4.4.1. Precipitation versus ultracentrifugation

Ultracentrifugation and precipitation techniques are among the most commonly used method for isolating ECVs from serum or plasma, yet both techniques are not applicable in clinical diagnostic setup. The precipitation method is simple and requires less time but, there are concerns about the potential co-isolation of non-ECVs such as protein complexes and lipoproteins by this method [Lötvall et al., 2014]. Since this study wanted an optimal method of isolating ECVs for downstream analysis, the precipitation technique was compared to the ultracentrifugation method. Surprisingly, ECVs' marker protein HSP70 was not detected after carefully adopting the precipitation technique for both serum and plasma sample (Figure 3-1A). The finding in this current study is at variance with previous studies where precipitation method was used to detect ECVs in plasma [Helwa et al., 2017], in urine [Alvarez, 2014] and condition cell cultured medium (Weng). But it is important to note that, different sources of biological materials (such as plasma, serum, culture medium) have varied composition, and therefore the same isolation technique may not be applicable to all samples. As those previous studies failed to describe how polymeric materials and potential protein contaminants were eliminated in their precipitation techniques, using this method to isolate ECVs from human serum or plasma remains debatable.

On the contrary, using ultracentrifugation method, ECV's marker protein HSP70 was detected in both plasma and serum sample suggesting that the isolate contained ECVs. Pelleting of ECVs by ultracentrifugation technique is a gold standard procedure for the isolation of the vesicles [Zarovni et al., 2015; Li et al., 2017]. Therefore, as this current study also isolated ECVs by this same technique, arguably suggest that, ultracentrifugation is a crucial step in the processing of ECVs. Again, the observation in this study is similar with several studies [Zarovni et al., 2015; Lambrecht et al., 2017; An et

al., 2018]. While in the precipitation technique pre-cleaning may be optional [Alvarez, 2014], ultracentrifugation is always performed after pre-cleaning. As the pelleting of ECVs by ultracentrifugation proceeds pre-cleaning of the sample (serum or plasma), possible contaminants might have been removed. Furthermore, ultracentrifugation may be a necessary step to concentrate the sparsely distributed vesicles. Finally, isolation of ECVs by ultracentrifugation appears more likely to yield suitable vesicles for downstream analysis.

To further ascertain if indeed pelleting of ECVs by ultracentrifugation was a major requirement, this study attempted to isolate ECVs from serum that has only undergone pre-cleaned stage (Figure 3-1B right). But from the western blot verification result, ECVs were not detected in the pre-cleaned serum compared to the pelleted serum or plasma (Figure 3-1B left). Several reasons could be attributed to this observation. That, in serum, ECVs are sparsely distributed and therefore the aliquoted volume for western blot analysis did not contain much ECVs, or the amount of the vesicles contained in the aliquoted serum was below the detection limit by the western blot technique. Another possible reason is that, the ECVs might have been highly contaminated or trapped in other protein aggregates. And that pre-enrichment process by ultracentrifugation at 100,000xg was necessary to concentrate the ECVs prior to western blot analysis. Again, the dilution of the pre-cleaned serum with PBS (2.4.3.3) prior to ultracentrifugation might have contributed to reducing the viscosity of the serum and increased the centrifugal force on the circulating ECVs and promoting pelleting. Finally, the washing of the pelleted ECVs after the first ultracentrifugation might have contributed to removing additional contaminants.

4.4.2. Purification of ECVs by density gradient technique

Although, pelleting by ultracentrifugation was useful to concentrate the ECVs, another concern that existed was that, aggregated proteins and large microvesicles could co-sediment with pelleted vesicles [Tauro et al., 2012] which can invariably compromise the purity of the isolated ECVs. Hence to avoid such potential contaminant, the differences in the flotation densities of ECVs and the other potential were exploited. To do this, ECVs

were purified by either iodixanol or sucrose gradient and the outcome compared. From the result (Figure 3-2), purification of ECVs by sucrose gradient showed unsatisfactory outcome. Possible reason for this observation may be attributed to the fact that, sucrose gradient is unable to properly discriminate ECVs from other larger protein aggregates or contaminants. This is possible because, a previous study has also observed that sucrose gradient did not sufficiently separate ECVs from non-ECVs [Cantin et al., 2008]. Since the formation of ECVs (exosomes and ectosomes) is defined by two pathways, purification technique ought to be carefully selected to avoid compounding the existing challenges. Thus, a suitable technique that can efficiently separate a ECVs population at a given time is preferred.

Contrary to the sucrose gradient, iodixanol gradient showed an efficient separable result (Figure 3-2) like previously reported [Cantin et al., 2008; Tauro et al., 2012]. While sucrose gradient has been used elsewhere [Raposo et al., 1996] to separate "so-called" vesicles, it is important to again recognised the source of the sample (such as blood, CSF, urine or conditioned cell culture medium) as different samples may have varied components. This study identified iodixanol gradient as suitable medium that can efficiently purify ECVs from either serum or plasma for downstream analysis. Again, though there are two types (continuous and discontinuous) of preparing the iodixanol gradient, this study found no difference between the two (data not shown). Therefore, the discontinuous method of preparing the iodixanol gradient was adopted for the purpose of convenience.

Next, as it is generally recommended that at least one membrane and one cytosolic marker protein for ECVs should be identified in a preparation in order to enable the usage of the term "ECVs" [Kanninen et al., 2016], this study went further to verify for additional markers in the isolate. The tetraspanin proteins, CD9 and CD63 as well as the cargo protein HSP70 were verified from an isolate simultaneously. These proteins were exclusively selected because they are abundantly found on or in ECVs and therefore demonstration them confirms the presence of the vesicles. Interestingly, within the same iodixanol fractions, the marker proteins CD9, CD63 and HSP70 were detected (Figure 3-3). Since these markers are generally used to characterise the vesicles, this study considered the isolate as ECVs.

Following the verification of ECVs' marker proteins (CD9, CD63 and HSP70) in the pellet of a single donor's serum, the study proceeds to evaluate the reproducibility of the procedure. A reproducible protocol is an important step for subsequent downstream analysis. Here, ECVs were verified from three (3) young health donors. Remarkably, ECVs' cargo protein HSP70 showed positive reactivity within the same iodixanol fractions for the 3 donors (Figure 3-4). This current finding further suggests that the iodixanol is a suitable medium for the purification of ECVs.

In addition to using composition (such as CD9, CD63 or HSP70) to characterise ECVs, the vesicles are further classified based on its buoyant density. It is presumed that ECVs will sediment into iodixanol gradient until it reaches an equilibrium density and float. The density of the iodixanol at which the ECVs float is assumed to be the density of the vesicle. Using this principle, this study moved a step further to determine the density of the isolates. And from the result (Figure 3-5), the densities of the iodixanol fractions that contained the ECVs ranged from 1.079g/ml to 1.196g/ml. This observed density range is like that reported previously [Tauro et al., 2012; Muller et al., 2014; Pérez-González et al., 2017].

Based on the recorded density range as well as the verified protein markers (CD9, CD63 and HSP70), the study assumed that, ECVs were successfully isolated, purified and verified by ultracentrifugation, iodixanol gradient and western blot techniques respectively.

4.4.3. Detection of ECVs' cargo protein using western blot technique

Following the successful isolation of ECVs by the establishment of protocol, the study next, demonstrates the cargo proteins in the vesicles using western blot as an initial platform. Tau protein was the focus however; HSP70 was included as additional cargo protein to further confirm the source of the targeted protein. Thus, qualitatively, the detection of HSP70 in the isolate will provide as a proof that ECVs were present. Also, quantitatively the volume of serum from which HSP70 could be detected, will be suggestive for the volume from which tau protein can be demonstrated.

As shown by the western blot analysis (Figure 3-11), using 11ml serum, tau protein was not obviously detected (Figure 3-11A), while the protein was weakly detected in the 80ml serum (Figure 3-11B). Since a weak positive reaction was observed for tau protein in the 80ml serum, it suggests that to efficiently demonstrate tau protein by western blot at least a volume of 80ml would be required. But this will be challenging, as obtaining 80ml serum will require sampling of at least 240ml whole blood, a quantity that cannot be practicable for routine diagnosis. Even the 11ml serum will require at least 33ml whole blood and this will also be a challenge.

4.4.4. ECVs isolation using the Bead-assisted technique

Though this study has shown that ECVs contain tau protein using the western blot analysis (Figure 3-11), quantification of the protein will require at least 80ml serum, several days for sample processing and the detected protein could not be addressed to it origin. Hence, this study aimed at another method that could quantify cargo proteins from specific ECVs (ndECVs) in considerably reduced time and more importantly require less starting material.

Hence, the flow cytometric platform was exploited. Flow cytometry is a simple well-established sensitive technique for high-throughput qualitative, quantitative or multiparametric analysis [Zhu et al., 2014]. Based on light scattering property of flow cytometer, information on the morphology, size and shape can be obtained. Also based on fluorescence labelling, flow cytometry technique can be used to analyse biochemical characteristic (such as antigens) of a cell or particle [Zhu et al., 2014]. However, the typical flow cytometers were designed for cells [Zhu et al., 2014] and therefore particles below 1µl are generally unable to scatter forward light. The scattering of light in the instrument is generally considered an indication that cell or particle is present [van der Pol et al., 2012].

Since the smallest ECVs are about 20nm [Muller et al., 2014], using the typical flow cytometer to measure these vesicles directly could pose a challenge, particularly regarding forward light scattering. To overcome this drawback, beads were used to capture the vesicles before flow cytometry analysis. Coupling ECVs onto beads have the

advantage of concentrating several vesicles on a single bead and thereby makes it appear large enough to scatter forward light [Morales-Kastresana; Jones, 2017]. Besides, human peripheral blood contains a mixture of components including various sizes of ECVs, nucleic acid aggregates and subcellular fragment [Muller et al., 2014] which are likely to remain in the supernatant following the low-speed (10,000xg) centrifugation (2.4.3.1). These aggregates or components can equally sediment along with the ECVs during the pelleting by ultracentrifugation process (2.4.3.3) and contaminate the recovered vesicles. However, using beads that have been coated with specific antibodies directed against ECVs' marker proteins (CD63 or CD171), one can selectively isolate ECVs which are devoid of any contaminants.

Based on this background information, this study next adopted the bead-assisted strategy of isolating ECV for flow cytometry analysis. The technique was first used to isolate general ECVs before using it to isolate cell type specific ECVs. This was done to ascertain the reliability of using the technique to isolate ndECVs. From the result (Figure 3-6), ECVs were isolated by the bead-based method and verified by the flow cytometry, a development that was interesting. Earlier, a study has used the bead-assisted technique to isolate ECVs except that the material used was cultured cells [Oksvold et al., 2015]. Altogether, the bead-based flow cytometry platform was suitable for isolation and detection of ECVs. Further, the procedure was rapid, simple and efficient for ECVs isolation and analysis

4.4.5. Isolation of cell type specific ECVs (ndECVs)

As ECVs contain repertoire of signatories from their parental cells, using beads coated with antibodies directed against the ndECVs' marker protein CD171, these cell type specific ECVs could be isolated and measured. This further makes the bead-assisted strategy for flow cytometry analysis an attractive technique. Having established a valid protocol for isolating ECVs in general (Figure 3-6), the study modified the procedure with the aim of capturing ndECVs using CD171 coated beads. Here also, ndECVs were successfully isolated from the serum of two independent young healthy donors (Figure 3-7B). As neuron derived ECVs are characterized by the marker protein CD171 and cultured

human neuroblastoma cell line SH-SY5Y were known to release ECVs which are CD171 positive [Park et al., 2015], it was included to provide as positive control. Remarkably, the technique isolated and measure ndECVs from the positive control (Figure 3-7A) hence, the isolation was considered successful. Following this positive finding, the study assumed that the bead-assisted technique was suitable for isolating ndECVs for downstream analysis. But a major concern that existed was whether to use plasma or serum.

4.4.6. Comparison of plasma and serum as a source of ndECVs

Is being speculated that, in the process of obtaining serum from blood, ECVs are trapped in the clot and this can potentially affect the recovered vesicles [Muller et al., 2014]. Likewise, in obtaining plasma from blood, the formation of heparin-ECV complex can also deplete the total quantity of the ECVs [Atai et al., 2013]. Considering these important concerns, there was the need to compare and identify the most suitable starting material. To address these concerns, ndECVs were isolated from both plasma and serum of a single donor and compared qualitatively. Interestingly, there was no major difference between the qualitative yield ndECVs from both sources (Figure 3-8). Therefore, either plasma or serum is just appropriate to be used for the isolation ndECVs. Thus, the choice of serum or plasma should be based on the availability. However, to avoid potential interference of heparin-ECV complex in plasma which could influence the recovery of ndECVs, this study opted to use serum.

Having isolated of ndECVs from human serum, next, the study focused on identifying the ideal minimum volume that could be used as starting material. It is important to identify the minimum volume of serum require per flow cytometry test to provide as a guide for subsequent analysis. After evaluating different volumes, the study observed that ndECVs can be detected and measured from at least 250μl of serum (Figure 3-9). Increasing the starting volume is not wrong, however, no significant variation in the measured vesicles was observed qualitatively (Figure 3-9) if the used beads are kept constant (5μl). This finding is attractive in the sense that not much blood will be required to perform this test should it be accepted in clinical settings.

Next, the study wanted to find out if the enrichment of ECVs via ultracentrifugation was a necessary step or it could be skipped. This could properly save time and uphold the integrity of the sample. In address this issue, beads coated with CD171 antibodies were used to isolate ndECVs from pelleted serum (2.4.3.3) or pre-cleaned serum (2.4.3.1). It was observed that ndECVs can be isolated from either pelleted or pre-cleaned serum (Figure 3-10). Although ndECVs could be isolated from pre-cleaned serum, pelleting by ultracentrifugation improve the isolation process and this was shown by the pronounced positive signal by the pelted vesicles (Figure 3-10). Altogether, using bead-assisted technique, ndECVs can be isolated from either pelleted or pre-cleaned serum, and that the choice should be based on the intended downstream analysis.

4.5. Detection and quantification of ECVs' cargo proteins (HSP70 & tau)

4.5.1. Flow cytometry analysis

Considering the high-throughput nature of flow cytometry, this study next attempted using the technique to detect and quantify tau proteins in ndECVs. But prior to this quantifying the tau protein, the study first aimed to quantify HSP70 in the vesicles. The demonstration of HSP70 in the vesicles using flow cytometry was due to it abundance in ECVs (Figure 3-1B, 3-2, 3-3C, & 3-4). Hence, using HSP70 as an initial target protein to be detected is not only suitable but also provides a guarantee for the established protocol. To further ensure the robustness of this platform, two positive controls were included. The first being SH-SY5Y cells and the second, pelleted ECVs from SH-SY5Y cell suspension. As the protein HSP70 is present in SH-SY5Y cells, it was important to include it serve as a proof of the principle.

Surprisingly, the cargo HSP70 was not detected in the ECVs obtained from the young healthy donor (Figure 3-12A & 3-12B) as well as ECVs obtained from the supernatant of the SH-SY5Y cell (Figure 3-12C & 3-12D). On the contrarily, the protein was detected in the cells of SH-SY5Y (Figure 3-12E & 3-12F). The detection of HSP70 in the cells suggests that the applied platform is possible except that at present it could not detect HSP70 in ECVs. The exact reason for this unexpected result appears complex however, the following speculations can be considered. To start with, one of the basic steps in this

procedure was fixation of the vesicles and its components by paraformaldehyde. Typically, paraformaldehyde functions by inducing cross-linkage among proteins to form bridges or mesh. The formation of this bridges help preserve the integrity of the components. But because some of the ECVs have a size of about 20nm [Muller et al., 2014], such a crossing linking characteristic of the fixative could further enhance rigidity. Indeed, prior to staining the cargo protein, the ECVs were permeabilised, but due to their small sizes and the rigidity confer by the fixative might have rendered the permeabilization ineffective.

Again, another possible reason why the ECVs' cargo could not be detected in the vesicles may be due to the large size of the antibody-fluorophore complex (HSP70-PE). Like the fluorophore allophycocyanin (APC) or phycocyanin (PC), the PE also belongs to the family phycobilisome which has a diameter of 11nm and a thickness of 6nm all enclosed in a central channel of a diameter 4.5nm [FICNER; HUBER, 1993]. Considering this size of the PE in addition to the antibody (anti-HSP70) may form a large complex that could not enter and stain the cargo in the ECVs. This justification is likely to hold because HSP70 in the SH-SY5Y cells were stained, possibly because the cells are larger than the vesicles. Based on the above discussion, this study suggests that a modification of the antibody and the fluorophore to a smaller size could be helpful.

4.5.2. ELISA analysis

While this study continues to identify the exact reason why the flow cytometry strategy was unable to detect the ECVs' cargo protein (HSP70), there was the need to proceed with the evaluation of tau protein in ndECVs from the clinical samples using alternative platform. The ELISA method was adopted as alternative approach to detect and quantify the protein in the vesicles. The reason for using ELISA was because it is a sensitive technique and it has been used extensively to evaluate tau proteins in plasma or serum [Vanmechelen et al., 2000; Sparks et al., 2012; Fiandaca et al., 2015; Guix et al., 2018]

However, in a study by Fiandaca and colleagues, 0.15ml of thromboplastin D was added to aid blood clotting. But generally, thromboplastin D is prepared from rabbit brain and therefore has the potential of introducing exogenous tau protein into samples [Guix et al.,

2018]. To avoid the possibility of such exogenous tau protein from thromboplastin D, Guix and colleagues substituted thrombin for thromboplastin D [Guix et al., 2018]. But, here also, thrombin can truncate or cleave the tau protein [Guo et al., 2017]. Hence neither thromboplastin D nor thrombin was added in this current study

From the ELISA analysis result (Figure 3-13), tau protein was detected and measured in the pure serum, ndECVs and non-ndECVs of the clinical samples using the 1G2 antibody ELISA assay. Also, tau protein was measured in the ECVs obtained from SH-SY5Y cells (positive control). The 1G2 antibody identifies tau proteins that are non-phosphorylated at epitope containing Thr175 or Thr181 [Lewczuk et al., 2017]. Since only a small fraction of the entire total tau protein is phosphorylated [Lewczuk et al., 2017], an antibody that target only phosphorylated site has the tendency to exclude most measurable tau proteins. Fortunately, the antibody (1G2) used in this current study was directed towards non-phosphorylated epitopes of the tau protein. And therefore, has the advantage of measuring most of the available protein as well as quantify the proteins that are not phosphorylated at stated epitopes [Lewczuk et al., 2017]. More so, this adopted ELISA technique was able measure tau in the ECVs of SH-SY5Y cells (positive control). The SY5Y cells has been transfected with cDNA for human tau protein (2.4.2 paragraph 2) and therefore the measurement of the protein in the vesicles further guarantees the validity of the applied platform.

Having measured tau protein in ndECVs, the study wanted to identify the possible correlation between tau protein in these vesicles and the available predictive markers (CSF tau, CSF p-tau & CSF β-amyloid) of AD. Unexpectedly, no obvious correlation existed between tau protein in ndECVs and these 3 diagnostic markers of AD (Figure 3-16). Possible reason for this finding may be due to the small sample size (28 participants). Of the total 28 participants, the assay measured tau protein in the ndECVs of only 7, therefore the observed weak correlation is not surprising. As no obvious correlation was observed between blood-based ndECVs' tau protein and any of the validated markers of AD, the use of this vesicle-based protein for the diagnosis of AD is currently not practicable. Further, due to the observed weak correlation, blood-based ndECVs' tau protein is not feasible to be used as a surrogate to any of the existing AD diagnostic markers (CSF tau, CSF p-tau & CSF β-amyloid).   Nevertheless, the measurement of tau

protein in ndECVs by this current study is interesting because it further contributes to the previous reports that, the protein is measurable in these vesicles [Fiandaca et al., 2015; Winston et al., 2016; Guix et al., 2018].

Like a previous work [Guix et al., 2018], the amount of tau protein measured in the ndECVs were less than that measured as free floating in serum. Thus, more tau proteins were measured in the pure serum compared to ndECVs or non-ndECVs (Figure 3-13). The exact reason for this observation appears complex but the following could be speculated. That, following the migration of tau protein in ndECVs from neurons in the brain into peripheral blood [Weinstein; Seshadri, 2014], the vesicles then release the tau protein to float freely in the tissue. Thus, peripheral blood may serve as the destination for the removal of the unneeded tau protein in the brain. And the fact that tau protein was detected in the ndECVs arguably suggests that, the vesicle is involved in the transportation of the protein into blood. Another possible reason could be that, tau protein encapsulated in migrant ndECVs becomes endocytosed by resident cells in the peripheral blood and reduce their quantity.   Moreover, a truncation activity of thrombin on tau protein could have resulted in a pseudo-high value since tau protein is highly susceptible to thrombin (common in peripheral blood) proteolytic cleavage [Guo et al., 2017].

Even though more tau proteins were measured in the serum compared to that of ndECVs, there was no strong correlation between the serum tau protein and CSF tau or CSF p-tau (Figure 3-15A & 3-15B). However, of major interest was the trend for a correlation between serum tau protein and CSF β-amyloid (Figure 15C). The observed trend for a negative correlation (-0.467) can be interpreted; as serum tau protein increases CSF β-amyloid decreases, a pattern that may suggest that AD related reduction of Aβ is accompanied by a serum tau increase.

The former interpretation is more likely because it has resemblance to current clinical diagnosis AD (1.3 paragraphs 3). While this finding is exciting, a larger sample size would be helpful to substantiate this observation.

Furthermore, as there are concerns that the neuropsychological tests are influenced by a person's education or race [Crum et al., 1993], the study correlated MMSE to either

serum tau or ndECVs' tau protein. With the aim that where a strong correlation might occur, could form basis for consideration or otherwise. The MMSE evaluate a person's orientation to a place and time [McKhann et al., 1984], and is graded on a 30-point scale. The following is how MMSE is graded: orientation, 10 points; ability to recall things, 6 points; ability to concentrate, 5 points; language skill, 8 points; and visuospatial function, 1-point [Folstein et al., 1975]. A score below 23 points is generally considered abnormal. The grading principle of Montreal Cognitive Assessment (MoCA) and the Saint Louis University Mental Status (SLUMS) are like that of MMSE except that a score of less than 25 is abnormal for MoCA [Nasreddine et al., 2005]. Here also, there was no obvious correlation between MMSE and serum tau protein (Figure 3-15D) or ndECVs' tau protein (Figure 3-15D). While this study has provided a basis for further study, a larger sample size would be required to show the relationship between MMSE and tau protein in the ndECVs. In addition to considering a larger sample size in future studies, the use of ultra-sensitive technique such as single molecule array (simoa) may be considered for the measurement of tau protein in the ndECVs. This study was unable to discriminate between cancer related ECVs that could also be CD171$^+$ from the neuron derived ECVs (CD171$^+$).

4.5.3. Tau protein in the ECVs of hibernating animals

As discussed earlier for SH-SY5Y cells (4.5.1, paragraph 1), hibernating hamsters (*Mesocricetus auratus)* were also included as a second positive control sample to further cornfim that tau protein in the vesicles were indeed measurable by the ELISA platform. The phenotypic lesions of AD have demonstrated in Caenorhabditis elegans, Drosophila melanogaster, Xenopus oocytes, mice, European squirrels and hamsters [Lewis et al., 2000; Arendt et al., 2003; Lee et al., 2005; Härtig et al., 2007]. This study included hamsters because hyperphosphorylated tau protein has been demonstrated in the brain of torpid state (7°C) hibernators [Arendt et al., 2003]. During reduced body temperature (hypothermic state) serine-threonine protein phosphatase activity is inhibited, while kinases activities are favoured resulting in the hyperphosphorylation of the tau protein in the brain [Planel et al., 2001; Planel et al., 2004; Planel et al., 2007; Whittington et al., 2011]. As AD is not localised to the brain, one will expect that such AD-like lesion in the

hibernators should be accessible in peripheral blood. This was the reason for the inclusion of the hamsters.

Remarkably, tau protein was measured in the serum and ECVs of the hibernating hamsters that were in the torpor state (5 – 10°C) as well as euthermic (~37°C) state non-hibernators (Figure 3-17). Even though tau proteins were measured in these two state hamsters, there was a significant difference in the measured means. Thus, more tau proteins were measured (both pure serum and ECVs) in the torpid state *M. auratus* compared to the euthermic state ones. This observation was interesting because it confirms that tau protein is measurable in peripheral blood.

In addition to these animals serving as positive control, the study made some observations that need to be discussed. In either serum or ECVs, the mean tau protein concentration in the torpid state was higher than that of the euthermic state (Figure 3-17A & 3-17B). The following speculations could be attributed to the observed higher tau protein in the torpid hamsters. Hypothermic state induces tau phosphorylation [Planel et al., 2004] which may represent a protective mechanism [Arendt et al., 2003], but prolong hypothermia may generate excessive hyperphosphorylation of the protein and accumulated in the neurons. Further inhibition of protein phosphatase 2A (PP2A) during hypothermia [Planel et al., 2001] promote the accumulation of the abnormal protein. In addition to the hyperphosphorylated tau protein being toxic to the cells, it is also proficient in sequestering other neuronal microtubule associated proteins, MAP1 and MAP2 [Alonso et al., 1997]. Due to the permeable state of the BBB during enforced hibernation [Baldwin, 1968; Wells, 1972], tau protein may use this channel to exit the brain cells into peripheral blood. But to avoid potential insult to neighbouring cells, tau protein from the brain may be transported in secluded manner. The demonstration of the tau protein in the ECVs further proofs that these vesicles are the potential culprit in the transportation of protein from the brain to the blood. The passage of tau protein through BBB is possible during hypothermic state because most of the physiological processes such as depolarization, calcium influx and signal transmission are maintained [Horowitz; Horwitz, 2019].

5. CONCLUSION

This study is the first to have attempted to measure tau protein in peripheral blood ndECVs using flow cytometry technique. While quantification of tau protein by flow cytometry platform was a challenge, ELISA technique was used as alternative to measure the proteins in the vesicles. Tau protein was measured in the peripheral blood (serum and ndECVs) of patients who have already undergone the routine clinical diagnosis for AD. However, the study did not observe any strong correlation between tau protein in ndECVs and the validated diagnostic markers (CSF tau, CSF p-tau, CSF β-amyloid or MMSE evaluation) of AD. Of interest is the trend for a negative correlation (r = -0.467, p=0.059) between serum tau protein and CSF β-amyloid, a pattern that may suggest that AD related reduction of Aβ is accompanied by a serum tau increase. Peripheral blood is a relevant source for tau protein measurement and therefore more studies are needed to evaluate the significance of blood serum tau content as a diagnostic biomarker for AD.

6. REFERENCES

Abner EL, Jicha GA, Shaw LM, Trojanowski JQ, Goetzl EJ. 2016. Plasma neuronal exosomal levels of Alzheimer's disease biomarkers in normal aging. Annals of clinical and translational neurology 3:399–403.

Akingbade OES, Gibson C, Kalaria RN, Mukaetova-Ladinska EB. 2018. Platelets: Peripheral Biomarkers of Dementia? Journal of Alzheimer's disease: JAD 63:1235–1259.

Albert MS, DeKosky ST, Dickson D, Dubois B, Feldman HH, Fox NC, Gamst A, Holtzman DM, Jagust WJ, Petersen RC, Snyder PJ, Carrillo MC, Thies B, Phelps CH. 2011. The diagnosis of mild cognitive impairment due to Alzheimer's disease: recommendations from the National Institute on Aging-Alzheimer's Association workgroups on diagnostic guidelines for Alzheimer's disease. Alzheimer's & dementia: the journal of the Alzheimer's Association 7:270–279.

Alkon DL, Sun M-K, Nelson TJ. 2007. PKC signaling deficits: a mechanistic hypothesis for the origins of Alzheimer's disease. Trends in pharmacological sciences 28:51–60.

Alladi S, Xuereb J, Bak T, Nestor P, Knibb J, Patterson K, Hodges JR. 2007. Focal cortical presentations of Alzheimer's disease. Brain 130:2636–2645.

Alonso AD, Grundke-Iqbal I, Barra HS, Iqbal K. 1997. Abnormal phosphorylation of tau and the mechanism of Alzheimer neurofibrillary degeneration: sequestration of microtubule-associated proteins 1 and 2 and the disassembly of microtubules by the abnormal tau. Proceedings of the National Academy of Sciences of the United States of America 94:298–303.

Alvarez ML. 2014. Isolation of urinary exosomes for RNA biomarker discovery using a simple, fast, and highly scalable method. Methods in molecular biology (Clifton, N.J.) 1182:145–170.

Alzheimer A. 1907. Uber eine eigenartige Erkrankung der Hirnrinde. Allgemeine Zeitschrift fur Psychiatrie und phychish-Gerichtliche Medizin:146–148.

Alzheimer's Association. 2019. 2019 Alzheimer's disease facts and figures. Alzheimer's & Dementia 15:321–387.

Alzheimer's Disease

An M, Wu J, Zhu J, Lubman DM. 2018. Comparison of an Optimized Ultracentrifugation Method versus Size-Exclusion Chromatography for Isolation of Exosomes from Human Serum. Journal of proteome research 17:3599–3605.

Arai T, Guo J-P, McGeer PL. 2005. Proteolysis of non-phosphorylated and phosphorylated tau by thrombin. The Journal of biological chemistry 280:5145–5153.

Arendt T, Stieler J, Strijkstra AM, Hut RA, Rüdiger J, van der Zee EA, Harkany T, Holzer M, Härtig W. 2003. Reversible paired helical filament-like phosphorylation of tau is an adaptive process associated with neuronal plasticity in hibernating animals. The Journal of neuroscience: the official journal of the Society for Neuroscience 23:6972–6981.

Arendt T, Stieler J, Ueberham U. 2017. Is sporadic Alzheimer's disease a developmental disorder? Journal of neurochemistry 143:396–408.

Arendt T, Stieler JT, Holzer M. 2016. Tau and tauopathies. Brain research bulletin 126:238–292.

Arevalo-Rodriguez I, Smailagic N, Roqué I Figuls M, Ciapponi A, Sanchez-Perez E, Giannakou A, Pedraza OL, Bonfill Cosp X, Cullum S. 2015. Mini-Mental State Examination (MMSE) for the detection of Alzheimer's disease and other dementias in people with mild cognitive impairment (MCI). The Cochrane database of systematic reviews:CD010783.

Atai NA, Balaj L, van Veen H, Breakefield XO, Jarzyna PA, van Noorden CJF, Skog J, Maguire CA. 2013. Heparin blocks transfer of extracellular vesicles between donor and recipient cells. Journal of neuro-oncology 115:343–351.

Avila J, Lucas JJ, Perez M, Hernandez F. 2004. Role of tau protein in both physiological and pathological conditions. Physiological reviews 84:361–384.

Baldwin M. 1968. Cerebral argyria after hibernation. Neurology 18:813–816.

Bartheld CS von, Altick AL. 2011. Multivesicular bodies in neurons: distribution, protein content, and trafficking functions. Progress in neurobiology 93:313–340.

Bebelman MP, Smit MJ, Pegtel DM, Baglio SR. 2018. Biogenesis and function of extracellular vesicles in cancer. Pharmacology & therapeutics 188:1–11.

Bekris LM, Yu C-E, Bird TD, Tsuang DW. 2010. Genetics of Alzheimer disease. Journal of geriatric psychiatry and neurology 23:213–227.

BERKELEY J. 2009. Neurodegenerative and Movement Disorders. Cerebrospinal Fluid in Clinical Practice: Elsevier, p 115–119.

BLASS JP, SHEU K-FR, PIACENTINI S, SORBI S. 1997. Inherent Abnormalities in Oxidative Metabolism in Alzheimer's Disease: Interaction with Vascular Abnormalities. Ann NY Acad Sci 826:382–385.

Blennow K, Zetterberg H, Fagan AM. 2012. Fluid biomarkers in Alzheimer disease. Cold Spring Harbor perspectives in medicine 2: a006221.

Bodea L-G, Eckert A, Ittner LM, Piguet O, Götz J. 2016. Tau physiology and pathomechanisms in frontotemporal lobar degeneration. Journal of neurochemistry 138 Suppl 1:71–94.

Bonotis K, Krikki E, Holeva V, Aggouridaki C, Costa V, Baloyannis S. 2008. Systemic immune aberrations in Alzheimer's disease patients. Journal of neuroimmunology 193:183–187.

Braak H, Braak E. 1991. Neuropathological stageing of Alzheimer-related changes. Acta neuropathologica 82:239–259.

Bramblett GT, Goedert M, Jakes R, Merrick SE, Trojanowski JQ, Lee VMY. 1993. Abnormal tau phosphorylation at Ser396 in alzheimer's disease recapitulates development and contributes to reduced microtubule binding. Neuron 10:1089–1099.

Brion JP. 1998. Neurofibrillary tangles and Alzheimer's disease. European neurology 40:130–140.

Brothers HM, Gosztyla ML, Robinson SR. 2018. The Physiological Roles of Amyloid-β Peptide Hint at New Ways to Treat Alzheimer's Disease. Frontiers in aging neuroscience 10:118.

Buée L, Bussière T, Buée-Scherrer V, Delacourte A, Hof PR. 2000. Tau protein isoforms, phosphorylation and role in neurodegenerative disorders. Brain research. Brain research reviews 33:95–130.

Buerger K, Zinkowski R, Teipel SJ, Tapiola T, Arai H, Blennow K, Andreasen N, Hofmann-Kiefer K, DeBernardis J, Kerkman D, McCulloch C, Kohnken R, Padberg F, Pirttilä T, Schapiro MB, Rapoport SI, Möller H-J, Davies P, Hampel H. 2002. Differential diagnosis of Alzheimer disease with cerebrospinal fluid levels of tau protein phosphorylated at threonine 231. Archives of neurology 59:1267–1272.

Calignon A de, Polydoro M, Suárez-Calvet M, William C, Adamowicz DH, Kopeikina KJ, Pitstick R, Sahara N, Ashe KH, Carlson GA, Spires-Jones TL, Hyman BT. 2012. Propagation of tau pathology in a model of early Alzheimer's disease. Neuron 73:685–697.

Cantin R, Diou J, Bélanger D, Tremblay AM, Gilbert C. 2008. Discrimination between exosomes and HIV-1: purification of both vesicles from cell-free supernatants. Journal of immunological methods 338:21–30.

Chen K, Huang J, Gong W, Zhang L, Yu P, Wang JM. 2006. CD40/CD40L dyad in the inflammatory and immune responses in the central nervous system. Cellular & molecular immunology 3:163–169.

Chivet M, Hemming F, Pernet-Gallay K, Fraboulet S, Sadoul R. 2012. Emerging role of neuronal exosomes in the central nervous system. Frontiers in physiology 3:145.

Chow VW, Mattson MP, Wong PC, Gleichmann M. 2010. An overview of APP processing enzymes and products. Neuromolecular medicine 12:1–12.

Colombo M, Raposo G, Théry C. 2014. Biogenesis, secretion, and intercellular interactions of exosomes and other extracellular vesicles. Annual review of cell and developmental biology 30:255–289.

Coronel R, Bernabeu-Zornoza A, Palmer C, Muñiz-Moreno M, Zambrano A, Cano E, Liste I. 2018. Role of Amyloid Precursor Protein (APP) and Its Derivatives in the Biology and Cell Fate Specification of Neural Stem Cells. Molecular neurobiology 55:7107–7117.

Crum RM, Anthony JC, Bassett SS, Folstein MF. 1993. Population-based norms for the Mini-Mental State Examination by age and educational level. JAMA 269:2386–2391.

Cummings J. 2012. Alzheimer's disease diagnostic criteria: practical applications. Alzheimer's research & therapy 4:35.

Davis DG, Schmitt FA, Wekstein DR, Markesbery WR. 1999. Alzheimer neuropathologic alterations in aged cognitively normal subjects. Journal of neuropathology and experimental neurology 58:376–388.

Dawkins E, Small DH. 2014. Insights into the physiological function of the β-amyloid precursor protein: beyond Alzheimer's disease. Journal of neurochemistry 129:756–769.

Fauré J, Lachenal G, Court M, Hirrlinger J, Chatellard-Causse C, Blot B, Grange J, Schoehn G, Goldberg Y, Boyer V, Kirchhoff F, Raposo G, Garin J, Sadoul R. 2006. Exosomes are released by cultured cortical neurones. Molecular and cellular neurosciences 31:642–648.

Favit A, Grimaldi M, Nelson TJ, Alkon DL. 1998. Alzheimer's-specific effects of soluble beta-amyloid on protein kinase C-alpha and -gamma degradation in human fibroblasts. Proceedings of the National Academy of Sciences of the United States of America 95:5562–5567.

Ferreira LK, Busatto GF. 2011. Neuroimaging in Alzheimer's disease: current role in clinical practice and potential future applications. Clinics (Sao Paulo, Brazil) 66 Suppl 1:19–24.

Fiandaca MS, Kapogiannis D, Mapstone M, Boxer A, Eitan E, Schwartz JB, Abner EL, Petersen RC, Federoff HJ, Miller BL, Goetzl EJ. 2015. Identification of preclinical Alzheimer's disease by a profile of pathogenic proteins in neurally derived blood

exosomes: A case-control study. Alzheimer's & dementia: the journal of the Alzheimer's Association 11:600-7. e1.

FICNER R, HUBER R. 1993. Refined crystal structure of phycoerythrin from Porphyridium cruentum at 0.23-nm resolution and localization of the gamma subunit. Eur J Biochem 218:103–106.

Folstein MF, Folstein SE, McHugh PR. 1975. "Mini-mental state". A practical method for grading the cognitive state of patients for the clinician. Journal of psychiatric research 12:189–198.

Frühbeis C, Fröhlich D, Krämer-Albers E-M. 2012. Emerging roles of exosomes in neuron-glia communication. Frontiers in physiology 3:119.

Galasko D, Hansen LA, Katzman R, Wiederholt W, Masliah E, Terry R, Hill LR, Lessin P, Thal LJ. 1994. Clinical-neuropathological correlations in Alzheimer's disease and related dementias. Archives of neurology 51:888–895.

Galton CJ, Patterson K, Xuereb JH, Hodges JR. 2000. Atypical and typical presentations of Alzheimer's disease: a clinical, neuropsychological, neuroimaging and pathological study of 13 cases. Brain 123 Pt 3:484–498.

Gasparini L, Racchi M, Binetti G, Trabucchi M, Solerte SB, Alkon D, Etcheberrigaray R, Gibson G, Blass J, Paoletti R, Govoni S. 1998. Peripheral markers in testing pathophysiological hypotheses and diagnosing Alzheimer's disease. The FASEB Journal 12:17–34.

Ghidoni R, Paterlini A, Albertini V, Glionna M, Monti E, Schiaffonati L, Benussi L, Levy E, Binetti G. 2011. Cystatin C is released in association with exosomes: a new tool of neuronal communication which is unbalanced in Alzheimer's disease. Neurobiology of aging 32:1435–1442.

Ghiso J, Matsubara E, Koudinov A, Choi-Miura NH, Tomita M, Wisniewski T, Frangione B. 1993. The cerebrospinal-fluid soluble form of Alzheimer's amyloid beta is complexed to SP-40,40 (apolipoprotein J), an inhibitor of the complement membrane-attack complex. The Biochemical journal 293 (Pt 1):27–30.

Glenner GG. 1982. Alzheimer's Disease (Senile Dementia). Journal of the American Geriatrics Society 30:59–62.

Glenner GG, Wong CW. 1984. Alzheimer's disease: Initial report of the purification and characterization of a novel cerebrovascular amyloid protein. Biochemical and biophysical research communications 120:885–890.

Glenner GG, Wong CW. 1986. The Nature and Pathogenesis of the Amyloid Deposits in Alzheimer's Disease. In: Marrink J, van Rijswijk MH, editors. Amyloidosis. Dordrecht: Springer Netherlands, p 227–242.

Goedert M, Spillantini MG, Potier MC, Ulrich J, Crowther RA. 1989. Cloning and sequencing of the cDNA encoding an isoform of microtubule-associated protein tau containing four tandem repeats: differential expression of tau protein mRNAs in human brain. The EMBO journal 8:393–399.

Gómez-Isla T, Price JL, McKeel DW, Morris JC, Growdon JH, Hyman BT. 1996. Profound loss of layer II entorhinal cortex neurons occurs in very mild Alzheimer's disease. J. Neurosci. 16:4491–4500.

Goossens J, Bjerke M, Struyfs H, Niemantsverdriet E, Somers C, van den Bossche T, van Mossevelde S, Vil B de, Sieben A, Martin J-J, Cras P, Goeman J, Deyn PP de, van Broeckhoven C, van der Zee J, Engelborghs S. 2017. No added diagnostic value of non-phosphorylated tau fraction (p-taurel) in CSF as a biomarker for differential dementia diagnosis. Alzheimer's research & therapy 9:49.

Greening DW, Xu R, Ji H, Tauro BJ, Simpson RJ. 2015. A protocol for exosome isolation and characterization: evaluation of ultracentrifugation, density-gradient separation, and immunoaffinity capture methods. Methods in molecular biology (Clifton, N.J.) 1295:179–209.

Grimm MOW, Mett J, Stahlmann CP, Haupenthal VJ, Zimmer VC, Hartmann T. 2013. Neprilysin and Aβ Clearance: Impact of the APP Intracellular Domain in NEP Regulation and Implications in Alzheimer's Disease. Frontiers in aging neuroscience 5:98.

Grundke-Iqbal I, Iqbal K, Tung YC, Quinlan M, Wisniewski HM, Binder LI. 1986. Abnormal phosphorylation of the microtubule-associated protein tau (tau) in Alzheimer cytoskeletal pathology. Proceedings of the National Academy of Sciences of the United States of America 83:4913–4917.

Gu Y, Oyama F, Ihara Y. 1996. Tau is widely expressed in rat tissues. Journal of neurochemistry 67:1235–1244.

Guix FX, Corbett GT, Cha DJ, Mustapic M, Liu W, Mengel D, Chen Z, Aikawa E, Young-Pearse T, Kapogiannis D, Selkoe DJ, Walsh DM. 2018. Detection of Aggregation-Competent Tau in Neuron-Derived Extracellular Vesicles. International journal of molecular sciences 19.

Guo JL, Lee VM-Y. 2011. Seeding of normal Tau by pathological Tau conformers drives pathogenesis of Alzheimer-like tangles. The Journal of biological chemistry 286:15317–15331.

Guo T, Noble W, Hanger DP. 2017. Roles of tau protein in health and disease. Acta neuropathologica 133:665–704.

Guzmán-Martinez L, Farías GA, Maccioni RB. 2013. Tau oligomers as potential targets for Alzheimer's diagnosis and novel drugs. Frontiers in neurology 4:167.

Hampel H, Blennow K, Shaw LM, Hoessler YC, Zetterberg H, Trojanowski JQ. 2010. Total and phosphorylated tau protein as biological markers of Alzheimer's disease. Experimental gerontology 45:30–40.

Hansson O, Zetterberg H, Buchhave P, Londos E, Blennow K, Minthon L. 2006. Association between CSF biomarkers and incipient Alzheimer's disease in patients with mild cognitive impairment: A follow-up study. The Lancet Neurology 5:228–234.

Harding C, Stahl P. 1983. Transferrin recycling in reticulocytes: pH and iron are important determinants of ligand binding and processing. Biochemical and biophysical research communications 113:650–658.

Härtig W, Stieler J, Boerema AS, Wolf J, Schmidt U, Weissfuss J, Bullmann T, Strijkstra AM, Arendt T. 2007. Hibernation model of tau phosphorylation in hamsters: selective

vulnerability of cholinergic basal forebrain neurons - implications for Alzheimer's disease. The European journal of neuroscience 25:69–80.

Hauser WA, Morris ML, Heston LL, Anderson VE. 1986. Seizures and myoclonus in patients with Alzheimer's disease. Neurology 36:1226–1230.

Hedley DW, Friedlander ML, Taylor IW, Rugg CA, Musgrove EA. 1983. Method for analysis of cellular DNA content of paraffin-embedded pathological material using flow cytometry. The journal of histochemistry and cytochemistry: official journal of the Histochemistry Society 31:1333–1335.

Helwa I, Cai J, Drewry MD, Zimmerman A, Dinkins MB, Khaled ML, Seremwe M, Dismuke WM, Bieberich E, Stamer WD, Hamrick MW, Liu Y. 2017. A Comparative Study of Serum Exosome Isolation Using Differential Ultracentrifugation and Three Commercial Reagents. PloS one 12: e0170628.

Hof PR, Cox K, Morrison JH. 1990. Quantitative analysis of a vulnerable subset of pyramidal neurons in Alzheimer's disease: I. Superior frontal and inferior temporal cortex. The Journal of comparative neurology 301:44–54.

Hogervorst E, Bandelow S, Combrinck M, Irani SR, Irani S, Smith AD. 2003. The validity and reliability of 6 sets of clinical criteria to classify Alzheimer's disease and vascular dementia in cases confirmed post-mortem: added value of a decision tree approach. Dementia and geriatric cognitive disorders 16:170–180.

Holzer M, Holzapfel H-P, Zedlick D, Brückner MK, Arendt T. 1994. Abnormally phosphorylated tau protein in Alzheimer's disease: Heterogeneity of individual regional distribution and relationship to clinical severity. Neuroscience 63:499–516.

Homolak J, Mudrovčić M, Vukić B, Toljan K. 2018. Circadian Rhythm and Alzheimer's Disease. Medical sciences (Basel, Switzerland) 6.

Horowitz JM, Horwitz BA. 2019. Extreme Neuroplasticity of Hippocampal CA1 Pyramidal Neurons in Hibernating Mammalian Species. Frontiers in neuroanatomy 13:9.

Hurd MD, Martorell P, Delavande A, Mullen KJ, Langa KM. 2013. Monetary costs of dementia in the United States. The New England journal of medicine 368:1326–1334.

Hyman BT, Kromer LJ, van Hoesen GW. 1987. Reinnervation of the hippocampal perforant pathway zone in Alzheimer's disease. Annals of neurology 21:259–267.

Hyman BT, Trojanowski JQ. 1997. Consensus recommendations for the postmortem diagnosis of Alzheimer disease from the National Institute on Aging and the Reagan Institute Working Group on diagnostic criteria for the neuropathological assessment of Alzheimer disease. Journal of neuropathology and experimental neurology 56:1095–1097.

Ibrahim A, Marbán E. 2016. Exosomes: Fundamental Biology and Roles in Cardiovascular Physiology. Annual review of physiology 78:67–83.

Ikeda T, Yamamoto K, Takahashi K, Yamada M. 1991. Immune system-associated antigens on the surface of peripheral blood lymphocytes in patients with Alzheimer's disease. Acta psychiatrica Scandinavica 83:444–448.

Irizarry MC. 2004. Biomarkers of Alzheimer disease in plasma. NeuroRx : the journal of the American Society for Experimental NeuroTherapeutics 1:226–234.

Jakobsen KR, Paulsen BS, Bæk R, Varming K, Sorensen BS, Jørgensen MM. 2015. Exosomal proteins as potential diagnostic markers in advanced non-small cell lung carcinoma. Journal of extracellular vesicles 4:26659.

Ju Y-ES, Lucey BP, Holtzman DM. 2014. Sleep and Alzheimer disease pathology—a bidirectional relationship. Nature reviews. Neurology 10:115–119.

Kalani A, Tyagi A, Tyagi N. 2014. Exosomes: mediators of neurodegeneration, neuroprotection and therapeutics. Molecular neurobiology 49:590–600.

Kalluri R. 2016. The biology and function of exosomes in cancer. The Journal of clinical investigation 126:1208–1215.

Kang J-E, Lim MM, Bateman RJ, Lee JJ, Smyth LP, Cirrito JR, Fujiki N, Nishino S, Holtzman DM. 2009. Amyloid-beta dynamics are regulated by orexin and the sleep-wake cycle. Science (New York, N.Y.) 326:1005–1007.

Kanninen KM, Bister N, Koistinaho J, Malm T. 2016. Exosomes as new diagnostic tools in CNS diseases. Biochimica et biophysica acta 1862:403–410.

Khan TK, Alkon DL. 2010. Early diagnostic accuracy and pathophysiologic relevance of an autopsy-confirmed Alzheimer's disease peripheral biomarker. Neurobiology of aging 31:889–900.

Khan TK, Alkon DL. 2015. Peripheral biomarkers of Alzheimer's disease. Journal of Alzheimer's disease: JAD 44:729–744.

KIDD M. 1963. Paired Helical Filaments in Electron Microscopy of Alzheimer's Disease. Nature 197:192–193.

KIDD M. 1964. ALZHEIMER'S DISEASE —AN ELECTRON MICROSCOPICAL STUDY. Brain 87:307–320.

Kolarova M, García-Sierra F, Bartos A, Ricny J, Ripova D. 2012. Structure and pathology of tau protein in Alzheimer disease. International journal of Alzheimer's disease 2012:731526.

Kowal EJK, Ter-Ovanesyan D, Regev A, Church GM. 2017. Extracellular Vesicle Isolation and Analysis by Western Blotting. Methods in molecular biology (Clifton, N.J.) 1660:143–152.

Kraepelin E. 1910. Psychiatrie, Ein Lehrbuch für Studierende und Ärzte. Leipzig: Ambrosius Barth.

Lachenal G, Pernet-Gallay K, Chivet M, Hemming FJ, Belly A, Bodon G, Blot B, Haase G, Goldberg Y, Sadoul R. 2011. Release of exosomes from differentiated neurons and its regulation by synaptic glutamatergic activity. Molecular and cellular neurosciences 46:409–418.

Laemmli UK. 1970. Cleavage of structural proteins during the assembly of the head of bacteriophage T4. Nature 227:680–685.

Lai CP-K, Breakefield XO. 2012. Role of exosomes/microvesicles in the nervous system and use in emerging therapies. Frontiers in physiology 3:228.

Lakhal S, Wood MJA. 2011. Exosome nanotechnology: an emerging paradigm shift in drug delivery: exploitation of exosome nanovesicles for systemic in vivo delivery of RNAi heralds new horizons for drug delivery across biological barriers. BioEssays: news and reviews in molecular, cellular and developmental biology 33:737–741.

Lambrecht J, Jan Poortmans P, Verhulst S, Reynaert H, Mannaerts I, van Grunsven LA. 2017. Circulating ECV-Associated miRNAs as Potential Clinical Biomarkers in Early Stage HBV and HCV Induced Liver Fibrosis. Frontiers in pharmacology 8:56.

Lane RE, Korbie D, Trau M, Hill MM. 2017. Purification Protocols for Extracellular Vesicles. Methods in molecular biology (Clifton, N.J.) 1660:111–130.

Lanier LL, Warner NL. 1981. Paraformaldehyde fixation of hematopoietic cells for quantitative flow cytometry (FACS) analysis. Journal of immunological methods 47:25–30.

Lee VM-Y, Kenyon TK, Trojanowski JQ. 2005. Transgenic animal models of tauopathies. Biochimica et biophysica acta 1739:251–259.

Lendon CL, Ashall F, Goate AM. 1997. Exploring the etiology of Alzheimer disease using molecular genetics. JAMA 277:825–831.

Leuzy A, Chiotis K, Lemoine L, Gillberg P-G, Almkvist O, Rodriguez-Vieitez E, Nordberg A. 2019. Tau PET imaging in neurodegenerative tauopathies—still a challenge. Molecular Psychiatry 24:1112–1134.

Lewczuk P, Lelental N, Lachmann I, Holzer M, Flach K, Brandner S, Engelborghs S, Teunissen CE, Zetterberg H, Molinuevo JL, Mroczko B, Blennow K, Popp J, Parnetti L, Chiasserini D, Perret-Liaudet A, Spitzer P, Maler JM, Kornhuber J. 2017. Non-Phosphorylated Tau as a Potential Biomarker of Alzheimer's Disease: Analytical and Diagnostic Characterization. Journal of Alzheimer's disease: JAD 55:159–170.

Lewis J, McGowan E, Rockwood J, Melrose H, Nacharaju P, van Slegtenhorst M, Gwinn-Hardy K, Paul Murphy M, Baker M, Yu X, Duff K, Hardy J, Corral A, Lin WL, Yen SH, Dickson DW, Davies P, Hutton M. 2000. Neurofibrillary tangles, amyotrophy and progressive motor disturbance in mice expressing mutant (P301L) tau protein. Nature genetics 25:402–405.

Li M, Zeringer E, Barta T, Schageman J, Cheng A, Vlassov AV. 2014. Analysis of the RNA content of the exosomes derived from blood serum and urine and its potential as biomarkers. Philosophical transactions of the Royal Society of London. Series B, Biological sciences 369.

Li P, Kaslan M, Lee SH, Yao J, Gao Z. 2017. Progress in Exosome Isolation Techniques. Theranostics 7:789–804.

Lindwall G, Cole RD. 1984. Phosphorylation affects the ability of tau protein to promote microtubule assembly. The Journal of biological chemistry 259:5301–5305.

Lötvall J, Hill AF, Hochberg F, Buzás EI, Di Vizio D, Gardiner C, Gho YS, Kurochkin IV, Mathivanan S, Quesenberry P, Sahoo S, Tahara H, Wauben MH, Witwer KW, Théry C. 2014. Minimal experimental requirements for definition of extracellular vesicles and their functions: a position statement from the International Society for Extracellular Vesicles. Journal of extracellular vesicles 3:26913.

Lu J, Helton TD, Blanpied TA, Rácz B, Newpher TM, Weinberg RJ, Ehlers MD. 2007. Postsynaptic positioning of endocytic zones and AMPA receptor cycling by physical coupling of dynamin-3 to Homer. Neuron 55:874–889.

Maas SLN, Breakefield XO, Weaver AM. 2017. Extracellular Vesicles: Unique Intercellular Delivery Vehicles. Trends in cell biology 27:172–188.

Mahmood T, Yang P-C. 2012. Western blot: technique, theory, and trouble shooting. North American journal of medical sciences 4:429–434.

Mandelkow E-M, Mandelkow E. 2012. Biochemistry and cell biology of tau protein in neurofibrillary degeneration. Cold Spring Harbor perspectives in medicine 2: a006247.

Maness PF, Schachner M. 2007. Neural recognition molecules of the immunoglobulin superfamily: signaling transducers of axon guidance and neuronal migration. Nature neuroscience 10:19–26.

Marešová P, Mohelská H, Dolejš J, Kuča K. 2015. Socio-economic Aspects of Alzheimer's Disease. CAR 12:903–911.

Markowitsch HJ, Staniloiu A. 2012. Amnesic disorders. The Lancet 380:1429–1440.

Masliah E, Hansen L, Mallory M, Albright T, Terry RD. 1991. Abnormal brain spectrin immunoreactivity in sprouting neurons in Alzheimer disease. Neuroscience letters 129:1–5.

Masliah E, Terry R. 1993. The role of synaptic proteins in the pathogenesis of disorders of the central nervous system. Brain pathology (Zurich, Switzerland) 3:77–85.

Matsumoto J, Stewart T, Banks WA, Zhang J. 2017. The Transport Mechanism of Extracellular Vesicles at the Blood-Brain Barrier. Current pharmaceutical design 23:6206–6214.

Mazanetz MP, Fischer PM. 2007. Untangling tau hyperphosphorylation in drug design for neurodegenerative diseases. Nature reviews. Drug discovery 6:464–479.

McKhann G, Drachman D, Folstein M, Katzman R, Price D, Stadlan EM. 1984. Clinical diagnosis of Alzheimer's disease: report of the NINCDS-ADRDA Work Group under the auspices of Department of Health and Human Services Task Force on Alzheimer's Disease. Neurology 34:939–944.

McKhann GM, Knopman DS, Chertkow H, Hyman BT, Jack CR, Kawas CH, Klunk WE, Koroshetz WJ, Manly JJ, Mayeux R, Mohs RC, Morris JC, Rossor MN, Scheltens P, Carrillo MC, Thies B, Weintraub S, Phelps CH. 2011. The diagnosis of dementia due to Alzheimer's disease: recommendations from the National Institute on Aging-Alzheimer's Association workgroups on diagnostic guidelines for Alzheimer's disease. Alzheimer's & dementia: the journal of the Alzheimer's Association 7:263–269.

Melo SA, Luecke LB, Kahlert C, Fernandez AF, Gammon ST, Kaye J, LeBleu VS, Mittendorf EA, Weitz J, Rahbari N, Reissfelder C, Pilarsky C, Fraga MF, Piwnica-Worms D, Kalluri R. 2015. Glypican-1 identifies cancer exosomes and detects early pancreatic cancer. Nature 523:177–182.

Michel CH, Kumar S, Pinotsi D, Tunnacliffe A, St George-Hyslop P, Mandelkow E, Mandelkow E-M, Kaminski CF, Kaminski Schierle GS. 2014. Extracellular monomeric tau protein is sufficient to initiate the spread of tau protein pathology. The Journal of biological chemistry 289:956–967.

Morales-Kastresana A, Jones JC. 2017. Flow Cytometric Analysis of Extracellular Vesicles. Methods in molecular biology (Clifton, N.J.) 1545:215–225.

Morris E, Chalkidou A, Hammers A, Peacock J, Summers J, Keevil S. 2016. Diagnostic accuracy of (18)F amyloid PET tracers for the diagnosis of Alzheimer's disease: a systematic review and meta-analysis. European journal of nuclear medicine and molecular imaging 43:374–385.

Morris GP, Clark IA, Vissel B. 2014a. Inconsistencies and controversies surrounding the amyloid hypothesis of Alzheimer's disease. Acta neuropathologica communications 2:135.

Morris JC, Heyman A, Mohs RC, Hughes JP, van Belle G, Fillenbaum G, Mellits ED, Clark C. 1989. The Consortium to Establish a Registry for Alzheimer's Disease (CERAD). Part I. Clinical and neuropsychological assessment of Alzheimer's disease. Neurology 39:1159–1165.

Morris JK, Honea RA, Vidoni ED, Swerdlow RH, Burns JM. 2014b. Is Alzheimer's disease a systemic disease? Biochimica et biophysica acta 1842:1340–1349.

Morris M, Knudsen GM, Maeda S, Trinidad JC, Ioanoviciu A, Burlingame AL, Mucke L. 2015. Tau post-translational modifications in wild-type and human amyloid precursor protein transgenic mice. Nature neuroscience 18:1183–1189.

Motter R, Vigo-Pelfrey C, Kholodenko D, Barbour R, Johnson-Wood K, Galasko D, Chang L, Miller B, Clark C, Green R. 1995. Reduction of beta-amyloid peptide42 in the

cerebrospinal fluid of patients with Alzheimer's disease. Annals of neurology 38:643–648.

Muller L, Hong C-S, Stolz DB, Watkins SC, Whiteside TL. 2014. Isolation of biologically active exosomes from human plasma. Journal of immunological methods 411:55–65.

Mustapic M, Eitan E, Werner JK, Berkowitz ST, Lazaropoulos MP, Tran J, Goetzl EJ, Kapogiannis D. 2017. Plasma Extracellular Vesicles Enriched for Neuronal Origin: A Potential Window into Brain Pathologic Processes. Frontiers in neuroscience 11:278.

Nagasaka Y, Dillner K, Ebise H, Teramoto R, Nakagawa H, Lilius L, Axelman K, Forsell C, Ito A, Winblad B, Kimura T, Graff C. 2005. A unique gene expression signature discriminates familial Alzheimer's disease mutation carriers from their wild-type siblings. Proceedings of the National Academy of Sciences of the United States of America 102:14854–14859.

Namba Y, Tomonaga M, Kawasaki H, Otomo E, Ikeda K. 1991. Apolipoprotein E immunoreactivity in cerebral amyloid deposits and neurofibrillary tangles in Alzheimer's disease and kuru plaque amyloid in Creutzfeldt-Jakob disease. Brain research 541:163–166.

Nasreddine ZS, Phillips NA, Bédirian V, Charbonneau S, Whitehead V, Collin I, Cummings JL, Chertkow H. 2005. The Montreal Cognitive Assessment, MoCA: a brief screening tool for mild cognitive impairment. Journal of the American Geriatrics Society 53:695–699.

Neve RL, Harris P, Kosik KS, Kurnit DM, Donlon TA. 1986. Identification of cDNA clones for the human microtubule-associated protein tau and chromosomal localization of the genes for tau and microtubule-associated protein 2. Brain research 387:271–280.

Nhan HS, Chiang K, Koo EH. 2015. The multifaceted nature of amyloid precursor protein and its proteolytic fragments: friends and foes. Acta neuropathologica 129:1–19.

Nichols E, Szoeke CEI, Vollset SE, Abbasi N, Abd-Allah F, Abdela J, Aichour MTE, Akinyemi RO, Alahdab F, Asgedom SW, Awasthi A, Barker-Collo SL, Baune BT, Béjot Y,

Belachew AB, Bennett DA, Biadgo B, Bijani A, Bin Sayeed MS, Brayne C, Carpenter DO, Carvalho F, Catalá-López F, Cerin E, Choi J-YJ, Dang AK, Degefa MG, Djalalinia S, Dubey M, Duken EE, Edvardsson D, Endres M, Eskandarieh S, Faro A, Farzadfar F, Fereshtehnejad S-M, Fernandes E, Filip I, Fischer F, Gebre AK, Geremew D, Ghasemi-Kasman M, Gnedovskaya EV, Gupta R, Hachinski V, Hagos TB, Hamidi S, Hankey GJ, Haro JM, Hay SI, Irvani SSN, Jha RP, Jonas JB, Kalani R, Karch A, Kasaeian A, Khader YS, Khalil IA, Khan EA, Khanna T, Khoja TAM, Khubchandani J, Kisa A, Kissimova-Skarbek K, Kivimäki M, Koyanagi A, Krohn KJ, Logroscino G, Lorkowski S, Majdan M, Malekzadeh R, März W, Massano J, Mengistu G, Meretoja A, Mohammadi M, Mohammadi-Khanaposhtani M, Mokdad AH, Mondello S, Moradi G, Nagel G, Naghavi M, Naik G, Nguyen LH, Nguyen TH, Nirayo YL, Nixon MR, Ofori-Asenso R, Ogbo FA, Olagunju AT, Owolabi MO, Panda-Jonas S, Passos VMdA, Pereira DM, Pinilla-Monsalve GD, Piradov MA, Pond CD, Poustchi H, Qorbani M, Radfar A, et al. 2019. Global, regional, and national burden of Alzheimer's disease and other dementias, 1990–2016: a systematic analysis for the Global Burden of Disease Study 2016. The Lancet Neurology 18:88–106.

Okamura N, Harada R, Ishiki A, Kikuchi A, Nakamura T, Kudo Y. 2018. The development and validation of tau PET tracers: current status and future directions. Clinical and translational imaging 6:305–316.

Oksvold MP, Neurauter A, Pedersen KW. 2015. Magnetic bead-based isolation of exosomes. Methods in molecular biology (Clifton, N.J.) 1218:465–481.

Osteikoetxea X, Sódar B, Németh A, Szabó-Taylor K, Pálóczi K, Vukman KV, Tamási V, Balogh A, Kittel Á, Pállinger É, Buzás EI. 2015. Differential detergent sensitivity of extracellular vesicle subpopulations. Organic & biomolecular chemistry 13:9775–9782.

Pan BT, Johnstone RM. 1983. Fate of the transferrin receptor during maturation of sheep reticulocytes in vitro: selective externalization of the receptor. Cell 33:967–978.

Parakh R, Roy E, Koo E, Black S. 2004. Pantomime and imitation of limb gestures in relation to the severity of Alzheimer's disease. Brain and cognition 55:272–274.

Park S, Ahn ES, Kim Y. 2015. Neuroblastoma SH-SY5Y cell-derived exosomes stimulate dendrite-like outgrowths and modify the differentiation of A375 melanoma cells. Cell biology international 39:379–387.

Parker WD, Parks JK. 1995. Cytochrome c oxidase in Alzheimer's disease brain: purification and characterization. Neurology 45:482–486.

Patel GK, Khan MA, Zubair H, Srivastava SK, Khushman M'd, Singh S, Singh AP. 2019. Comparative analysis of exosome isolation methods using culture supernatant for optimum yield, purity and downstream applications. Scientific reports 9:5335.

Patters BJ, Kumar S. 2018. The role of exosomal transport of viral agents in persistent HIV pathogenesis. Retrovirology 15:79.

Pawlowski M, Meuth SG, Duning T. 2017. Cerebrospinal Fluid Biomarkers in Alzheimer's Disease-From Brain Starch to Bench and Bedside. Diagnostics (Basel, Switzerland) 7.

Pedersen KW, Kierulf B, Neurauter A. 2017. Specific and Generic Isolation of Extracellular Vesicles with Magnetic Beads. Methods in molecular biology (Clifton, N.J.) 1660:65–87.

Pérez-González R, Gauthier SA, Kumar A, Saito M, Saito M, Levy E. 2017. A Method for Isolation of Extracellular Vesicles and Characterization of Exosomes from Brain Extracellular Space. Methods in molecular biology (Clifton, N.J.) 1545:139–151.

Peterson C, Goldman JE. 1986. Alterations in calcium content and biochemical processes in cultured skin fibroblasts from aged and Alzheimer donors. Proceedings of the National Academy of Sciences of the United States of America 83:2758–2762.

Pîrşcoveanu DFV, Pirici I, Tudorică V, Bălşeanu TA, Albu VC, Bondari S, Bumbea AM, Pîrşcoveanu M. 2017. Tau protein in neurodegenerative diseases - a review. Romanian journal of morphology and embryology = Revue roumaine de morphologie et embryologie 58:1141–1150.

Planel E, Miyasaka T, Launey T, Chui D-H, Tanemura K, Sato S, Murayama O, Ishiguro K, Tatebayashi Y, Takashima A. 2004. Alterations in glucose metabolism induce hypothermia leading to tau hyperphosphorylation through differential inhibition of

kinase and phosphatase activities: implications for Alzheimer's disease. The Journal of neuroscience: the official journal of the Society for Neuroscience 24:2401–2411.

Planel E, Richter KEG, Nolan CE, Finley JE, Liu L, Wen Y, Krishnamurthy P, Herman M, Wang L, Schachter JB, Nelson RB, Lau L-F, Duff KE. 2007. Anesthesia leads to tau hyperphosphorylation through inhibition of phosphatase activity by hypothermia. The Journal of neuroscience: the official journal of the Society for Neuroscience 27:3090–3097.

Planel E, Yasutake K, Fujita SC, Ishiguro K. 2001. Inhibition of protein phosphatase 2A overrides tau protein kinase I/glycogen synthase kinase 3 beta and cyclin-dependent kinase 5 inhibition and results in tau hyperphosphorylation in the hippocampus of starved mouse. The Journal of biological chemistry 276:34298–34306.

Polanco JC, Scicluna BJ, Hill AF, Götz J. 2016. Extracellular Vesicles Isolated from the Brains of rTg4510 Mice Seed Tau Protein Aggregation in a Threshold-dependent Manner. The Journal of biological chemistry 291:12445–12466.

Portet F, Scarmeas N, Cosentino S, Helzner EP, Stern Y. 2009. Extrapyramidal signs before and after diagnosis of incident Alzheimer disease in a prospective population study. Archives of neurology 66:1120–1126.

Pozarowski P, Darzynkiewicz Z. 2004. Analysis of cell cycle by flow cytometry. Methods in molecular biology (Clifton, N.J.) 281:301–311.

Prendergast EN, Souza Fonseca MA de, Dezem FS, Lester J, Karlan BY, Noushmehr H, Lin X, Lawrenson K. 2018. Optimizing exosomal RNA isolation for RNA-Seq analyses of archival sera specimens. PloS one 13: e0196913.

Price JL, McKeel DW, Buckles VD, Roe CM, Xiong C, Grundman M, Hansen LA, Petersen RC, Parisi JE, Dickson DW, Smith CD, Davis DG, Schmitt FA, Markesbery WR, Kaye J, Kurlan R, Hulette C, Kurland BF, Higdon R, Kukull W, Morris JC. 2009. Neuropathology of nondemented aging: presumptive evidence for preclinical Alzheimer disease. Neurobiology of aging 30:1026–1036.

Puig KL, Combs CK. 2013. Expression and function of APP and its metabolites outside the central nervous system. Experimental gerontology 48:608–611.

Rabinovici GD, Jagust WJ. 2009. Amyloid imaging in aging and dementia: testing the amyloid hypothesis in vivo. Behavioural neurology 21:117–128.

Rahayel S, Frasnelli J, Joubert S. 2012. The effect of Alzheimer's disease and Parkinson's disease on olfaction: a meta-analysis. Behavioural brain research 231:60–74.

Raposo G, Nijman HW, Stoorvogel W, Liejendekker R, Harding CV, Melief CJ, Geuze HJ. 1996. B lymphocytes secrete antigen-presenting vesicles. The Journal of experimental medicine 183:1161–1172.

Raposo G, Stoorvogel W. 2013. Extracellular vesicles: exosomes, microvesicles, and friends. The Journal of cell biology 200:373–383.

Ray S, Britschgi M, Herbert C, Takeda-Uchimura Y, Boxer A, Blennow K, Friedman LF, Galasko DR, Jutel M, Karydas A, Kaye JA, Leszek J, Miller BL, Minthon L, Quinn JF, Rabinovici GD, Robinson WH, Sabbagh MN, So YT, Sparks DL, Tabaton M, Tinklenberg J, Yesavage JA, Tibshirani R, Wyss-Coray T. 2007. Classification and prediction of clinical Alzheimer' s diagnosis based on plasma signaling proteins. Nature Medicine 13:1359 EP -.

Ray WJ, Ashall F, Goate DPhil AM. 1998. Molecular pathogenesis of sporadic and familial forms of Alzheimer's disease. Molecular Medicine Today 4:151–157.

Rezai-Zadeh K, Gate D, Szekely CA, Town T. 2009. Can peripheral leukocytes be used as Alzheimer's disease biomarkers? Expert review of neurotherapeutics 9:1623–1633.

Riccardi C, Nicoletti I. 2006. Analysis of apoptosis by propidium iodide staining and flow cytometry. Nature Protocols 1:1458–1461.

Richartz-Salzburger E, Batra A, Stransky E, Laske C, Köhler N, Bartels M, Buchkremer G, Schott K. 2007. Altered lymphocyte distribution in Alzheimer's disease. Journal of psychiatric research 41:174–178.

Robinson S, Pool R, Giffin RB. 2008. Emerging safety science: Workshop summary. Washington DC: National Academies Press. xvi, 134.

Saint-Aubert L, Lemoine L, Chiotis K, Leuzy A, Rodriguez-Vieitez E, Nordberg A. 2017. Tau PET imaging: present and future directions. Molecular neurodegeneration 12:19.

Saman S, Kim W, Raya M, Visnick Y, Miro S, Saman S, Jackson B, McKee AC, Alvarez VE, Lee NCY, Hall GF. 2012. Exosome-associated tau is secreted in tauopathy models and is selectively phosphorylated in cerebrospinal fluid in early Alzheimer disease. The Journal of biological chemistry 287:3842–3849.

Sastre B, Cañas JA, Rodrigo-Muñoz JM, Del Pozo V. 2017. Novel Modulators of Asthma and Allergy: Exosomes and MicroRNAs. Frontiers in immunology 8:826.

Simons M, Raposo G. 2009. Exosomes—vesicular carriers for intercellular communication. Current opinion in cell biology 21:575–581.

Simpson RJ, Jensen SS, Lim JWE. 2008. Proteomic profiling of exosomes: current perspectives. Proteomics 8:4083–4099.

Sims NR, Finegan JM, Blass JP. 1987. Altered metabolic properties of cultured skin fibroblasts in Alzheimer's disease. Annals of neurology 21:451–457.

Słomka A, Urban SK, Lukacs-Kornek V, Żekanowska E, Kornek M. 2018. Large Extracellular Vesicles: Have We Found the Holy Grail of Inflammation? Frontiers in immunology 9:2723.

Soria FN, Pampliega O, Bourdenx M, Meissner WG, Bezard E, Dehay B. 2017. Exosomes, an Unmasked Culprit in Neurodegenerative Diseases. Frontiers in neuroscience 11:26.

Sparks DL, Kryscio RJ, Sabbagh MN, Ziolkowski C, Lin Y, Sparks LM, Liebsack C, Johnson-Traver S. 2012. Tau is reduced in AD plasma and validation of employed ELISA methods. American journal of neurodegenerative disease 1:99–106.

Spires-Jones TL, Stoothoff WH, Calignon A de, Jones PB, Hyman BT. 2009. Tau pathophysiology in neurodegeneration: a tangled issue. Trends in Neurosciences 32:150–159.

Steen HB. 2004. Flow cytometer for measurement of the light scattering of viral and other submicroscopic particles. Cytometry. Part A: the journal of the International Society for Analytical Cytology 57:94–99.

Stelzma RA, Schnitzlein NH, and Murllagh RF. 1995. An english translation of alzheimer's 1907 paper, "über eine eigenartige erkankung der hirnrinde":3.

Stieler JT, Lederer C, Brückner MK, Wolf H, Holzer M, Gertz HJ, Arendt T. 2001. Impairment of mitogenic activation of peripheral blood lymphocytes in Alzheimer's disease. Neuroreport 12:3969–3972.

Stokholm J, Vogel A, Gade A, Waldemar G. 2006. Heterogeneity in executive impairment in patients with very mild Alzheimer's disease. Dementia and geriatric cognitive disorders 22:54–59.

Strittmatter WJ, Roses AD. 1996. Apolipoprotein E and Alzheimer's disease. Annual review of neuroscience 19:53–77.

Süssmuth SD, Reiber H, Tumani H. 2001. Tau protein in cerebrospinal fluid (CSF): a blood-CSF barrier related evaluation in patients with various neurological diseases. Neuroscience letters 300:95–98.

Tai Y-L, Chen K-C, Hsieh J-T, Shen T-L. 2018. Exosomes in cancer development and clinical applications. Cancer science 109:2364–2374.

Tan J, Town T, Mullan M. 2002. CD40-CD40L interaction in Alzheimer's disease. Current opinion in pharmacology 2:445–451.

Tariot PN, Aisen P, Cummings J, Jakimovich L, Schneider L, Thomas R, Becerra L, Loy R. 2009. The ADCS valproate neuroprotection trial: Primary efficacy and safety results. Alzheimer's & Dementia 5: P84-P85.

Tariq SH, Tumosa N, Chibnall JT, Perry MH, Morley JE. 2006. Comparison of the Saint Louis University mental status examination and the mini-mental state examination for detecting dementia and mild neurocognitive disorder—a pilot study. The American journal of geriatric psychiatry: official journal of the American Association for Geriatric Psychiatry 14:900–910.

Tauro BJ, Greening DW, Mathias RA, Ji H, Mathivanan S, Scott AM, Simpson RJ. 2012. Comparison of ultracentrifugation, density gradient separation, and immunoaffinity capture methods for isolating human colon cancer cell line LIM1863-derived exosomes. Methods (San Diego, Calif.) 56:293–304.

Terry RD, Peck A, DeTeresa R, Schechter R, Horoupian DS. 1981. Some morphometric aspects of the brain in senile dementia of the Alzheimer type. Annals of neurology 10:184–192.

Théry C, Amigorena S, Raposo G, Clayton A. 2006. Isolation and characterization of exosomes from cell culture supernatants and biological fluids. Current protocols in cell biology Chapter 3: Unit 3.22.

Théry C, Zitvogel L, Amigorena S. 2002. Exosomes: composition, biogenesis and function. Nature reviews. Immunology 2:569–579.

Thinakaran G, Koo EH. 2008. Amyloid precursor protein trafficking, processing, and function. The Journal of biological chemistry 283:29615–29619.

Tollefson GD, Godes M, Warren JB, Haus E, Luxenberg M, Garvey M. 1989. Lymphopenia in primary degenerative dementia. Journal of psychiatric research 23:191–199.

Trams EG, Lauter CJ, Norman Salem, JR., Heine U. 1981. Exfoliation of membrane ecto-enzymes in the form of micro-vesicles. Biochimica et Biophysica Acta (BBA) - Biomembranes 645:63–70.

Tycko R. 2016. Molecular Structure of Aggregated Amyloid-β: Insights from Solid-State Nuclear Magnetic Resonance. Cold Spring Harbor perspectives in medicine 6.

van der Pol E, van Gemert MJC, Sturk A, Nieuwland R, van Leeuwen TG. 2012. Single vs. swarm detection of microparticles and exosomes by flow cytometry. Journal of thrombosis and haemostasis: JTH 10:919–930.

van Niel G, D'Angelo G, Raposo G. 2018. Shedding light on the cell biology of extracellular vesicles. Nature reviews. Molecular cell biology 19:213–228.

Vanmechelen E, Vanderstichele H, Davidsson P, van Kerschaver E, van der Perre B, Sjögren M, Andreasen N, Blennow K. 2000. Quantification of tau phosphorylated at threonine 181 in human cerebrospinal fluid: a sandwich ELISA with a synthetic phosphopeptide for standardization. Neuroscience letters 285:49–52.

Vogel A, Upadhya R, Shetty AK. 2018. Neural stem cell derived extracellular vesicles: Attributes and prospects for treating neurodegenerative disorders. EBioMedicine 38:273–282.

Wang X, Huang T, Bu G, Xu H. 2014. Dysregulation of protein trafficking in neurodegeneration. Molecular neurodegeneration 9:31.

Weingarten MD, Lockwood AH, Hwo SY, Kirschner MW. 1975. A protein factor essential for microtubule assembly. Proceedings of the National Academy of Sciences of the United States of America 72:1858–1862.

Weinstein G, Seshadri S. 2014. Circulating biomarkers that predict incident dementia. Alzheimer's research & therapy 6:6.

Wekerle H, Flügel A, Neumann H. 2000. Neuronal Control of the Immune Response in the Central Nervous System: From Pathogenesis to Therapy. In: Christen Y, Patterson P, Kordon C, editors. Neuro-Immune Interactions in Neurologic and Psychiatric Disorders. Berlin, Heidelberg: Springer Berlin Heidelberg, p 111–123.

Wells LA. 1972. Permeability of the blood-brain barrier system to rubidium in euthermia, hibernation and hypothermia. Comparative Biochemistry and Physiology Part A: Physiology 42:551–557.

Whittington RA, Virág L, Marcouiller F, Papon M-A, El Khoury NB, Julien C, Morin F, Emala CW, Planel E. 2011. Propofol directly increases tau phosphorylation. PloS one 6: e16648.

Whitwell JL, Dickson DW, Murray ME, Weigand SD, Tosakulwong N, Senjem ML, Knopman DS, Boeve BF, Parisi JE, Petersen RC, Jack CR, Josephs KA. 2012. Neuroimaging correlates of pathologically defined subtypes of Alzheimer's disease: a case-control study. The Lancet Neurology 11:868–877.

Winston CN, Goetzl EJ, Akers JC, Carter BS, Rockenstein EM, Galasko D, Masliah E, Rissman RA. 2016. Prediction of conversion from mild cognitive impairment to dementia with neuronally derived blood exosome protein profile. Alzheimer's & dementia (Amsterdam, Netherlands) 3:63–72.

Wren MC, Lashley T, Årstad E, Sander K. 2018. Large inter- and intra-case variability of first-generation tau PET ligand binding in neurodegenerative dementias. Acta neuropathologica communications 6:34.

Wyss-Coray T. 2006. Inflammation in Alzheimer disease: driving force, bystander or beneficial response? Nature Medicine 12:1005–1015.

Yang L, Rieves D, Ganley C. 2012. Brain amyloid imaging—FDA approval of florbetapir F18 injection. The New England journal of medicine 367:885–887.

Yoo YK, Lee J, Kim H, Hwang KS, Yoon DS, Lee JH. 2018. Toward Exosome-Based Neuronal Diagnostic Devices. Micromachines 9.

Yoon SC, Kwon Y-A, Kim H, Kim S, Ahn Jo S, Kim DK. 2010. Altered cell viability and proliferation activity of peripheral lymphocytes in patients with Alzheimer's disease. Psychiatry investigation 7:68–71.

Zarovni N, Corrado A, Guazzi P, Zocco D, Lari E, Radano G, Muhhina J, Fondelli C, Gavrilova J, Chiesi A. 2015. Integrated isolation and quantitative analysis of exosome shuttled proteins and nucleic acids using immunocapture approaches. Methods (San Diego, Calif.) 87:46–58.

Zeringer E, Barta T, Li M, Vlassov AV. 2015. Strategies for isolation of exosomes. Cold Spring Harbor protocols 2015:319–323.

Zhang Y, Hu Y-W, Zheng L, Wang Q. 2017. Characteristics and Roles of Exosomes in Cardiovascular Disease. DNA and cell biology 36:202–211.

Zheng H, Koo EH. 2011. Biology and pathophysiology of the amyloid precursor protein. Molecular neurodegeneration 6:27.

Zhu S, Ma L, Wang S, Chen C, Zhang W, Yang L, Hang W, Nolan JP, Wu L, Yan X. 2014. Light-scattering detection below the level of single fluorescent molecules for high-resolution characterization of functional nanoparticles. ACS nano 8:10998–11006.

7.   APPENDICES

7.1.   Curriculum Vitae

David Larbi Simpong

Date of birth   08.08.1984

Place of birth   Aburi, Eastern Region, Ghana

Address   Tarostraße 18/204, 04103 Leipzig, Germany

Mobile   +4915213310009

E-Mail   dsimpong@ucc.edu.gh

Professional and academic career

Since 2016   working group of Professor Dr. med of Thomas Arendt

                  Quantification of tau protein in peripheral blood

                  Lymphocyte activation test as blood biomarker for Alzheimer's disease

2014 – 2016   Pathology techniques lecturer, Department of Medical Laboratory

                  Science, University of Cape Coast, Ghana

Since 2014   qualified to practice as clinical laboratory scientist (PIN-09034112)

                  Certification by Allied Health Professional Council Ghana

Education

Since 2016   PhD student, Universität Leipzig

2011 – 2013   Master of philosophy in pathology student, University of Ghana

2005 – 2009   BSc. Medical Laboratory Scientist student, University of Cape Coast

Scholarship

Since 2016   Government scholarship Ghana (MoE) and

                  Deutscher Akademischer Austauschdienst (DAAD)

Languages

English   Mother tongue

Deutsch   Up to B1

Others

Since 2015   Good knowledge in GraphPad Prism, SPSS, EndNote and Citavi

June 2018   Participant of 68th Lindau Nobel Laureate Meeting

2010 – 2011   Senior Research Assistant, University of Cape Coast

2009 – 2010   Medical Laboratory Scientist Intern, Cape Coast teaching hospital, Ghana

Interest   Long distance running, football, acrobatics, watching of movies

7.2.   Publications

Oberstadt M, Stieler J, **Simpong DL**, Römuß U, Urban N, Schaefer M, Arendt T, Holzer M. 2018. TDP-43 self-interaction is modulated by redox-active compounds Auranofin, Chelerythrine and Riluzole. Scientific reports 8:2248.

Simpong DL, Asmah RH, Krampah C, Akakpo PK, Adu P, Asante D-B, Naporo S, Adjei AA, Gyasi RK. 2018a. HER-2 Protein Overexpression in Patients with Gastric and Oesophageal Adenocarcinoma at a Tertiary Care Facility in Ghana. TheScientificWorldJournal 2018:1564150.

Awuku YA, **Simpong DL**, Alhassan IK, Tuoyire DA, Afaa T, Adu P. 2017. Prevalence of helicobacter pylori infection among children living in a rural setting in Sub-Saharan Africa. BMC public health 17:360.

Simpong DL, Awuku YA, Kye-Amoah KK, Morna MT, Adoba P, Anin SK, Adu P. 2018b. High Iodine Deficiency among Pregnant Women in Periurban Ghana: A Hospital-Based Longitudinal Study. Journal of nutrition and metabolism 2018:9706805.

Simpong DL, Adu P, Bashiru R, Morna MT, Yeboah FA, Akakpo K, Ephraim RKD. 2016. Assessment of iodine status among pregnant women in a rural community in ghana - a cross sectional study. Archives of public health = Archives belges de sante publique 74:8.

Asante D-B, Asmah RH, Adjei AA, Kyei F, **Simpong DL**, Brown CA, Gyasi RK. 2017. Detection of Human Papillomavirus Genotypes and Epstein-Barr Virus in Nasopharyngeal Carcinomas at the Korle-Bu Teaching Hospital, Ghana. TheScientificWorldJournal 2017:2721367.

Afrifa J, Gyekye SA, Owiredu WKBA, Ephraim RKD, Essien-Baidoo S, Amoah S, **Simpong DL**, Arthur AR. 2015. Application of sigma metrics for the assessment of quality control in clinical chemistry laboratory in Ghana: A pilot study. Nigerian medical journal : journal of the Nigeria Medical Association 56:54–58.

7.3. Declaration of the independent writing of this thesis

Erklärung über die eigenständige Abfassung der Arbeit

Hiermit erkläre ich, dass ich die vorliegende Arbeit selbstständig und ohne unzulässige Hilfe oder Benutzung anderer als der angegebenen Hilfsmittel angefertigt habe. Ich versichere, dass Dritte von mir weder unmittelbar noch mittelbar eine Vergütung oder geldwerte Leistungen für Arbeiten erhalten haben, die im Zusammenhang mit dem Inhalt der vorgelegten Dissertation stehen, und dass die vorgelegte Arbeit weder im Inland noch im Ausland in gleicher oder ähnlicher Form einer anderen Prüfungsbehörde zum Zweck einer Promotion oder eines anderen Prüfungsverfahrens vorgelegt wurde. Alles aus anderen Quellen und von anderen Personen übernommene Material, das in der Arbeit verwendet wurde oder auf das direkt Bezug genommen wird, wurde als solches kenntlich gemacht. Insbesondere wurden alle Personen genannt, die direkt an der Entstehung der vorliegenden Arbeit beteiligt waren. Die aktuellen gesetzlichen Vorgaben in Bezug auf die Zulassung der klinischen Studien, die Bestimmungen des Tierschutzgesetzes, die Bestimmungen des Gentechnikgesetzes und die allgemeinen Datenschutzbestimmungen wurden eingehalten. Ich versichere, dass ich die Regelungen der Satzung der Universität Leipzig zur Sicherung guter wissenschaftlicher Praxis kenne und eingehalten habe.

7.4. Acknowledgement